MASARYKOVA UNIVERZITA
PŘÍRODOVĚDECKÁ FAKULTA
ÚSTAV TEORETICKÉ FYZIKY A ASTROFYZIKY

Fenomenologie modelu MEMe v blízkosti kritické hustoty hmoty

DIPLOMOVÁ PRÁCE

Bc. Alena Vanžurová

Vedoucí práce:
Dr. Sante Carloni, M.A., Ph.D.

Brno 2026

Bibliografický záznam

Autor:	Bc. Alena Vanžurová Přírodovědecká fakulta, Masarykova univerzita Ústav teoretické fyziky a astrofyziky

Název práce:	Fenomenologie modelu MEMe v blízkosti kritické hustoty hmoty
Studijní program:	PřF B-FYZ Fyzika
Studijní obor:	Astrofyzika
Vedoucí práce:	Dr. Sante Carloni, M.A., Ph.D.
Konzultant:	doc. RNDr. Lenka Přibylová, Ph.D.
Akademický rok:	2025/2026
Počet stran:	xiv + 115
Klíčová slova:	kosmologie; bounce; modifikovaná gravitace; dynamické systémy; fázové portréty

Bibliographic entry

Author:	Bc. Alena Vanžurová Faculty of Science, Masaryk University Department of theoretical physics and astrophysics

Title of Thesis:	Phenomenology of the MEMe model close to the critical matter density
Degree programme:	Physics
Field of study:	Astrophysics
Supervisor:	Dr. Sante Carloni, M.A., Ph.D.
Consultant:	doc. RNDr. Lenka Přibylová, Ph.D.
Academic year:	2025/2026
Number of pages:	xiv + 115
Key words:	cosmology; bounce; modified gravity; dynamical systems; phase portraits

Abstrakt

Tato práce se zaměřuje na prozkoumání možných kosmologických vývojových scénářu v rámci modelu Minimal Exponential Measure (MEMe), jenž je příkladem minimálně modifikované teorie gravitace typu I a vychází ze zobecnění vazby mezi časoprostorem a hmotou. Takové rozšíření obecné relativity má potenciál nejen objasnit nedávné zrychlení expanze našeho vesmíru, ale také poskytnout přirozenou cestu jak se vyhnout počáteční singularitě. Naše studie se soustředí především na druhý z uvedených aspektů. Začínáme přehledem základních typů modifikované gravitace, abychom vytvořili ucelený obraz o výzkumu probíhajícím v této oblasti. Další součástí je stručné uvedení do teorie nelineárních dynamických systémů s důrazem na její význam pro kosmologické aplikace. Pomocí technik dynamických systémů zjistíme, že bounce zabraňuje MEMe modelu dosáhnout singularity ve všech prostorových geometriích, nezávisle na volbě počátečních podmínek v rámci fyzikální domény.

Abstract

This thesis aims to investigate possible cosmological evolutions within the Minimal Exponential Measure (MEMe) model, an example of type-I Minimally Modified Gravity theory, based on a generalization of coupling between geometry and matter. This extension of General Relativity has the potential not only to account for recent accelerated expansion of the Universe but may also provide a natural mechanism for avoiding the initial singularity. The primary focus of our study is on the latter aspect. We commence with an overview of modified gravity scenarios to establish a coherent picture of ongoing research in this area. A brief introduction to the theory of nonlinear dynamical systems is included, emphasizing its relevance to cosmological applications. Through employing dynamical systems techniques, we find that the bounce mechanism prevents the MEMe theory from reaching singularity in all spatial geometries, regardless of the choice of initial conditions within a physical domain.

MUNI
SCI

MASARYKOVA UNIVERZITA
PŘÍRODOVĚDECKÁ FAKULTA
KOTLÁŘSKÁ 2, 611 37 BRNO
IČ: 00216224
DIČ: CZ00216224

ZADÁNÍ DIPLOMOVÉ PRÁCE

Akademický rok: 2025/2026

Ústav:	Ústav teoretické fyziky a astrofyziky
Studentka:	Bc. Alena Vanžurová
Program:	Fyzika
Specializace:	Astrofyzika

Ředitel *ústavu* PřF MU Vám ve smyslu Studijního a zkušebního řádu MU určuje diplomovou práci s názvem:

Název práce:	Fenomenologie modelu MEMe v blízkosti kritické hustoty hmoty
Název práce anglicky:	Phenomenology of the MEMe model close to the critical matter density
Jazyk práce:	angličtina

Oficiální zadání:
General Relativity (GR) has proven extremely successful in explaining a wide range of gravitational phenomena. However, in some contexts, like the dark universe, Einstein's theory seems incomplete. This fact has led the research community to explore extensions of GR that might fit the current evidence. Among these extensions, the Minimal Exponential Measure model (MEMe), despite its simplicity, has demonstrated remarkable potential in describing the current dark phenomenology [1,2,3,4]. However, this model also presents some intriguing peculiarities, notably the decoupling of matter from spacetime at a critical density. The primary objective of this project is to study this last phenomenon. Leveraging dynamic system techniques [5], we will delve into the dynamics of the theory, striving to deduce the range of initial conditions that lead to the decoupling. Our ultimate goal is to infer the implications for gravitational collapse and black hole formation in these theories, thereby contributing to our understanding of their relevance as extensions of GR.

Vedoucí práce:	Dr. Sante Carloni, M.A., Ph.D.
Konzultant:	doc. RNDr. Lenka Přibylová, Ph.D.
Datum zadání práce:	19. 5. 2024
V Brně dne:	26. 1. 2026

Zadání bylo schváleno prostřednictvím IS MU.

Bc. Alena Vanžurová, 8. 12. 2025
Dr. Sante Carloni, M.A., Ph.D., 10. 12. 2025
Mgr. Dušan Hemzal, Ph.D., 12. 12. 2025

Acknowledgements

First and foremost, I am immensely grateful to my kind supervisor, Sante, for the aptest metaphors and analogies, new Italian words, endless patience, tireless beating of my pessimism, countless learning opportunities, and for noticing the spark of my potential to explore the fascinating realms of theoretical cosmology. He stood by me all the way, from "why is this index up and the other one down?" to "the dynamics of Einstein–Cartan cosmology has the same topology as the MEMe model on the boundary where the cosmological constant vanishes", and, despite my "czech shyness", brought me into (phase) spaces I never knew I had dreamed of. Next, I sincerely thank my mathematical advisor, Lenka, whose enthusiasm served as the driving force that prevented my analysis from descending into chaos and, most importantly, fuelled my own enthusiasm for any future work in the field of dynamical systems theory. A special thanks goes to Aďka, for her supportive and refreshing presence during this period of shared challenges and uncertainties. The genuine conversations with my closest friends and the environment they create have been quiet but foundational to my growth and elation, and I cannot fully express my gratitude to them for that. I would also like to thank all the encouraging and inspiring souls I was fortunate enough to meet during my master's studies, who completely transformed my perception of the scientific community and made me feel that perhaps I do belong there after all.

Declaration

Hereby I declare that I have prepared my Master's thesis independently under the guidance of the supervisor with the use of cited works.

Brno, 2026

Bc. Alena Vanžurová

It'll be just lovely for you to play – it'll be so hard.
And there's so much more fun when it is hard!

— Pollyanna

Contents

List of Figures

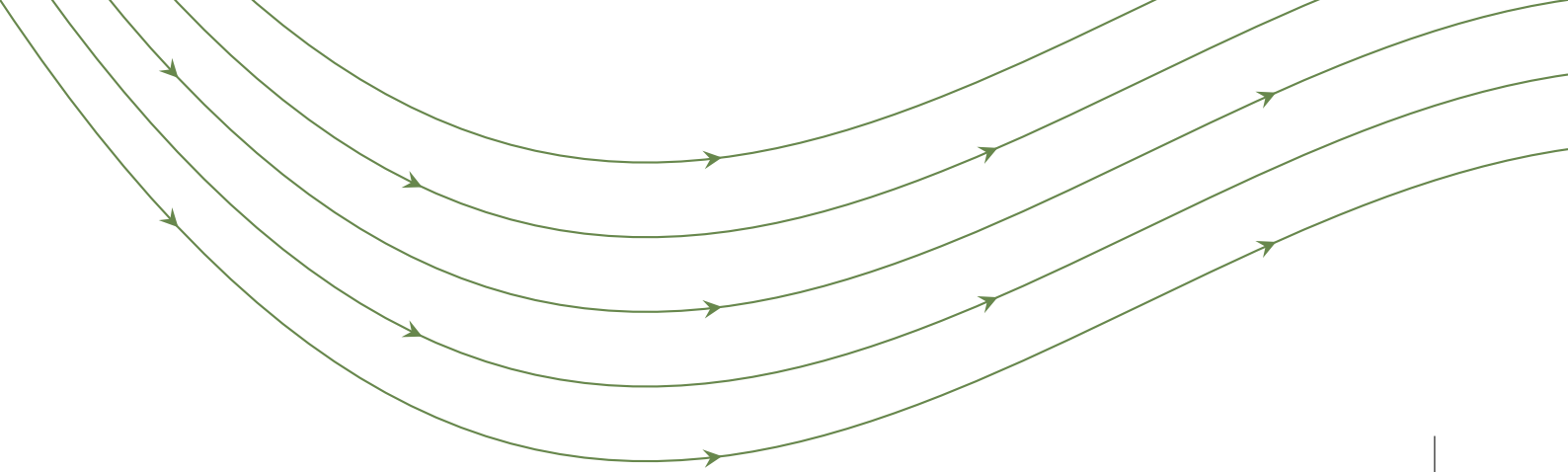

Introduction

Contemporary cosmology, which is experiencing an exciting era of precise measurements, faces several ongoing challenges. In particular, the search for an explanation of the Universe's *accelerated expansion*, as well as understanding the nature of *additional gravitating component* necessary for the initiation of structure formation has been central in recent gravitational and cosmological research. These components, commonly referred to as *dark*, collectively constitute the majority of the Universe's content. Another area of ongoing inquiry concerns the *initial singularity*, where our current understanding of physics becomes insufficient. Not to mention that much of the existing knowledge in the cosmological field relies on assumptions that are inherently difficult to empirically verify, such as the *cosmological principle* or the universal character of gravity throughout the entire cosmos.

Dark components are primarily handled by introducing new cosmic ingredients that encapsulate unknown physics. Current models include two such ingredients: *dark energy*, connected with accelerated expansion, and *dark matter*, associated, in cosmology, with structure formation. None of these dark components have been directly detected as yet, but many different theoretical models have been proposed. On the other hand, the problem of singularities is somewhat more nuanced, as they are generally linked to the limitations or breakdown of a particular theoretical framework and therefore less easy to model.

Over the past century, many researchers have approached these issues through the framework of *modified gravity*, rather than inventing exotic components to account for the unexplained phenomena. Specifically, certain theoretical extensions of General Relativity – our most accurate theory of gravity to date – offer potential alternatives to dark energy and/or dark matter within specific conditions. Additionally, some of these models have the capacity to circumvent the Big Bang singularity, which is considered inevitable in the standard cosmological model.

In this study, our aim is to examine a relatively recent generalization of General Relativity [1] that *relaxes the assumption of minimal coupling* between spacetime geometry and the energy-momentum tensor. This paradigm is guided by the recognition that the

deviations from General Relativity typically emerge when dealing with non-vacuum solutions to the Einstein equations. It suggests that we may be overlooking potential effects resulting from complex matter distributions, analogous to the extension of Hooke's law to three-dimensional continua in elasticity theory.

Above all, we will focus on the cosmological implications of the simplest realization of this Generalized Coupling Theory (GCT), dubbed as the Minimal Exponential Measure (MEMe) model. The impact of any modified theory on the evolution of the Universe can be effectively examined through mathematical techniques of *dynamical systems* – stability analysis of equilibrium points and phase space visualisation. The search for suitable variables in dynamical systems analysis is akin to selecting appropriate *lens*: each choice brings certain aspects of the dynamics into sharp focus while inevitably concealing others. Since previous analysis of the MEMe model utilized variables that highlighted features of *late-time* cosmology, we will seek an alternative approach that offers an elaborated response to questions related to bounce occurrence within the context of *early-universe* cosmology.

After crossing to the area of dynamical systems, our discussion will examine the structure of various phase portraits by combining analytical tools for equation manipulation with numerical methods. Analytical calculations are carried out using *Wolfram Mathematica* software, while numerical integrations are performed in *Python* utilizing standard routines. The visualization of the resulting trajectories is generated via the *Plotly* library. Interactive versions of selected phase portraits are available online.

In Chapter 1, we highlight the key aspects of General Relativity and explore potential avenues for its extensions. The initial section provides an overview of possible modified theories, followed by an introduction to standard cosmology and the corresponding formulations of cosmological equations derived from these alternative theoretical frameworks. Chapter 2 is dedicated to a concise introduction to nonlinear dynamical systems and the analytical tools employed to study them, ultimately leading to their application to cosmological equations discussed in Chapter 1. The characteristics of the examined MEMe model and its forecasts are detailed in Chapter 3, where we also present a summary of the analysis of the late Universe's evolution obeying the cosmological equations of the MEMe model, originally carried out in [1]. Finally, Chapter 4 presents a revised perspective on the linearized cosmological equations of the MEMe model and elaborates the analysis for each possible spatial geometry of our Universe.

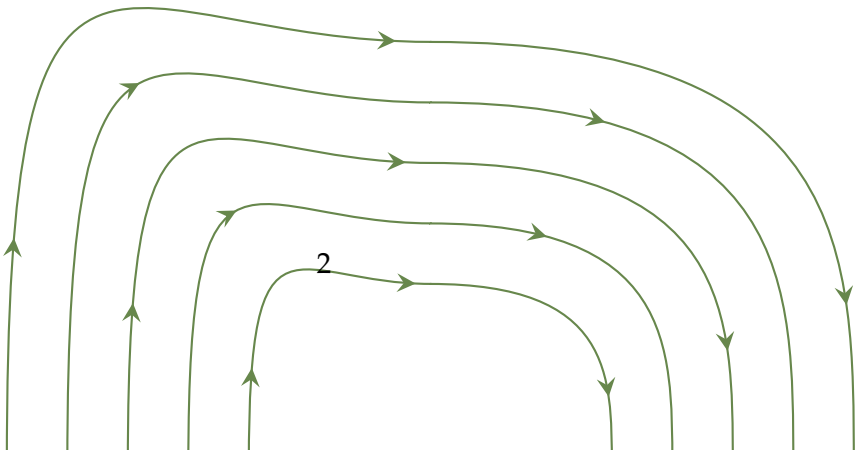

1

Modified gravity

Keep in mind that every single generation before us has worked under the assumption that they possessed all the major tools for understanding the universe, and they were all wrong, without exception.

— David Eagleman

The opening chapter of this thesis is devoted to the very broad topic of going *beyond Einstein*, and serves as a concise sampler of the ideas developed in this area. However, even in this form, the grievousness and boundlessness of this topic will perhaps become apparent [2].

First, it is advisable to provide the reader with an answer to the question that immediately comes to mind: why would one even consider something so radical – why would one doubt the ultimateness of the General Relativity (GR)? It is reasonable to inquire, given that from the glass-half-full perspective, GR continues to meet increasingly precise local tests of gravity without any significant issues and its strong-field regime predictions remain robust as well [3].

Simultaneously, each physical theory is inherently formulated and validated within a limited range of applicability, and increasing evidence suggests that we are now nearing the boundaries of GR's natural domain. From a glass-half-empty perspective (assuming the glass even has a bottom), GR alone does not provide a satisfactory description in the low-energy, large-distance regime (dubbed as IR regime), where cosmic acceleration emerges, nor in the high-energy, short-distance regime (dubbed as UV regime), where the theory itself ceases to be predictive, as the curvature invariants diverge. These complementary limitations do not diminish the effectiveness of GR within its applicable range, but indicate that it may not represent the ultimate word on gravity. But even if it does, dissecting it and exploring controlled extensions may deepen our understanding of how and why its structure works so remarkably well [4].

Historically, theoretical modification attempts appeared immediately after the theory of General Relativity was proposed [2]. Nowadays, these theories are mainly motivated

by the following arguments. First, GR and Quantum Mechanics (QM) both originated in the early twentieth century, with the latter one alone subsequently evolving into relativistic Quantum Field Theory (QFT). Although developed contemporaneously and demonstrating similar levels of empirical success, GR and QFT frameworks are grounded in different and incompatible conceptual structures. Particularly, in GR, spacetime itself is a dynamical entity whose geometry encodes the gravitational field, whereas QFT is formulated on a fixed background spacetime and relies on a clearly defined notion of time evolution and particle states. This tension between background independence and background dependence is a central obstacle to unifying gravity with the other fundamental interactions and suggests that at least one of the two theories should be regarded as an effective description.

Second, the singularities predicted by GR, even in the presence of physically reasonable matter, indicate a breakdown of the theory rather than its completion. Third, if we leave the issue of cosmological singularity aside, the subsequent early Universe still introduces additional challenges that can only be addressed through extensions of GR. Lastly, the treatment of inertia within GR does not fully align with Mach's principle, a discrepancy that Einstein himself was never entirely satisfied with [5].

Only the dusk of 20th century revealed that most of the Universe components may be unknown [6, 7, 8, 9]. Since then, our best fit to observations – Cosmological Concordance model ΛCDM – contains two dark elements. Dark matter was previously proposed to explain the flat rotation curves of galaxies by Vera Rubin [10], and Fritz Zwicky demonstrated its necessity in accounting for the galaxies' motion within large clusters [11] already in 1937, but the requirement for dark energy to explain the accelerated expansion of our Universe is what really plunged the well-established physical understanding into uncertainty.

1.1 What GR is made of

Due to the rich diversity of the GR modifications land, one needs to properly understand what makes GR so special, only then it is possible to decide whether it is feasible to change its anatomy and how. In this section, a structure of GR will be summarized very shortly. For further insights into the different levels of understanding in the study of GR, see the following literature [12, 13, 14, 15].

To start, the existence of Einstein's picture relies on the fundamental assumption that a gravitational theory can be constructed utilizing the principles of differential geometry. In the simplest language and notorious interpretation, the concept of gravitational force can be understood as a manifestation of the curvature of four-dimensional *Lorentzian* manifold named *spacetime*, which is caused by the presence of matter and energy. A *manifold* is a smooth topological space that locally resembles Euclidean space $\mathbb{R}^n$. A Lorentzian manifold is a specific type of *pseudo-Riemannian* manifold characterized by exactly one timelike dimension. Unlike *Riemannian* manifolds [16], which have a positive-definite metric tensor for measuring lengths and angles, pseudo-Riemannian manifolds generalize this concept by allowing non-degenerate metric with an arbitrary

signature. This introduces directions that can be classified as *timelike, spacelike* or *null*. Flat Lorentzian manifolds correspond to *Minkowski* spacetime, which is also sometimes called *pseudo-Euclidean*.

The design of Einstein's theory is based on several core principles. The name of the theory itself refers to the *principle of relativity*, by which the laws of physics should be the same in all reference frames [17]. This leads to the mathematical *principle of general covariance* (or *diffeomorphism invariance*), which requires that equations are tensorial and therefore invariant under coordinate transformations. This ensures that no single reference frame is privileged and that spacetime points are considered equivalent.

From a physics-oriented standpoint, the famous *Equivalence Principle* (EP) pertains to the results of local measurements. Its weak formulation, rooted in the observations of Galileo and later formalized by Newton, is fundamental to classical mechanics. This *Weak Equivalence Principle* (WEP) states that the *inertial mass* of an object – that is, its resistance to acceleration – is equal to its *passive gravitational mass*, which determines its response to gravitational forces. This means that all bodies *fall* in a gravitational field with the same acceleration, regardless of their internal composition. Einstein expanded upon this concept to incorporate the laws of electrodynamics. The *Einstein Equivalence Principle* (EEP) asserts that all non-gravitational phenomena are locally unaffected by gravity when conducted within a freely falling frame. In other words, all free-falling observers and inertial observers are locally indistinguishable. This principle implies *Lorentz invariance*, ensuring that physics remains unchanged under rotations and boosts in the local tangent space, no direction is special and the speed of light, c, is universal. Equally, by EEP, it is understood that the non-gravitational laws of physics locally reduce to those described by special relativity. The most stringent formulation is the *Strong Equivalence Principle* (SEP), which allows the freely falling bodies to possess their own gravitational fields. Consequently, SEP applies to objects that exert a gravitational force on themselves, such as stars, planets, or black holes. GR with a cosmological constant is believed to be the only gravitational theory that satisfies the SEP [18]. Finally, by the *correspondence principle*, the theory is expected to recover Newtonian gravity in the weak field limit and slow motion of sources.

This represents the core of general relativity and its physical interpretation. To capture the skeleton of a theory, understanding of underlying mathematical framework is essential. The Lorentz manifold is equipped with *two* additional structures: the aforementioned *metric tensor*, $g_{\mu\nu}$, encoding how distances and time intervals are measured, and *affine connection*, $\Gamma^{\alpha}_{\ \mu\nu}$, which specifies how vectors at different spacetime points are related, providing the notion of parallel transport and covariant differentiation. The former is described through the line-element

$$\mathrm{d}s^2 = g_{\mu\nu}\,\mathrm{d}x^\mu\,\mathrm{d}x^\nu\,, \tag{1.1}$$

while the latter is not fixed a priori. In GR, however, the connection is not treated as an independent structure. Instead, it is uniquely determined by two physical requirements:

(i) *Metric compatibility*, ensuring that lengths and angles are preserved under parallel transport,

$$\nabla_\alpha g_{\mu\nu} = 0\,, \tag{1.2}$$

and

(ii) *Vanishing torsion*, corresponding to symmetry in the lower indices of the connection,

$$\Gamma^\alpha{}_{\mu\nu} = \Gamma^\alpha{}_{\nu\mu}\,. \tag{1.3}$$

These two conditions uniquely fix the affine connection to be the *Levi-Civita connection*,

$$\Gamma^\alpha{}_{\mu\nu} = \frac{1}{2} g^{\alpha\beta}\left(\partial_\mu g_{\nu\beta} + \partial_\nu g_{\mu\beta} - \partial_\beta g_{\mu\nu}\right)\,, \tag{1.4}$$

thereby eliminating it as an independent degree of freedom. The spacetime curvature is then completely characterized by the fourth-order Riemann tensor

$$R^\alpha{}_{\beta\mu\nu} = \partial_\mu \Gamma^\alpha{}_{\beta\nu} - \partial_\nu \Gamma^\alpha{}_{\beta\mu} + \Gamma^\delta{}_{\beta\nu}\Gamma^\alpha{}_{\delta\mu} - \Gamma^\delta{}_{\beta\mu}\Gamma^\alpha{}_{\delta\nu} \tag{1.5}$$

and its contractions, namely the Ricci tensor

$$R_{\alpha\beta} = g^{\gamma\delta} R_{\gamma\alpha\delta\beta} \tag{1.6}$$

and Ricci curvature scalar

$$R = g^{\alpha\beta} R_{\alpha\beta}\,. \tag{1.7}$$

On a journey to Einstein Field Equations (EFE), we should emphasize a fundamental mathematical theorem that establishes their uniqueness [19]. It can be stated as [20]:

Theorem 1.1.1 (Lovelock's theorem) *The only possible second-order Euler–Lagrange expression obtainable in a four dimensional space from a scalar density $\mathcal{L}(g_{\mu\nu}, \partial g_{\mu\nu}, \partial^2 g_{\mu\nu})$, which is linear in the Ricci scalar R, is*

$$\alpha\sqrt{-g}\left[R^{\mu\nu} - \frac{1}{2} g^{\mu\nu} R\right] + \lambda\sqrt{-g}\, g^{\mu\nu}\,, \tag{1.8}$$

where α and λ are constants, $R_{\mu\nu}$ and R are the Ricci tensor and scalar curvature respectively.

This theorem demonstrates that any attempt to formulate a gravitational theory within a four-dimensional pseudo-Riemannian spacetime, based solely on an action principle involving the metric tensor and its derivatives, which is linear in the Ricci scalar, inevitably leads to Einstein's equations with a cosmological constant. Therefore, the standard action consists of the gravitational part, including the Einstein–Hilbert term and a cosmological constant term, denoted by S_{EH} and S_Λ, and a matter component, S_{m}, as described by

$$S = S_{\mathrm{EH}} + S_\Lambda + S_{\mathrm{m}} = \int \mathrm{d}^4x\sqrt{-g}\left[\frac{1}{2\kappa}(R - 2\Lambda) + \mathcal{L}_{\mathrm{m}}(g_{\mu\nu}, \psi)\right]. \tag{1.9}$$

Here, the $\mathcal{L}_{\mathrm{m}}$ represents the Lagrangian of matter fields, g stands for the determinant of the metric $g_{\mu\nu}$, $\kappa = 8\pi G/c^4$ is the gravitational coupling constant and Λ is a cosmological constant. The variation of the action (1.9) with respect to the metric yields the well-known EFE

$$R_{\mu\nu} - \frac{1}{2}g_{\mu\nu}R + \Lambda g_{\mu\nu} = \kappa T_{\mu\nu}\,, \tag{1.10}$$

and the energy-momentum tensor of the matter fields, $T_{\mu\nu}$, is accordingly defined by

$$T_{\mu\nu} \equiv \frac{2}{\sqrt{-g}}\frac{\delta(\sqrt{-g}\mathcal{L}_{\mathrm{m}})}{\delta g_{\mu\nu}}\,. \tag{1.11}$$

Lastly, the diffeomorphism invariance of the action leads to the Bianchi-contracted identities,

$$\nabla_\nu T^{\mu\nu} = 0\,, \tag{1.12}$$

which imply that in GR, energy conservation is a consequence of the underlying geometric symmetries of spacetime, rather than an explicit physical stipulation.

What we have just committed is known as a *variational approach* to gravity. The variational formulation is a foundational aspect of modern theoretical physics, as it offers a unified and systematic method for deriving field equations from a single scalar quantity – the action. The *principle of stationary action* is based on the requirement that the physical evolution of a system renders the action stationary under infinitesimal variations of the dynamical variables. In other words, among all possible configurations, the actual configuration satisfies

$$\delta S = 0\,, \tag{1.13}$$

which leads to the Euler–Lagrange equations of classical mechanics [21]. In field theory, this condition is applied with respect to variations of the fields – in this case, the metric tensor field – while maintaining fixed boundary conditions as appropriate. This approach is especially effective when considering gravity because it ensures general covariance and naturally gives rise to conservation laws through the underlying symmetries, as demonstrated shortly through the equation (1.12). Additionally, in the context of GR extensions that we aim to discuss, it provides a more fundamental framework that allows for straightforward modifications of the gravitational or matter Lagrangian, which is an important flexibility for the development and comparison of alternative theories of gravity.

We will also present another important theorem with significant implications for the weak field limit of GR. It states [22]

Theorem 1.1.2 (Jebsen–Birkhoff's theorem) *All spherically symmetric solutions of Einstein's equations in vacuum must be static and asymptotically flat (in the absence of* $\mathbf{\Lambda}$*).*

Although our Universe may not present real scenarios where the Jebsen–Birkhoff's theorem strictly applies – as perfect spherical symmetry or true vacuum conditions are idealized cases – it plays a significant role in understanding the gravitational fields around (nearly) isolated masses. Specifically, the theorem states that the *exterior* gravitational

field of a static spherically symmetric system located in vacuum can be described by the *Schwarzschild solution* and is independent of the system's internal dynamics. Additionally, Jebsen–Birkhoff's theorem indicates that certain types of gravitational radiation – such as that from a star pulsating in a spherically symmetric manner – are not possible. The theorem also reinforces the relativistic extension of the Newtonian picture, suggesting that far from massive objects, their gravitational influence diminishes, leading to asymptotically flat spacetime. This justifies treating the weak field limit of GR as a perturbation around Minkowski spacetime, providing a solid foundation for many approximations used in gravitational physics [20].

1.2 Usual ways of modification

A logical next step is to consider the implications of relaxing some of the assumptions or breaking some rules of the GR game discussed in previous section. A suitable starting point for exploring alternative theories of gravity is provided by Lovelock's theorem 1.1.1. This theorem outlines five conditions that GR must satisfy:

- *Equations of Motion (EoM) are of second order,*
- *there are no additional gravitational fields aside from a single rank-2 tensor field,*
- *general covariance holds (there is a minimal coupling between matter and geometry),*
- *the theory is local,*
- *the space-time is four-dimensional.*

Under these conditions, the theory is uniquely determined, indicating that the only consistent field equations are those of Einstein (1.10). Any significant extension of the theory must, at a minimum, violate one of these assertions, thereby circumventing Lovelock's theorem. From this broad point of view, we can classify Modified Gravity (MG) models as

- *those that go beyond second order in EoM,*
- *those that add new gravitational field content,*
- *those allowing non-minimal coupling to matter fields,*
- *those that break principle of locality,*
- *those that add higher dimensions.*

Speaking of second, third and fourth options, they remain distinct ways to evade the Lovelock's theorem, but at a deeper level they are often mathematically interchangeable: non-minimal (spacetime-matter) couplings or non-local terms can typically be reformulated as local theories with extra fields, see for example [23]. Conceptually, these three

categories can be seen as different representations of the same underlying flexibility and may be transformed into one another. Furthermore, the new fields inherently do not require their own minimal coupling. This indicates that, from a technical standpoint, it is most straightforward to address these mechanisms collectively within the overarching framework for additional fields. This reduction may seem reasonable, but there is one more widely studied category that falls outside the scope of Lovelock's theorem:

- *the extension or complete transformation of the geometrical framework.*

Overall, within this work, all modifications of gravity can ultimately be organized into four main classes, which will guide the structure of the subsequent discussion:

1. *gravity with extra non-minimally coupled fields,*
2. *gravity with extra dimensions,*
3. *gravity with extra curvature invariants,*
4. *gravity with extra geometrical structures.*

Before elaborating the various possibilities outlined in this introduction, we will also acknowledge that new types of models may emerge through the combination of two or more modification categories and, as we will observe, may converge into each other under certain conditions. At the same time, it is important to assert that many such toy models serve primarily as theoretical laboratories: they are often motivated by mathematical consistency, symmetry principles, or dynamical richness, rather than by direct derivation from underlying physical mechanisms.

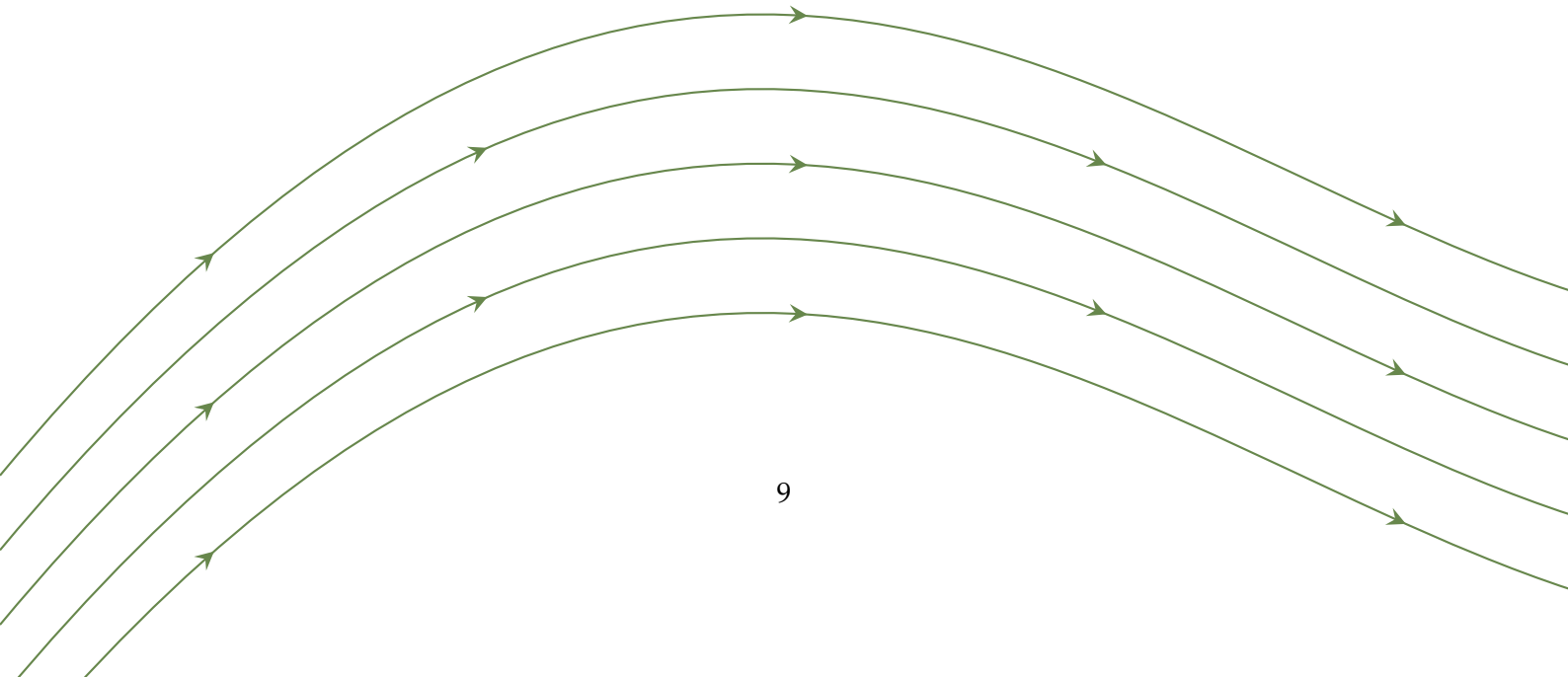

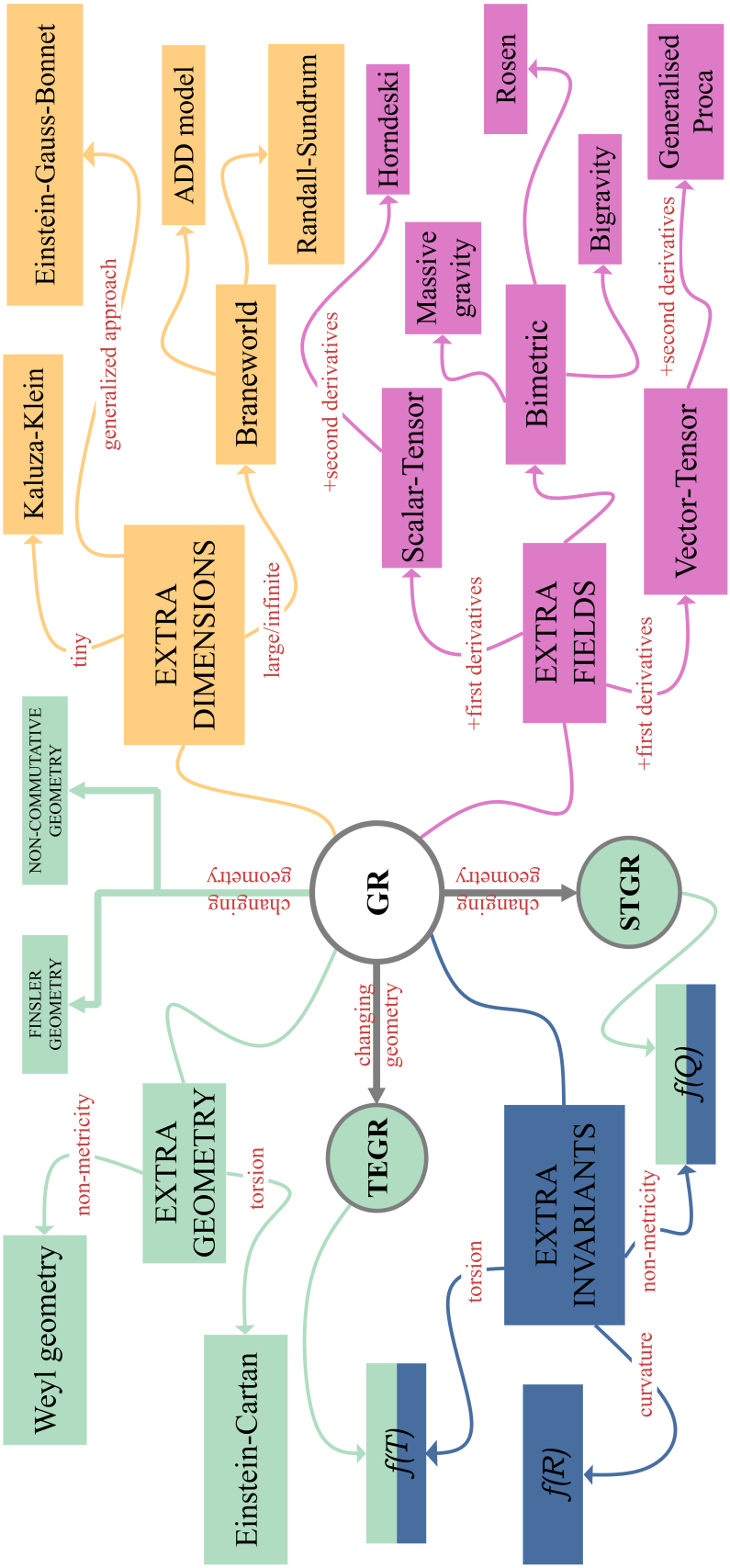

Figure 1.1: A streamlined classification of the modified gravity theories, as discussed further in this chapter.

1.2.1 Gravity with extra field(s)

First, we will explore the question of what happens if our gravitational action includes additional dynamical fields beyond the standard metric field used in GR, which are non-minimally coupled to the geometry. The simplest scenario to consider is the introduction of an extra scalar field. However, there is also no reason to exclude the possibility of incorporating extra vector fields, other rank-2 tensors, or even higher-rank fields, many of which exhibit similarities to Modified Newtonian Dynamics (MOND) in their non-relativistic limit [24]. Moreover, a multi-field extension, such as Tensor-Vector-Scalar (TeVeS) theories, is also permitted. We will restrict ourselves to the largest known family of well-behaved classical field extensions of GR.

Scalar-Tensor theories

Among the proposed modified gravity theories, scalar-tensor gravity has become one of the most popular and well-established. It originated from the work of Brans and Dicke, who sought to encompass Mach's principle into Einstein's gravitational theory, which at the time had existed for approximately 50 years [5]. This extension of GR supports the simplest concept of a *varying gravitational constant* G that depends on the distribution of matter content in our Universe. This can be modelled by an additional non-minimally coupled scalar field within the gravitational sector. Although the EEP ensures that gravity can be locally removed for non-gravitational phenomena, it does not guarantee that gravity can be globally transformed away or that its coupling strength must be universal. Generalized scalar-tensor theories are frequently employed as prototypes to model deviations from GR, due to their relatively simple field equations, which can be solved analytically [20]. They have also become an essential tool for describing the inflationary paradigm [25].

The most general Lagrangian density for the covariant local action constructed from a metric and a scalar field is [2]

$$\mathcal{L} = \frac{1}{2\kappa}\sqrt{-g}\left[f(\Phi)R - g(\Phi)\nabla_\mu\Phi\nabla^\mu\Phi - 2\lambda(\Phi)\right] + \mathcal{L}_{\mathrm{m}}(\psi, g_{\mu\nu})\right] , \tag{1.14}$$

where f, g, h and λ are all allowed to be arbitrary functions of the scalar field Φ and $\mathcal{L}_{\mathrm{m}}$ denotes the Lagrangian density of the matter fields ψ. We can set $f(\Phi) \to \phi$ without loss of generality, then equation (1.14) can be rewritten as

$$\mathcal{L} = \frac{1}{2\kappa}\sqrt{-g}\left[\phi R - \frac{\omega(\phi)}{\phi}\nabla_\mu\phi\nabla^\mu\phi - 2V(\phi)\right] + \mathcal{L}_{\mathrm{m}}(\psi, g_{\mu\nu}) , \tag{1.15}$$

where $\omega(\phi)$ is an arbitrary function known as the *coupling parameter*, while $V(\phi)$ represents the potential of a scalar field ϕ. The corresponding field equations are obtained by the variation of action built from (1.15). Varying with respect to the metric tensor brings

$$\phi G_{\mu\nu} + \left[\Box\phi + \frac{\omega}{2\phi}(\nabla\phi)^2 + V\right]g_{\mu\nu} - \nabla_\mu\nabla_\nu\phi - \frac{\omega}{\phi}\nabla_\mu\phi\nabla_\nu\phi = \kappa T_{\mu\nu} , \tag{1.16}$$

and varying with respect to the additional degree of freedom, ϕ, gives

$$(2\omega + 3)\Box\phi + \frac{\partial\omega}{\partial\phi}(\nabla\phi)^2 + 4V - 2\phi\frac{\partial V}{\partial\phi} = \kappa T \ , \tag{1.17}$$

where T is a trace of $T_{\mu\nu}$.

Scalar-tensor theories also possess the property that, after applying a *conformal* rescaling of the metric – specifically, a transformation of the form

$$\tilde{g}_{\mu\nu} = \Omega^2 g_{\mu\nu} \ , \tag{1.18}$$

where Ω is a nonvanishing regular function – and performing an appropriate field redefinition, the gravitational sector can be expressed in the standard Einstein–Hilbert form [26]. Any deviations from General Relativity are then manifested through scalar-matter interactions, meaning that a conformal transformation "shuffles" the coupling of the scalar field ϕ from the curvature sector into the matter sector [20].

In the limit as $\omega \to$ (positive) constant and $V \to 0$, this theory reduces to the original Brans–Dicke theory [5], and it recovers General Relativity with a cosmological constant in the limits $\omega \to \infty$, $\frac{\partial\omega}{\partial\phi}\frac{1}{\omega^2} \to 0$ and $V \to$ constant.

It is important to note at this point that the expression (1.15), commonly identified as *generalized Brans–Dicke theory*, still assumes that the scalar field influences the action solely through ϕ and its first derivatives. Horndeski theory [27] extends this framework by allowing second derivatives of the scalar field within the action, while maintaining second-order equations of motion (and the same number of propagating degrees of freedom). Galileon theories [28] can be viewed as the flat-spacetime limit of this extended construction. The investigation extends to higher (than second) derivatives of the scalar field within the context of beyond Horndeski theories [29].

Vector-Tensor theories

While a scalar field introduces one additional degree of freedom through its single component, the addition of a four-vector field, u^μ, involves up to four additional degrees of freedom. A general action for such theories can be expressed as

$$S = \int \mathrm{d}^4x\sqrt{-g}\left[\frac{1}{2\kappa}R + \mathcal{L}(g^{\mu\nu}, u^\nu)\right] + S_\mathrm{m}(g^{\mu\nu}, \psi) \ , \tag{1.19}$$

where S_m is the matter action with matter fields ψ that couple only to the metric $g_{\mu\nu}$. A particular and commonly studied subclass of (1.19) are Einstein-æther theories, where u^μ has a time-like direction. The simplest form of Lagrangian density of Vector-Tensor theory $\mathcal{L}$ is quadratic in derivatives of u^ν [20]

$$\mathcal{L}_\mathrm{EA}(g^{\mu\nu}, u^\nu) = \frac{1}{2\kappa}[K^{\mu\nu}{}_{\alpha\beta}\nabla_\mu u^\alpha \nabla_\nu u^\beta + \lambda(u^\nu u_\nu + 1)] \ , \tag{1.20}$$

where

$$K^{\mu\nu}{}_{\alpha\beta} = c_1 g^{\mu\nu}g_{\alpha\beta} + c_2\delta^\mu{}_\alpha\delta^\nu{}_\beta + c_3\delta^\mu{}_\beta\delta^\nu{}_\alpha - c_4 u^\mu u^\nu g_{\alpha\beta} \tag{1.21}$$

and λ is a Lagrange multiplier (an auxiliary variable introduced to directly enforce a constraint on a system [21]). This is a so called *linear* version of Einstein-æther, however, a generalized nonlinear form can be constructed by allowing for a function $F(K)$ in (1.20) as

$$\mathcal{L}_{\text{GEA}}(g^{\mu\nu}, u^{\nu}) = \frac{1}{2\kappa}[F(K) + \lambda(u^{\nu}u_{\nu} + 1)]\,, \tag{1.22}$$

where $K = K^{\mu\nu}{}_{\alpha\beta}\nabla_{\mu}u^{\alpha}\nabla_{\nu}u^{\beta}$. The corresponding gravitational field equations are detailed in [20]. A notable characteristic of these theories is the spontaneous breaking of local Lorentz invariance, resulting in a preferred reference frame. This feature can significantly influence cosmological solutions, particularly in the context of early-universe perturbations and the renormalization of the Newton constant.

Generalized Proca theories [30] constitute the vector-tensor analogue of Horndeski scalar-tensor theories, incorporating derivative self-interactions and curvature couplings. In this framework, Lorentz and diffeomorphism invariance are maintained at the level of action.

Bimetric theories

The inclusion of an extra two-rank tensor field is primarily motivated by the concept of a *massive graviton*, specifically exploring whether a spin-2 particle could acquire a nonzero mass through mechanisms similar to how particles in the Standard Model obtain mass via spontaneous symmetry breaking through the Higgs field [2]. This approach necessitates the introduction of an extra metric, which may be a reference metric, as in theories of *massive gravity* [31], or a dynamical metric, as in *bigravity* models [32].

In general bimetric language, the second metric does not necessarily assign a mass to the graviton, it can serve as an auxiliary or measurement-related function. The oldest theory of this kind is that of Rosen [33, 34], where the extra metric is considered to be flat, $\tilde{g}_{\alpha\beta} = \eta_{\alpha\beta}$. It produces results that are virtually indistinguishable from those of General Relativity in the post-Newtonian limit, except for one parameter [20]. Nevertheless, its predictions fail in pulsar observations. Other formulations of bimetric theory are Drummond's theory [35] and bimetric MOND [36].

Viability

The inclusion of additional fields in modified gravity theories provides a flexible phenomenological framework capable of replicating the effects traditionally attributed to dark matter and, as will be demonstrated, achieving desired cosmological evolution. However, this approach presents several challenges. Additional fields generally introduce new propagating degrees of freedom that require careful management to prevent instabilities such as ghost, gradient, or tachyonic modes. Their interactions with the metric and matter may differ from minimal coupling, which could potentially lead to violations of the EEP or the emergence of fifth forces – phenomena that are tightly constrained by laboratory, solar system, and astrophysical observations. Maintaining the

viability of these theories often relies on *screening mechanisms* to suppress the influence of extra fields on well-tested scales [37].

Additionally, many models necessitate tuning of functions or parameters to match observational data, raising concerns regarding their naturalness and predictive robustness. Consequently, while theories that involve extra gravitational fields constitute a broad and versatile class of MG models, their overall viability depends on achieving a careful balance among theoretical consistency, phenomenological control, and compliance with empirical constraints.

1.2.2 Gravity with extra dimensions

Since Riemannian geometry is not limited to four dimensions, we have access to tools suitable for analysing higher-dimensional theories of gravity. The upcoming paragraphs will provide a brief overview of a few models concerning the concept of additional dimensions, focusing on spatial dimensions, although extra temporal dimensions have also been investigated in the past [38]. This is, of course, the category in which *stringy theories* are rooted, as their consistent formulations require higher-dimensional spacetimes, ranging from ten dimensions to twenty-six dimensions in the bosonic case. It is argued that in these frameworks the observable four-dimensional gravity emerges either through dimensional reduction, localization mechanisms, or higher-curvature corrections.

Kaluza–Klein theory

The initial foundational effort was made by Theodor Kaluza in 1921, who sought to unify GR and electromagnetism by extending the concept of spacetime fabric to include a hidden fifth dimension [39]. Oskar Klein then proposed that the extra dimension was not extended as the other spatial dimensions, but *compactified*, rolled up into a tiny circle at every point in space [40].

The compactification is achieved through the dimensional reduction of the GR analogue on a circle of radius $L/2\pi$, where the scale L is typically taken to be of the order of the Planck length ($\sim l_{\rm Pl}$). This process involves extending the Einstein–Hilbert action to $D = n + 1$ dimensions,

$$S[\gamma] = \frac{1}{16\pi G_D} \int \mathrm{d}^D X \sqrt{-\gamma}\mathcal{R}\,, \tag{1.23}$$

with G_D being the Newton's constant in D dimensions, γ_{AB} being the D dimensional metric with corresponding Ricci tensor, $\mathcal{R}_{AB}$, and Ricci scalar , $\mathcal{R} = \gamma^{AB}\mathcal{R}_{AB}$. The metric is then expressed as a Fourier series and truncated to include only massless modes in the four-dimensional theory, with massive modes becoming excited only through processes with energies exceeding the compactification scale, $1/L$. This indicates that the late-time dynamics of Kaluza–Klein (KK) theory is most effectively analysed within the framework of four-dimensional effective theories. Conversely, during early times, when the three-dimensional spatial dimensions are comparable in size to the extra

dimensions, the validity of this effective description diminishes [20]. It is found that the n-dimensional effective action is then

$$S_{\text{eff}}[g, a, \phi] = \frac{L}{16\pi G_D} \int \mathrm{d}^n x \sqrt{-g} \left(R - \frac{1}{2}(\nabla\phi)^2 - \frac{1}{4} e^{-2(n-1)\alpha\phi} F^2 \right) , \tag{1.24}$$

where $\alpha = 1/\sqrt{2(n-1)(n-2)}$, $\beta = -(n-2)\alpha$ and $F^2 = F_{\mu\nu}F^{\mu\nu}$ is the electromagnetic field strength. This is known as the Einstein–Maxwell–Dilaton system in n dimensions, reducing to Kaluza–Klein theory in the case of $n = 4$. It is important to note that the dilaton field, ϕ, appears in the resulting effective theory and cannot be eliminated. This aspect has been a point of concern for the original researchers.

The braneworld paradigm

Unlike the standard KK scenario, the braneworld model introduces additional spatial dimensions that may be significantly larger or even infinite in extent [41, 42, 43]. This is possible by relaxing the requirement that all fields propagate through the extra dimension(s) in the same way. In this illustration, the Standard Model fields are confined to 3 + 1 dimensional hypersurface, referred to as *the brane*, which is embedded within a higher-dimensional spacetime, known as *the bulk*. Then gravity is understood to propagate freely throughout the bulk, making it the only fundamental force that extends beyond the brane. This concept is motivated by the observed weakness of gravity at small scales relative to the other three fundamental forces, which renders it challenging to probe

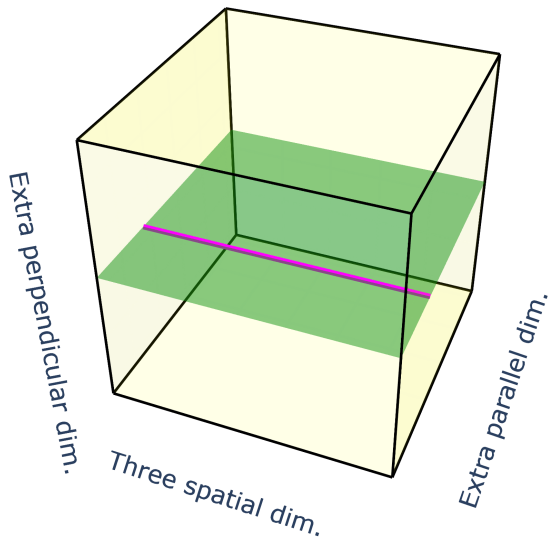

Figure 1.2: A graphical representation of a braneworld model. The magenta line denotes the three known spatial dimensions, while the green plane depicts a $3+d$ brane containing additional spatial dimensions parallel to our world. Only gravity can propagate through the entire yellow bulk, which encompasses also extra transverse dimensions.

at short distances. The brane world setup can be naturally interpreted as a configuration of fundamental objects known as D-branes embedded within a higher-dimensional target space, as described in string theory [44, 20].

In the Arkani-Hamed, Dimopoulos, and Dvali (ADD) model [45], the bulk space is assumed to be flat, whereas in the Randall–Sundrum gravity framework, the bulk is characterized as an anti-de Sitter space. The latter one was initially presented in two variants – one including two branes (RS1)[46] and the other featuring a single brane (RS2)[47] – but its definition can be generalized to encompass models with similar characteristics.

Einstein–Gauss–Bonnet Gravity

Regarding the fifth condition of Lovelock's theorem, in dimensions greater than four, the variation of the Einstein–Hilbert action does not yield Einstein's equations of GR; instead, it leads to an extension known as Einstein–Gauss–Bonnet (EGB) gravity. This alters gravitational dynamics while maintaining second-order field equations. In essence, GR is a particular case within a wider class of theories characterized by an action that includes an additional *Lovelock tensor*, which arises from variation of the Gauss–Bonnet term.

Viability

Theories of gravity in higher dimensions are theoretically well motivated by pursuits of unification and requirements of quantum consistency. However, current laboratory, astrophysical, and cosmological observations impose strong constraints on these models. Nowadays, gravity is not considered to operate as a ten-dimensional force, as required by superstring theory, for example. Emergent phenomena such as Kaluza–Klein excitations, radion fields [48], and bulk graviton modes generally lead to deviations from Newtonian gravity, fifth forces, and alterations in cosmological evolution, none of which have been observed to date. Consequently, viable extra-dimensional models are limited to narrow regions of parameter space and often depend on fine-tuning or stabilization mechanisms. While not outright excluded, these theories are presently considered as constrained effective frameworks rather than as definitive alternatives to standard four-dimensional gravity.

1.2.3 Gravity with extra curvature invariants

Relaxing the requirement that equations of motion be second-order leads us to consider the next category of theoretical models. In particular, constructing the Einstein–Hilbert action solely with the Ricci scalar represents the simplest option that satisfies all physical constraints. But additional scalar curvature invariants are permitted by general covariance, and in principle, infinitely many such terms can be included. Such a generalization may be beneficial, as it could lead to a more rapid decay of the graviton propagator in the UV regime, thereby enhancing the theory's renormalization properties [20]. Considering

any of the linear and quadratic contractions of the Riemann curvature tensor, the general scalar density appearing in generalized action can be constructed as

$$\mathcal{L} = \frac{\sqrt{-g}}{\chi} f(R, R_{\mu\nu}R^{\mu\nu}, R_{\mu\nu\rho\sigma}R^{\mu\nu\rho\sigma}) \,, \tag{1.25}$$

where f is an arbitrary function of its arguments and χ is a constant determined from the Newtonian limit.

In the weak field limit (or low energies), one can treat gravity as an effective field theory and discover that the Ricci scalar is selected not because other curvature invariants are forbidden, but because it represents the leading term in

$$\mathcal{L} = \frac{\sqrt{-g}}{\chi}(R + \alpha R^2 + \beta R_{\mu\nu}R^{\mu\nu} + \gamma R_{\mu\nu\rho\sigma}R^{\mu\nu\rho\sigma}) \,, \tag{1.26}$$

where α, β and γ are constants. The last term may be eliminated by redefining α and β without any loss of generality in solutions [20]. A systematic approach to studying higher order gravity models has been proposed in [49].

$f(R)$ theories

These toy models were brought on the stage in the context of inflation [25], but they gained significant popularity following the discovery of recent cosmic acceleration and have since become among the most extensively studied topics in the field. The so-called $f(R)$ theories, the simplest viable subclass of higher-order theories, extend the standard action by accounting for a general nonlinear function of the Ricci scalar, resulting in field equations of fourth order. The corresponding action is [50]

$$S = \frac{1}{2\kappa}\int \mathrm{d}^4x\sqrt{-g}f(R) + S_{\mathrm{m}}(g_{\mu\nu}, \psi) \tag{1.27}$$

which, after performing a variation with respect to the metric (and a mathematical jump related to surface terms), gives the field equations

$$f'(R)R_{\mu\nu} - \frac{1}{2}f(R)g_{\mu\nu} - [\nabla_\mu\nabla_\nu - g_{\mu\nu}\Box]f'(R) = \kappa T_{\mu\nu} \,, \tag{1.28}$$

where prime denotes a differentiation with respect to the argument. A useful approach to investigate properties of $f(R)$ gravity, such as stability or the weak field limit, is to consider the trace of equation (1.28),

$$f'(R)R - 2f(R) + 3\Box f'(R) = \kappa T \,, \tag{1.29}$$

where $T = g^{\mu\nu}T_{\mu\nu}$. Unlike in GR, this trace relates T and R in a differential manner, resulting in a broader set of solutions compared to Einstein's theory. Specifically, the condition $T = 0$ no longer implies $R = 0$, not even $R = \text{const}$. This is why Jebsen–Birkhoff's theorem 1.1.2 does not generally hold in metric $f(R)$ theories. For more details, see [50].

An entirely different set of field equations of the $f(R)$ theory can be obtained using *Palatini approach* instead of standard *metric variational approach* above. In the Palatini approach, the assumption of a Levi-Civita connection is relaxed, allowing the metric and connection to be treated as independent fields for the purpose of varying the action. The resulting field equations are

$$f'(\mathcal{R})\mathcal{R}_{\mu\nu} - \frac{1}{2}f(\mathcal{R})g_{\mu\nu} = \kappa T_{\mu\nu}\,, \tag{1.30}$$

$$\bar{\nabla}_\lambda(\sqrt{-g}f'(\mathcal{R})g^{\mu\nu}) = 0\,, \tag{1.31}$$

where $\mathcal{R}$ is the Ricci scalar constructed from a general connection (more discussed in the following subsection 1.2.4).

An intriguing aspect of $f(R)$ theories is that both formalisms allow for conformal transformations of the field equations into the form of the scalar-tensor theory described previously. Namely, it can be shown that the field equations of the $f(R)$ gravity in the metric formalism (1.28) are dynamically equivalent to the equations (1.16) and (1.17) with a vanishing coupling parameter, $\omega = 0$, while rewriting the field equations of Palatini formalism (1.30)(1.31) casts a scalar-tensor theory with $\omega = -3/2$ [50, 20].

A third method for investigating $f(R)$ theories of gravity is the *metric-affine approach*, where even the matter action is allowed to depend on both metric and connection (unlike on metric alone, as in the case of both aforementioned procedures). Meaning that

$$S = \frac{1}{2\kappa}\int \mathrm{d}^4x\sqrt{-g}f(\mathcal{R}) + S_{\mathrm{m}}(g_{\mu\nu}, \Gamma^{\mu}{}_{\nu\sigma}, \psi) \tag{1.32}$$

and $\mathcal{R}_{\mu\nu}$ is a function of the connection only, as in the Palatini procedure. A comprehensive analysis of various matter fields and their influence within the framework of metric-affine gravity is presented in [51]. However, in this most general case, it is not possible to formulate the $f(R)$ theory in a scalar-tensor language, as the metric-affine $f(R)$ gravity does not qualify as a metric theory (while the Palatini $f(R)$ formulation does indeed correspond to a metric theory, according to [52]).

Viability

Summarizing the viability of higher-order theories, or of $f(R)$ gravity in particular, is not an easy task, as some of the constraints identified in the literature (like background evolution or perturbations in cosmology) are not independent of the model or parametrization, and the utility of certain parametrizations may be limited. As a result, these constraints cannot be expressed straightforwardly using simple mathematical equations that are directly applicable to a general function.

That said, there are certain cases in which well-defined viability criteria can be straightforwardly established. Several kinds of short time scale instabilities must be overcome in order to represent an alternative to GR. For example, a Dolgov–Kawasaki instability [53] is sufficient to rule out many prototypes of metric $f(R)$ gravity, and is avoided if and only if $f''(R) \geq 0$. Another issue concerns the significantly inaccurate

post-Newtonian limit: in order for metric $f(R)$ theories to serve as viable alternatives to dark energy and simultaneously satisfy weak field tests, they must enforce effective screening mechanisms to suppress extraneous degrees of freedom [50]. On the other hand, proceeding with the Palatini $f(R)$ formalism introduces a multiple severe challenges, including an ill-posed Cauchy problem in the presence of most matter fields [54], a lack of predictive capability, problematic strong coupling at low energies [55] and the emergence of singularities in systems that are otherwise well-described by weak fields [56, 57].

1.2.4 Gravity with extra geometrical structures

As quoted previously, a spacetime manifold possesses a metric structure, but it also admits a separately defined affine structure, characterized by a connection. In GR, these structures are related through the Levi-Civita connection (1.4) associated with the metric, resulting in a well-known Riemannian geometry [58]. In terms of Metric Affine theories of Gravity (MAG) [59], a general connection is an independent object in four dimensions and can be split in the following way:

$$\Gamma^{\alpha}{}_{\mu\nu} = \{^{\alpha}{}_{\mu\nu}\} + L^{\alpha}{}_{\mu\nu}(Q) + K^{\alpha}{}_{\mu\nu}(T). \tag{1.33}$$

The first term is the Levi-Civita connection, second term is the *Disformation tensor*, which measures the incompatibility of the metric with the connection (*non-metricity*), and the third term is the *Contorsion tensor*, the anti-symmetric part, which encodes *torsion*. The complete definition is:

$$L^{\alpha}{}_{\mu\nu} = \frac{1}{2}Q^{\alpha}{}_{\mu\nu} - Q_{(\mu}{}^{\alpha}{}_{\nu)}\,, \tag{1.34}$$

where

$$Q_{\alpha\mu\nu} \equiv \nabla_{\alpha} g_{\mu\nu}, \tag{1.35}$$

and

$$K^{\alpha}{}_{\mu\nu} = \frac{1}{2}T^{\alpha}{}_{\mu\nu} + T_{(\mu}{}^{\alpha}{}_{\nu)}\,, \tag{1.36}$$

where

$$T^{\alpha}{}_{\mu\nu} \equiv \Gamma^{\alpha}{}_{\mu\nu} - \Gamma^{\alpha}{}_{\nu\mu}\,. \tag{1.37}$$

The $L^{\alpha}{}_{\mu\nu}$ and $K^{\alpha}{}_{\mu\nu}$ collectively quantify the deviation of the affine connection from the Riemannian Levi-Civita connection and are known as the *Distortion tensor*. This decomposition enables the separation of any object into its Riemannian component and additional non-Riemannian contributions [2]. The geometrical meaning of each structure is visualised in Figure 1.3.

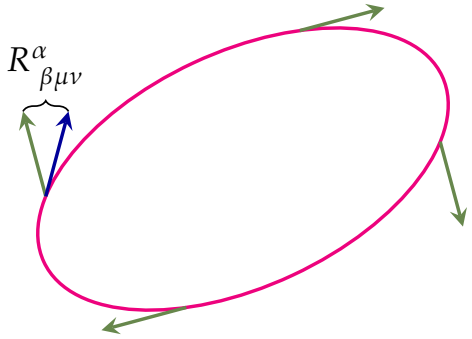

The curvature of spacetime forces a vector to undergo rotation when it is transported along a closed curve.

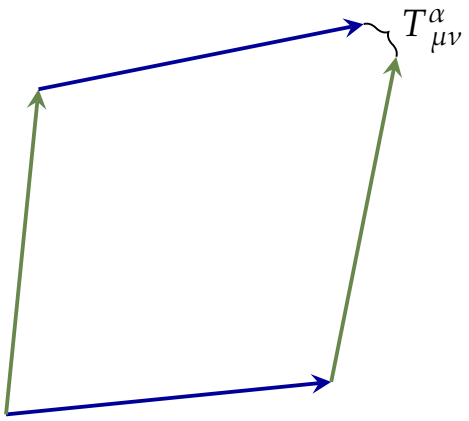

The torsion component can be represented by the failure of parallelograms, formed when two vectors are transported along each other, to close properly.

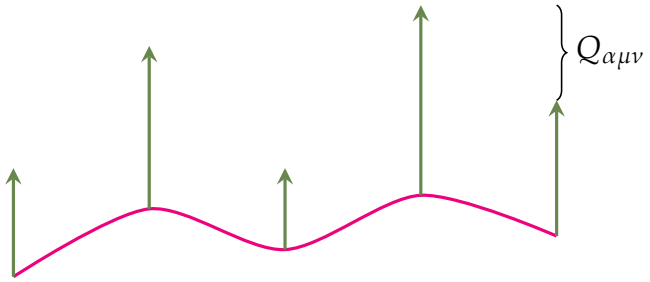

The non-metricity causes the alteration of a vector's length during its transport.

Figure 1.3: These illustrations depict the geometrical interpretation of curvature, torsion, and non-metricity in the absence of the remaining two.

The generalized connection (1.33) opens a whole new intriguing world to explore, metaphorically referred to as "Affinesia" [60]. Within this world, GR is merely one of the specifically calibrated geometrical interpretations, surrounded by many non-Riemannian neighbourhoods (see Figure 1.4).

The primary motivation for considering the torsion component stems from the fact that fermionic matter carries *intrinsic spin*, which may act as an additional source of the gravitational field alongside energy-momentum. This consideration naturally leads to an extension of GR in which spin couples to spacetime torsion. In contrast, the inclusion of non-metricity is not currently directly associated with a specific physical source, but it is instead considered as a broader generalization of the underlying geometric framework. Furthermore, from a microscopic perspective, the presence of torsion and non-metricity could be interpreted as arising from hypothetical spacetime defects, analogous to those

observed in condensed matter systems [61].

By carefully restricting the connection described in equation (1.33), one can derive the teleparallel equivalents of GR. In particular, constraining the affine connection to consist solely of torsion yields Teleparallel Gravity (TEGR)[62], while imposing non-metricity alone leads to Symmetric Teleparallel Gravity (STGR)[63]. A comprehensive overview of these three faces of GR is provided in [64]. To reproduce Einstein–Hilbert-like action in these frameworks, we need to introduce specific contractions of torsion tensor (1.37) and non-metricity tensor (1.35). That is,

$$\mathbb{T} = -\frac{1}{4}T_{\alpha\mu\nu}T^{\alpha\mu\nu} - \frac{1}{2}T_{\alpha\mu\nu}T^{\mu\alpha\nu} + T_\alpha T^\alpha \tag{1.38}$$

is a *torsion scalar* with a trace

$$T_\mu = T^\alpha{}_{\mu\alpha}\,, \tag{1.39}$$

and

$$\mathbb{Q} = \frac{1}{4}Q_{\alpha\beta\gamma}Q^{\alpha\beta\gamma} - \frac{1}{2}Q_{\alpha\beta\gamma}Q^{\beta\alpha\gamma} - \frac{1}{4}Q_\alpha Q^\alpha + \frac{1}{2}Q_\alpha \tilde{Q}^\alpha \tag{1.40}$$

defines a *non-metricity scalar* with

$$Q_\alpha = Q_{\alpha\lambda}{}^\lambda \quad \text{and} \quad \tilde{Q}_\alpha = Q^\lambda{}_{\lambda\alpha}\,. \tag{1.41}$$

The corresponding actions for teleparallel equivalents of GR can be constructed by enforcing the constraints mentioned above. More technically, the gravitational part of the pure GR action (1.9) should be properly written as

$$S_{\text{GR}} = \int \mathrm{d}^4x \left[\frac{\sqrt{-g}}{2\kappa}R + \lambda_\alpha{}^{\mu\nu}T^\alpha{}_{\mu\nu} + \hat{\lambda}^\alpha{}_{\mu\nu}Q_\alpha{}^{\mu\nu}\right], \tag{1.42}$$

where $\lambda_\alpha{}^{\mu\nu}$ and $\hat{\lambda}^\alpha{}_{\mu\nu}$ are Lagrange multiplier fields imposing constraints on the connection being symmetric and metric compatible (as stated in Section 1.1), which then results in Einstein–Hilbert term of (1.9) alone. Similarly, by casting suitable Lagrange multipliers to enforce geometry without curvature and non-metricity, one can reproduce the dynamics of GR with

$$S_{\text{TEGR}} = -\frac{1}{2\kappa}\int \mathrm{d}^4x\sqrt{-g}\,\mathbb{T}\,. \tag{1.43}$$

Although we have expressed the TEGR action using $\sqrt{-g}$, its usual formulation fundamentally relies on the use of *tetrad (or vierbein) fields*. These tetrads define a local orthonormal frame at each point in spacetime, facilitating the definition of the torsion tensor and ensuring the action is properly defined. This approach involves additional geometric structures that are beyond the scope of this discussion.

We can also recover GR behaviour constraining the geometry to be fully ascribed to non-metricity. This leads to the following action:

$$S_{\text{STGR}} = -\frac{1}{2\kappa}\int \mathrm{d}^4x\sqrt{-g}\,\mathbb{Q}\,, \tag{1.44}$$

which represents the Symmetric Teleparallel Gravity equivalent of Einstein–Hilbert action.

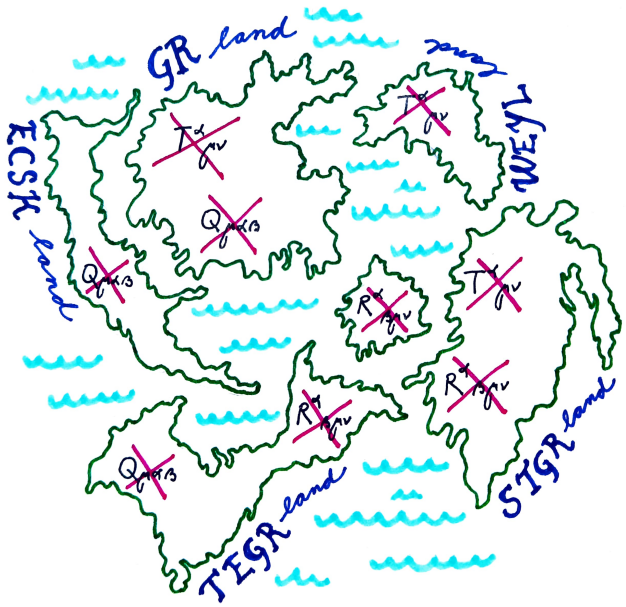

Figure 1.4: Illustration of the "Affinesia" map: a schematic representation of the space of possible geometric structures in MAG.

Einstein–Cartan theory

The concept of incorporating torsion into spacetime, alongside curvature, and establishing a relation between torsion and the density of intrinsic angular momentum was initially introduced by Élie Cartan in 1922 [65]. In the late 1950s, the theory was independently reformulated by Sciama and Kibble. Consequently, this theoretical framework is also commonly referred to as the Einstein–Cartan–Sciama–Kibble (ECSK) theory. Relaxing the assumption of GR that the affine connection (1.33) has a vanishing antisymmetric component, while retaining the assumption of metric compatibility ($Q_{\alpha\mu\nu} = 0$), yields the Lagrangian density [66]

$$\mathcal{L} = \frac{1}{2\kappa}\sqrt{-g}\left(R + \partial_\rho K_\alpha{}^{\rho\alpha} - T_\alpha{}^{\mu\nu}K_{\mu\nu}{}^{\alpha} - 2\Lambda\right) + \mathcal{L}_{\mathrm{m}}\ , \tag{1.45}$$

which is used to construct the lowest-order gravitational action that is linear in the curvature scalar and quadratic in torsion. The second term in brackets of (1.45) can be ignored, as it represents a pure divergence.

The deviation of ECSK from GR is quite slight – the influence of spin and torsion becomes significant only at matter densities that are notably high, though still substantially below the Planck density, where quantum gravitational phenomena are thought to primarily occur. For further reading on Einstein-Cartan theory, see [59, 67, 68].

Other geometries

Instead of curvature and torsion components, as utilized in Einstein–Cartan theory, one can consider a connection that includes curvature and non-metricity, which corresponds to Weyl geometry [69, 70]. Affine connections constructed solely from torsion and non-metricity, with zero curvature, are theoretically feasible. However, unlike the extensively studied Einstein–Cartan or Weyl geometries, these theories lack a definitive geometric interpretation and generally involve a surplus of independent degrees of freedom, which challenges their physical constraining.

An orthogonal approach to MAG is to change the very concept of a metric itself. Making the metric also direction dependent, one can study a generalized geometry of Finsler [71, 72]. A different development involves introducing non-commutative gravity, where spacetime coordinates do not commute. This approach fundamentally alters the manifold structure and replaces traditional differential geometry with an algebraic framework. Consequently, this methodology diverges from classical geometric interpretations and can be viewed as a quantum deformation of spacetime itself [73].

$f(\mathbb{T})$ and $f(\mathbb{Q})$ extensions

After discussing two equivalent formulations of General Relativity – TEGR and STGR – one might consider whether modifying these frameworks, or in better words, developing their extensions, could lead to a wide range of additional possibilities.

Regarding the higher-order theories for example, one could also play with functions of a torsion scalar $\mathbb{T}$ and a non-metricity scalar $\mathbb{Q}$. If one performs this dynamical change on TEGR or STGR formulations, it is not equivalent to the $f(R)$ scenario. This is due to the fact that the equivalence with GR is delicate and only valid at the level of the action linear in a corresponding geometric scalar $(R, \mathbb{T}, \mathbb{Q})$, in which case they are related through their boundary terms as

$$R = -\mathbb{T} + B_{\mathbb{T}} = -\mathbb{Q} + B_{\mathbb{Q}} \ . \tag{1.46}$$

Once the linear dependence is broken, the boundary terms will be embodied within nonlinear functions, making it impossible to eliminate them. As a result, the three formulations will no longer be different representations of the same physics and will instead become fundamentally distinct. These extensions of Teleparallel Gravity [74, 75, 76] and Symmetric Teleparallel Gravity [77, 78, 79] have garnered increasing attention over the past decade.

Viability

Among the non-Riemannian extensions of gravity, Einstein–Cartan theory offers a minimal and fully consistent extension of GR that involves the intrinsic spin of matter. It offers a solution to significant challenges in gravity and cosmology without the need to introduce exotic matter, an inflation field, or singularities [80]. The primary limitation is that its relevance is confined to densities encountered only in the early Universe or

potentially within black holes. Consequently, directly observing spin-torsion coupling remains beyond the capabilities of current experimental physics.

The original Weyl theory predicted the path-dependent behaviour of atomic clocks, specifically, it precluded the existence of sharp spectral lines in atoms [81]. To date, this has not been observed. Therefore, Weyl's geometry remains speculative, despite certain theoretical studies suggesting otherwise when the theory is interpreted correctly [82].

Teleparallel modifications based on torsion, such as $f(\mathbb{T})$ theories, face challenges related to the violation of the local Lorentz invariance. Conversely, symmetric teleparallel extensions involving non-metricity, such as $f(\mathbb{Q})$ theories, maintain covariance and exhibit significantly improved theoretical consistency. The broader category of metric-affine theories, which encompass both torsion and non-metricity, has yet to develop fully viable formulations. Additionally, although investigations primarily concentrate on astrophysical and cosmological phenomenology, certain studies addressing the theoretical consistency of teleparallel modified gravity have identified common issues such as strong coupling [83], the formulation of the Cauchy problem [84], and the presence of ghost instabilities [85, 2].

1.3 Minimally modified gravity

Regarding the viability of previously proposed mechanisms for modifying gravity through conventional approaches, there is a recurring emphasis on serious problems associated with the introduction of additional Degrees of Freedom (DoF). These can be interpreted as new propagating modes that cannot be eliminated through gauge symmetry or constraints. To elaborate on this issue, GR possesses two local physical DoF, corresponding to two polarization states of gravitational waves. A novel line of investigation initiated in 2017 questions whether GR is unique in this property or if there exist modifications to GR that preserve the same number of DoF. We will refer to these types of modification theories as Minimally Modified Gravity (MMG).

The process of determining the DoF is best understood through the Hamiltonian formalism of GR, which is implemented using the Arnowitt–Deser–Misner (ADM) formalism first introduced in 1962 [86]. We need to decompose a spacetime metric in (1.1) as [87]

$$\mathrm{d}s^2 = -N^2\,\mathrm{d}t^2 + h_{ij}(\,\mathrm{d}x^i + N^i\,\mathrm{d}t)(\,\mathrm{d}x^j + N^j\,\mathrm{d}t)\,, \tag{1.47}$$

where h_{ij} is a 3-dimensional spatial metric, N is a scalar function called a *lapse* and N^i is a three-vector called a *shift*. This is needed because Hamiltonian mechanics relies on configuration variables $q(t)$ and canonical momenta $p(t)$, which necessitate a concept of time evolution t, while GR itself does not presume a preferred time. Using ADM variables, we introduce a *time direction* and track evolution between two spatial hypersurfaces. The number of independent components remains the same as in $g_{\mu\nu}$ – ten in total.

The Einstein–Hilbert action can be rewritten as

$$S = \int \mathrm{d}t\,\mathrm{d}^3x\sqrt{h}N(K_{ij}K^{ij} - K^2 + R^{(3)})\,, \tag{1.48}$$

where

$$K_{ij} = (\partial_t h_{ij} - \nabla_i N_j - \nabla_j N_i) \tag{1.49}$$

is the extrinsic curvature, h is the determinant of h_{ij} and $R^{(3)}$ denotes the Ricci scalar in three dimensions. To exhibit time evolution, a variable must appear with a time derivative in the Lagrangian, which is only met by h_{ij}, whereas N and N^i are nondynamical. To clarify further, the canonical momenta given by

$$\pi^{ij} = \frac{\partial L}{\partial \dot{h}_{ij}} \tag{1.50}$$

are nonzero, while

$$\pi_N = \frac{\partial L}{\partial \dot{N}} \approx 0 \quad \text{and} \quad \pi_i = \frac{\partial L}{\partial \dot{N}^i} \approx 0 \tag{1.51}$$

are constraint equations, thus we obtain four primary constraints. The symbol $\approx$ is used to indicate that these relations hold only in the subspace defined by the constraints, i.e. on-shell. These relations must be preserved in time, meaning that

$$\frac{\mathrm{d}\pi_N}{\mathrm{d}t} \approx 0 \quad \text{and} \quad \frac{\mathrm{d}\pi_i}{\mathrm{d}t} \approx 0 \tag{1.52}$$

bring next four secondary constraints. In summary, ten independent components are, in case of General Relativity, reduced to two physical DoF due to diffeomorphism invariance, which generates eight first-class constraints (four primary + four secondary) that eliminate eight phase-space dimensions, leaving only the two transverse-traceless modes of the spatial metric.

Via canonical transformation, MMG seeks modifications that maintain the first-class character of the ADM constraints, ensuring that exactly two physical DoF are preserved. If one restricts to theories that have actions linear in the lapse function, (1.48) can be generalized as

$$S = \int \mathrm{d}t\, \mathrm{d}^3x \sqrt{h} N F(K_{ij}, R_{ij}, \nabla_i, h^{ij}, t)\,, \tag{1.53}$$

where F is a spatial scalar function, that must satisfy self-consistency condition found in [87]. It is subsequently established that there are two distinct categories of such theories.

1.3.1 Type-I

Within the first kind of minimal modification, there exists a field redefinition (or a canonical transformation of variables) that restores the theory to the form of GR. Shortly, an *Einstein frame* can be identified – the theory is reformulated as GR with a nontrivial way of coupling to matter, which also implies that in case of vacuum solutions, these theories are actually equivalent to GR [4, 88]. We can also state that matter couples minimally to the metric in the *Jordan frame* instead.

1.3.2 Type-II

A slightly different procedure is employed in the second type of MMG. After performing a canonical transformation of GR, one adds a cosmological constant to the game. Instead of adding matter fields in this transformed frame, one transforms the theory back to the original frame, which no longer corresponds to GR [89]. Matter fields can subsequently be incorporated. As one might expect, due to this modification, it is no longer possible to recast the theory as GR through any change of variables. This results in genuinely new dynamics, with or without matter fields, while still preserving exactly two DoF. Thus, an Einstein frame does not exist in this context. The previously mentioned theory of massive gravity can be represented using this formalism. Another example of type-II MMG is *Cuscuton* theory [90], which can be considered as the incompressible limit of a scalar field theory.

1.4 Cosmological context

So far, we have attempted to summarize the most recognized efforts to modify gravitational physics to date. The real adventure begins when we explore what these theories can reveal to us in regimes where GR alone has little to say. Any such insights must ultimately be confronted with and verified by relevant observations. Since this work focuses on the cosmological analysis of a specific modified gravity scenario, it is necessary to incorporate cosmological concepts at a certain point. In this section, we will briefly review the current leading description of cosmic evolution and then present the corresponding evolution equations in some alternative scenarios.

Even though cosmology initially emerged as a discipline concerning the large scales and global evolution of spacetime, it is now also increasingly regarded as a laboratory for high energy physics. From the 1970s, with the development of particle physics and QFT, the early Universe turned out to be a unique and powerful tool for probing fundamental interactions at energies far exceeding those achievable through terrestrial experiments. With phenomena such as inflation, phase transitions and symmetry breaking, baryogenesis and relic particle abundances, it provides a window into physics at extreme regimes. In modern cosmology, these two perspectives are inherently interconnected: the evolution of spacetime and the behaviour of fundamental fields are often analysed jointly, with observational data informing both gravitational dynamics and microscopic physics.

The cosmological arena is clearly one of the places where new theories would manifest themselves. Nevertheless, we shall also note that cosmological solutions can hardly stand on their own. They are often degenerate, since different gravitational theories can lead to identical cosmological evolutions. To distinguish between theories, it is necessary to examine strong-field regimes and less symmetric systems, typically encountered in astrophysical contexts, like binary pulsars, black hole mergers and gravitational lensing.

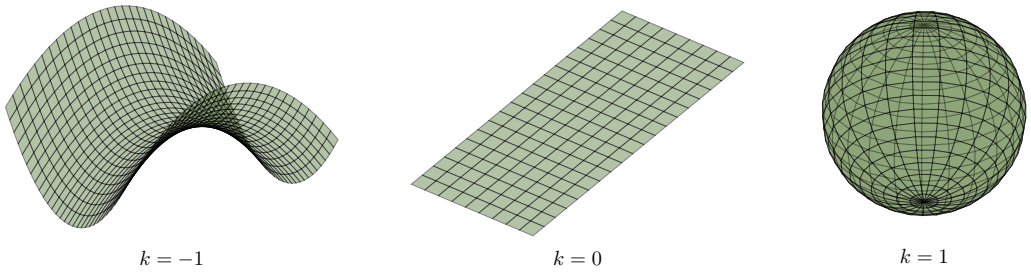

Figure 1.5: Schematic representations of spatial geometries with constant intrinsic curvature within the FLRW metric, visualized as two-dimensional surfaces embedded in three-dimensional space.

1.4.1 Standard GR cosmology

The cosmological perspective effectively smooths out the small-scale structures in the Universe. Postulating that the Universe is *homogeneous* and *isotropic* at sufficiently large scales may seem somewhat audacious, but it is the only approach that allows us to describe the entire Universe with a concise set of equations. This working assumption is known as the *cosmological principle*, and it is a core building block of our Standard cosmological model. As a result of this principle, the Universe exhibits maximal spatial symmetry, such that hypersurfaces at constant time have uniform curvature. This is mathematically encoded in the *Friedmann–Lemaître–Robertson–Walker* (FLRW) metric describing the line element in pseudospherical coordinates $x^\mu = (t, r, \theta, \phi)$ as

$$\mathrm{d}s^2 = g_{\mu\nu}\,\mathrm{d}x^\mu\,\mathrm{d}x^\nu = -\,\mathrm{d}t^2 + a(t)^2\left(\frac{\mathrm{d}r^2}{1-kr^2} + r^2\,\mathrm{d}\theta^2 + r^2\sin^2\theta\,\mathrm{d}\phi^2\right), \tag{1.54}$$

where $k = -1, 0, 1$ represents the spatial curvature of an open, flat or closed universe, respectively, and $a(t)$ is a positive function of the time coordinate called the *scale factor*. The scale factor is the sole independent geometric parameter that characterizes the evolution of a homogeneous and isotropic spacetime. Importantly, the FLRW metric is determined by symmetry considerations *alone* and does not depend on the particular theory of gravity employed. Also, these symmetry considerations give rise to a preferred way of slicing spacetime into spatial hypersurfaces, effectively establishing a notion of *cosmic time*. Without this, it would be impossible to define the Universe's history, as global time parameter cannot be universally specified in GR. This process of slicing is known as *foliation* and is closely related to the ADM decomposition (1.47). In this context, the scale factor $a(t)$ describes the expansion or contraction of three-dimensional hypersurfaces over cosmic time.

To obtain the cosmological equations, we insert a FLRW metric into the left-hand side of the EFE (1.10). The imposed symmetries restrict the most general energy-momentum

tensor on the right-hand side of (1.10) to be that of a *perfect fluid*,

$$T_{\mu\nu} = p g_{\mu\nu} + (\rho + p) u_\mu u_\nu \,. \tag{1.55}$$

Any other choice would not be compatible with FLRW universe. Thereby, the matter content is characterized solely in terms of its rest-frame mass density, $\rho(t)$, and isotropic pressure $p(t)$. No shear stresses, viscosity, or heat conduction are present. The vector $u^\mu = (-1, 0, 0, 0)$ denotes the four-velocity of an observer comoving with the fluid. Additionally, the energy density and pressure of barotropic perfect fluid are connected through an *Equation of State* (EoS),

$$p = w\rho \,, \tag{1.56}$$

and w is known as the EoS parameter taking the value $w = 0$ for a non-relativistic (dust-like) fluid or $w = 1/3$ for a relativistic (radiation-like) fluid. Values of w outside the $[0, 1]$ range are generally not consistent with established macroscopic physics; however, for instance, an unconventional value $w = -1$ is employed when modelling a cosmological constant to align with astronomical observations.

Given the FLRW metric (1.54) and the perfect fluid ansatz (1.55), the *Friedmann equation*,

$$H^2 = \frac{\kappa}{3}\rho + \frac{\Lambda}{3} - \frac{k}{a^2} \,, \tag{1.57}$$

arises as the time-time component of the EFE, while the *acceleration equation*,

$$2\dot{H} + 3H^2 = -\kappa p + \Lambda - \frac{k}{a^2} \,, \tag{1.58}$$

follows from the spatial components of the EFE. We have defined the *Hubble parameter* as

$$H = \frac{\dot{a}}{a} \tag{1.59}$$

with an over-dot indicating the derivative with respect to t. From equations (1.57) and (1.58), we obtain one more piece of information,

$$\dot{\rho} + 3H(\rho + p) = 0 \,, \tag{1.60}$$

and that is known as the *energy conservation equation*. Although, an equivalent expression can be obtained more straightforwardly by applying the Bianchi identity (1.12). This implies that one of the three listed differential equations is secretly redundant, implying that the complete description of the cosmological dynamics requires only two independent equations. Once the EoS relating ρ and p is specified through (1.56), (1.60) can be solved for $\rho(a)$, resulting in

$$\rho \propto a^{-3(w+1)} \,. \tag{1.61}$$

Substituting this into (1.57) then provides the general expression for the evolution of the scale factor. For illustration, in the case of a flat universe ($k = 0$), if matter dominates, it evolves as a power-law function of time:

$$a(t) \propto t^{\frac{2}{3(w+1)}} \,, \tag{1.62}$$

whereas, if the cosmological constant dominates, the solution takes an exponential form:

$$a(t) \propto e^{Ht} \quad \text{with} \quad H = \sqrt{\frac{\Lambda}{3}}\,. \tag{1.63}$$

This exponential growth characterizes the so-called *de Sitter universe*.

While two equations are sufficient to determine $a(t)$, the acceleration equation, although not independent, remains physically significant, as it directly specifies the sign and magnitude of $\ddot{a}$, indicating whether the expansion or contraction is accelerating or decelerating. This is most easily provided by the combined form obtained after substituting (1.57) into (1.58), yielding

$$\frac{\ddot{a}}{a} = -\frac{\kappa}{6}(\rho + 3p)\,. \tag{1.64}$$

It is also important to highlight that this brief analysis considers only a single perfect fluid with a constant EoS parameter w. The situation could become significantly more complex if multiple fluids are involved, as energy and momentum conservation for an individual fluid component may not hold due to potential interactions with other fluid components. For a more thorough understanding of the various solutions and the overall cosmological challenges in greater detail, we refer the reader to [14, 91, 92].

1.4.2 Selected cosmologies beyond GR

The appropriate time has now come to demonstrate how various gravitational paradigms modify the structure of the classical FLRW differential equations (1.57)–(1.58) just presented. In this way, we will get closer to the heart of this thesis. Rather than pursuing an exhaustive survey, we focus on three prototype theories chosen from the MG review above to illustrate how different mechanisms propagate to cosmological field equations. These will also serve as testers for the methodology outlined in the following chapter.

Brans–Dicke cosmology

We mentioned that the Brans–Dicke theory is derived from the general scalar-tensor theory (1.15) in the limit of $\omega \to$ const. and $V \to 0$. However, in subsequent generalizations of this theory, the latter can be included. This minor adjustment brings an extended action [93],

$$S_{\text{BD}} = \int \mathrm{d}^4x\sqrt{-g}\left[\frac{\phi}{2}R - \frac{\omega_{\text{BD}}}{2\phi}(\partial\phi)^2 - V(\phi) + \kappa\mathcal{L}_{\text{m}}\right], \tag{1.65}$$

where, since ϕ is a scalar field, its covariant derivative reduces to an ordinary partial derivative, and a constant Brans–Dicke parameter ω_{BD} is introduced. It has been demonstrated through Solar System experiments that this parameter is strongly bounded with $\omega_{\text{BD}} \gtrsim 10^4$ [94].

Following the standard procedure, the cosmological equations derived from (1.65) instead of (1.9) are

$$3\phi H^2 + 3H\dot{\phi} - \frac{\omega_{\text{BD}}}{2}\frac{\dot{\phi}^2}{\phi} - V = \kappa\rho\,, \tag{1.66}$$

$$2\phi\dot{H} - H\dot{\phi} + \omega_{\text{BD}}\frac{\dot{\phi}^2}{\phi} + \ddot{\phi} = -\kappa(1+w)\rho\,, \tag{1.67}$$

$$\ddot{\phi} + 3H\dot{\phi} - \frac{2}{3+2\omega_{\text{BD}}}\left(2V - \phi\frac{\partial V}{\partial\phi}\right) = \frac{\kappa(1-3w)}{3+2\omega_{\text{BD}}}\rho\,, \tag{1.68}$$

where we have assumed spatially flat FLRW geometry ($k = 0$), for simplicity, and used the over-dot for the derivative with respect to cosmic time t. Furthermore, the conservation law for the matter fluid – as expressed in (1.60) – standardly holds. This again leads to the redundancy of one of the four equations. When comparing the set (1.66)–(1.68) to (1.57) and (1.58), it is evident that an additional equation has emerged. It corresponds to an extra DoF – the scalar field ϕ – which encodes a spacetime-dependent effective Newton's gravitational constant, i. e. how the strength of the gravitational interaction changes in time and space.

$f(R)$ cosmology

As indicated in the Section 1.2.3, cosmology has played a significant role in motivating the recent increased interest in $f(R)$ gravity as a means of explaining the observed cosmic acceleration without invoking dark energy. Recall the related action

$$S_{f(R)} = \int \mathrm{d}^4x\sqrt{-g}[f(R) + 2\kappa\mathcal{L}_{\text{m}}]\,, \tag{1.69}$$

where $f(R)$ stands for arbitrary action of a Ricci scalar. Varying (1.69) with respect to the metric tensor and assuming FLRW geometry (1.54) yield equations

$$H^2 + \frac{k}{a^2} = \frac{1}{3F}\left[\frac{1}{2}(FR - f) - 3H\dot{F} + 2\kappa\rho\right], \tag{1.70}$$

$$2\dot{H} + H^2 + \frac{k}{a^2} = -\frac{1}{F}\left[\frac{1}{2}(FR - f) + \ddot{F} - 3H\dot{F} + 2\kappa p\right], \tag{1.71}$$

where we defined

$$F = \frac{\partial f}{\partial R}\,, \tag{1.72}$$

according to [93], and

$$R = 6\left(\dot{H} + 2H^2 + \frac{k}{a^2}\right) \tag{1.73}$$

is a Ricci scalar evaluated on FLRW spacetime. The system appears to be less complex than the previous Brans–Dicke formulation, as once the Bianchi identities for $T_{\mu\nu}$ are imposed, the second equation can be derived by differentiating the first with respect to cosmic time. But note that the Ricci scalar R becomes a dynamical variable and can be viewed as an effective additional scalar field. Also, we have remained silent so far about the fact that a specific function $f(R)$ has to be chosen to provide equations with any meaning. We will soon see that analysing such systems can be challenging due to the increased number of variables involved.

The geometrical nature of dark energy can be viewed through interpretation of the system above as GR combined with effective fluids. Notice, for example, that by incorporating the geometric terms of (1.70) into

$$\rho_{\text{eff}} = \frac{R}{2} - \frac{f}{F} - 3H\frac{\dot{F}}{F}\,, \tag{1.74}$$

the cosmological constant – traditionally regarded as an external energy source – is effectively replaced by the influence of spacetime curvature. However, this is a useful demonstration for a vacuum case exclusively,

$$H^2 + \frac{k}{a^2} = \frac{\rho_{\text{eff}}}{3}\,, \tag{1.75}$$

as the matter would enter equations with modified coupling [50].

The procedure of reformulating modified gravitational field equations into an Einstein-like form by transferring non-Einsteinian geometric contributions to the matter sector, as demonstrated with equations (1.74) and (1.75), is known as the *Ellis trick*, named after the South African cosmologist George F. R. Ellis. This technique enables us to interpret the additional contributions as components of an effective energy-momentum tensor and it is commonly used in cosmological contexts.

Einstein–Cartan cosmology

We will close this selection and chapter with a cosmological dynamics in realms of the theory that enriches GR by encompassing torsion effects. In contrast to the two previous candidates proposed to explain the accelerated expansion of the late-time Universe, Einstein–Cartan theory may offer an alternative to inflation, as its deviations from GR become significant only at very high densities, potentially encountered in the early Universe, as previously discussed.

Although torsion is incorporated into the spacetime geometry, its field equation is purely algebraic, allowing torsion to be expressed in terms of the *matter spin density*. Consequently, its effects manifest themselves as effective modifications to the energy–momentum tensor rather than as independent geometric DoF. In other words, torsion does not exist independently of matter, it interacts with the intrinsic spin of microscopic fermions. Building on that, a cosmological description necessitates a coarse-graining over these microscopic DoF. Assuming an unpolarized and isotropic spin

distribution, the average linear spin density vanishes, while quadratic spin contributions remain and produce an effective correction proportional to the squared fermion number density. For clarity and conciseness, we present only the resulting field equations and their physical interpretations; the extensive derivations are available in the articles [95, 96]. Following the convention established therein, they can be expressed as follows:

$$G^{\mu\nu} = \kappa\theta^{\mu\nu} \tag{1.76}$$

with

$$\theta^{\mu\nu} = \langle T^{\mu\nu}\rangle + \langle \tau^{\mu\nu}\rangle = (\rho + p - \frac{\kappa}{2}\sigma^2)u^\mu u^\nu - (p - \frac{\kappa}{4}\sigma^2)g^{\mu\nu} \tag{1.77}$$

describing the effective gravitational sources in the macroscoping limit. Here, σ^2 represents the *spin density scalar*. By substituting the FLRW metric into the modified field equations (1.76), we derive the altered cosmological equations corresponding to its (00) and (ii) components again:

$$H^2 + \frac{k}{a^2} = \frac{\kappa}{3}\left(\rho - \frac{\kappa}{4}\sigma^2\right), \tag{1.78}$$

$$2\dot{H} + 3H^2 + \frac{k}{a^2} = -\kappa\left(p - \frac{\kappa}{4}\sigma^2\right). \tag{1.79}$$

Reformulating the modified acceleration equation into the form of (1.64) gives

$$\frac{\ddot{a}}{a} = -\frac{\kappa}{6}(\rho + 3p - \kappa\sigma^2) \tag{1.80}$$

and one can immediately observe that accelerated expansion ($\ddot{a} > 0$) can occur even in the presence of positive pressure, provided that the condition

$$\kappa\sigma^2 > \rho + 3p \tag{1.81}$$

is met. Introducing the abbreviated notation for the spin density expression (as in [97])

$$\rho_s = \frac{\kappa\sigma^2}{4} \tag{1.82}$$

enables the formulation of an additional continuity equation

$$\dot{\rho}_s + 6H\rho_s = 0\,. \tag{1.83}$$

It should be emphasized at this point that this description is not an Ellis trick, even though it may resemble one. In Einstein–Cartan theory, the contribution associated with matter spin arises from eliminating an auxiliary field via its algebraic field equation, reflecting the absence of independent torsional DoF. By contrast, in $f(R)$ gravity previously encountered the effective stress–energy resulted from a rearrangement of dynamical geometric terms and therefore reflects an interpretational choice rather than a dynamical necessity.

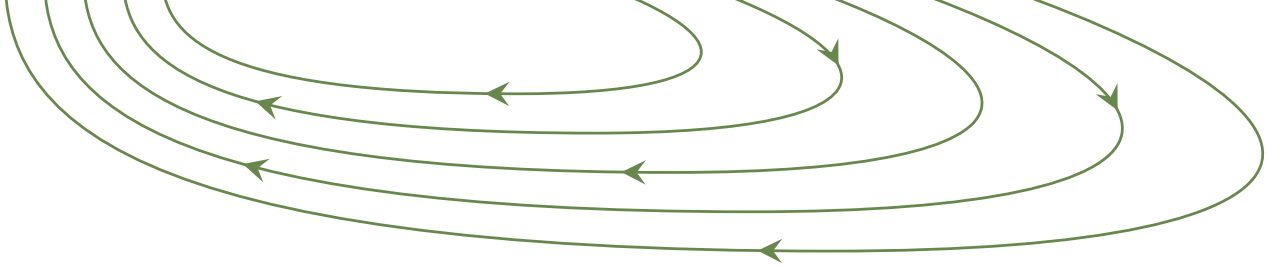

2

Dynamical systems approach

Everything changes but change.

— Israel Zangwill

The theory of dynamical systems serves as a "sonic screwdriver" in the study of various disciplines. Specifically, it offers a mathematical unifying framework to investigate time evolution in classical mechanics systems, electronics, (bio)chemistry, population dynamics, epidemiology, physiology, neuroscience, hydrodynamics, economics, and more, facilitating the extraction of fundamental structural insights.

Rather than seeking exact solutions to *ordinary differential equations* (ODEs), Poincaré in the late 1800s proposed a *geometrical* method for their analysis, initially applied in the context of celestial dynamics. He addressed longstanding challenges faced by Newton and subsequent generations of mathematicians and physicists in extending analytical methods to resolve the *three-body problem*.

Once a person enters a region of *nonlinear* ODEs, obtaining explicit analytical solutions becomes increasingly difficult and often impossible. This complexity arises because nonlinear interactions connect variables in ways that invalidate the applicability of the *superposition principle*, which typically allows us to decompose a linear problem into smaller, manageable parts that can be solved individually and then recombined. Linear systems are simply the sum of their individual components, but most real-world phenomena do not behave in this manner – their parts interact with one another in peculiar ways.

Motivated by these challenges, a broad spectrum of physical systems has been studied through the language of phase space and qualitative dynamics. Nonlinear oscillators have played a significant role in the development, as despite their relatively simple mathematical structures, they demonstrate complex behaviour, such as self-excited oscillations, bifurcations, limit cycles, and, in certain regimes, *chaotic dynamics*. Prominent models include the van der Pol oscillator of the 1920s [98], the Duffing oscillator [99], or later electronic circuits like the Chua system in the 1980s [100]. When interactions among multiple oscillatory units are introduced, additional collective phenomena emerge,

most notably *synchronization*, which can be modelled using approaches of Kuramoto. The notion that deterministic dynamical systems can produce irregular and seemingly random behaviour was substantially advanced by Edward Lorenz's work in the 1960s [101]. His simplified model of atmospheric convection unveiled the well-known chaotic attractor, illustrating the concept of chaos in deterministic systems.

It should be stressed that there exist two main types of dynamical systems: already mentioned *differential equations*, which treat time as *continuous*, but also *difference equations*, where time is *discrete*. The latter are also termed *iterated maps*, and while they are applicable in various scientific contexts as models of natural phenomena, such as period-doubling cascades, and uncover simple pathways to chaos, as the solutions "hop" along their orbits, they will not be discussed here further. We will confine our attention exclusively on continuous-time systems as they can directly correspond to cosmological ODEs.

Through this chapter, we will follow the introductions of standard textbooks on the topic of nonlinear dynamical systems, such as [102, 103, 104, 105], along with relevant interactive publications [106, 107], to provide a succinct overview of the methodology. Afterwards, we will connect this technique to the field of cosmology, referencing detailed studies, such as [108, 109, 110]. To properly introduce the renowned technique, the following pages will include a substantial amount of mathematical formalism, but relevant connections to physics will be drawn whenever applicable.

2.1 Language of ODEs

The rigorous content of this chapter should be preceded by addressing a key nuance: in a practical sense, a dynamical system *is* what the dynamical system *does*; in principle, the dynamics can be inferred through empirical observation alone. The mathematics just serves to capture, in a very concise and predictive way, the essence of what is already present in the *physical* behaviour.

A dynamical system can thus be understood as an abstract system composed of *a space* and *a mathematical rule* that describes the evolution of elements (or *states*) within that space. Rather than concentrating on the detailed analytical properties of differential equations, which form the basis of the dynamical systems theory, we will initially take a more abstract approach by describing the evolution through a flow mapping that associates each initial state with its subsequent development. This perspective highlights the geometric structure of the phase space and the qualitative characteristics of trajectories, which are essential to the analysis of dynamical behaviour.

Definition 2.1.1 *By a **dynamical system** we understand a triplet $\{T, \mathbf{X}, \phi^t\}$, where T is a numerical set, identified with time, $\mathbf{X}$ is a metric space called **phase space**, and ϕ^t is a parametric system of evolutionary operators with parameter $t \in T$ defined as a mapping $\phi^t : \mathbf{X} \to \mathbf{X}$ that takes some initial state $\mathbf{x}_i \in \mathbf{X}$ and maps it to some other state $\mathbf{x}_t = \phi^t \mathbf{x}_i \in \mathbf{X}$.*

As noted previously, we are going to deal exclusively with continuous systems, where the time set $T = \mathbb{R}$ and the state space $\mathbf{X} \subseteq \mathbb{R}^n$. It can be stated that $\mathbf{X}$, often also dubbed *phase portrait*, contains the entire dynamical "repertoire" of the system.

Definition 2.1.2 *By a **deterministic dynamical system** we understand a dynamical system* $\{T, \mathbf{X}, \phi^t\}$ *with a property* $\phi^0 = \mathbf{id}$*, where* $\mathbf{id}$ *is an identity on* $\mathbf{X}$*.*

The above definition simply excludes random phenomena by disallowing spontaneous changes in the state of dynamical systems. Additionally, when the evolution is governed solely by the previous state and does not depend on the passage of time itself, the system is classified as *autonomous* deterministic dynamical system. This indicates that if the state described by the n dynamical variables evolves according to the system of n ODEs

$$\dot{\mathbf{x}} = \frac{\mathrm{d}\mathbf{x}}{\mathrm{d}t} = \mathbf{f}(\mathbf{x}) \,, \tag{2.1}$$

the vector field $\mathbf{f}$, composed of functions $f_1(\mathbf{x}), \ldots, f_n(\mathbf{x})$ in $\mathbb{R}^n$, does not depend explicitly on time, only implicitly through the state variables, which means that $\mathbf{f}(\mathbf{x}(t))$. This reflects a physical property known as *time-translation symmetry*, implying that the evolution laws remain invariant over time. Fortunately, if one deals with a finite-dimensional *non-autonomous* system, it is possible to recast it as an autonomous one at the cost of enlarging the phase space – instead of treating time as an external parameter, it is promoted to a dynamical variable that flows uniformly to preserve the original parametrization. This construction is closely related to the standard reduction of higher-order ODEs. As a reminder, one could consider a generalized ODE of order n, but this can be equivalently transformed into a system of n first-order equations by introducing new variables to represent the successive derivatives of the original variable. This reformulation naturally defines an n-dimensional phase space in which the dynamics is represented as a vector field whose integral curves correspond to the solutions of the original equation.

Definition 2.1.3 *A **trajectory** or **orbit** with initial condition* $\mathbf{x}_\mathrm{i} \in \mathbf{X}$ *is an ordered subset of phase space* $\mathbf{X} : \{\mathbf{x} \in \mathbf{X} : \mathbf{x} = \phi^t \mathbf{x}_\mathrm{i}, \forall t \in T \text{ for which } \phi^t \mathbf{x}_\mathrm{i} \text{ is defined}\}$*. By **phase portrait** of the dynamical system we understand the distribution of trajectories in the phase space* $\mathbf{X}$*.*

To avoid ambiguity between a point in phase space $\mathbf{x} \in \mathbf{X}$ and a time-dependent $\mathbf{x}(t)$, a particular solution to (2.1) is often denoted by $\psi(t)$ to emphasize that it represents a phase space trajectory. At each point $\mathbf{x}$, the vector field $\mathbf{f}(\mathbf{x})$ controls the instantaneous direction of motion; consequently, it is tangent to the orbit $\psi(t)$ and can be interpreted as the velocity of the moving point within the phase space. It is important to clarify that this concept *does not* pertain to the velocity of a physical particle or the physical system under examination.

In the abstract setting regarded above in Definitions 2.1.1 and 2.1.2, the flow ϕ^t is already assumed to exist and defines the evolution uniquely. When the evolution is generated by an autonomous ODE system of the form of (2.1), the existence of such a flow is guaranteed under regularity conditions on the vector field $\mathbf{f}(\mathbf{x})$, such as *Lipschitz*

continuity. This ensures that each initial condition $\mathbf{x}_i$ produces a unique trajectory $\psi(t)$, so that the flow ϕ^t can be identified with the solution of the corresponding initial value problem. For detailed technical discussion, see the *Existence and Uniqueness* theorem in [111]. Physically, this reflects *causality*: the state of the system at one instant fully determines its future evolution.

However, the existence-uniqueness is a local result, as it is established over a maximal interval of time. Since we are interested in long-term behaviour, we aim for solutions that can be extended for all $t \in \mathbb{R}$, provided they remain within the domain where the vector field $\mathbf{f}(\mathbf{x})$ is defined. This extension is obtained via *Maximality* and *Extendibility* theorems, which can be further studied in [108]. Technically, it is also possible for solutions of the ODE to be extendable only as $t \to \infty$ and not as $t \to -\infty$, or vice versa. In such scenarios, one can define a *positive semi-flow* ϕ_+^t (or, similarly, a *negative semi-flow* ϕ_-^t).

2.1.1 Fixed points and stability

Throughout the history of physics, it has been widely acknowledged that systems tend to evolve toward *equilibrium* states, a behaviour commonly linked to the thermodynamical principle of *entropy maximization*. That said, a comprehensive discussion of these concepts would involve subtle and ongoing debates regarding the fundamental origins of *irreversibility* of time. For the purposes of dynamical systems analysis, such considerations are not necessary; the reason why physicists (and mathematicians) are obsessed with fixed points is their structural importance. They dictate the long-term behaviour of solutions and organize the overall dynamics. In the simplest words: an equilibrium point $\mathbf{x}_0$ corresponds to the steady state of a physical system, and since this state remains constant over time, the velocity of the point $\mathbf{x}_0$ in the state space is zero.

Definition 2.1.4 *A point $\mathbf{x}_0 \in \mathbf{X}$ is called an **equilibrium point** (also a **stationary**, **singular**, **critical** or **fixed point**) of the dynamical system if $\phi^t \mathbf{x}_0 = \mathbf{x}_0$ holds for all $t \in \mathbb{R}$. Equivalently, equilibrium points of the autonomous dynamical system (2.1) satisfy $\mathbf{f}(\mathbf{x}_0) = 0$.*

It is worth highlighting two special types of trajectories – narrow, finely tuned channels (which effectively have measure zero in phase space) – along which the flow is precisely aligned with the stable and unstable directions of specific fixed points.

Definition 2.1.5 *An orbit connecting different equilibrium points is named a **heteroclinic orbit**. An orbit that connects an equilibrium point to itself is known as a **homoclinic orbit**.*

From a physical standpoint, fixed points are meaningful only insofar as they are stable, since equilibria that cannot withstand arbitrarily small perturbations are unlikely to be observed in nature. Hence, the next pertinent question is whether the system can achieve such a steady state and, if so, whether small deviations from it tend to diminish, amplify, or remain persistent over time. Resolving this question involves analysing the local behaviour of trajectories near the critical point.

Definition 2.1.6 *An equilibrium point $\mathbf{x}_0$ is called **stable** if it satisfies:*

- *Lyapunov stability: for every arbitrarily small neighbourhood ε of the point $\mathbf{x}_0$ there exists a neighbourhood δ of the point $\mathbf{x}_0$ such that $\forall \mathbf{x} \in \delta$ and $\forall t > 0$ holds $\phi^t \mathbf{x} \in \varepsilon$.*
- *Asymptotic stability: there exists a neighbourhood δ_0 of the equilibrium point $\mathbf{x}_0$ such that $\phi^t \mathbf{x} \to \mathbf{x}_0$ for $\mathbf{x} \in \delta_0$ as $t \to \infty$.*

*A stable equilibrium is often referred to as **attractor** and a maximal δ_0 of $\mathbf{x}_0$ is called a **basin of attraction**.*

Similarly, these definitions can be expressed in the language of trajectories: if some solution of (2.1) at time t_0 satisfies $\|\psi(t_0) - \mathbf{x}_0\| < \delta$ and then for all $t \geq t_0$ the solution $\psi(t)$ exists and satisfies $\|\psi(t) - \mathbf{x}_0\| < \varepsilon$, the fixed point $\mathbf{x}_0$ is considered Lyapunov stable. If there also exists a number δ_0 such that $\|\psi(t_0) - \mathbf{x}_0\| < \delta_0$ and $\lim_{t\to\infty} \psi(t) = \mathbf{x}_0$, then $\mathbf{x}_0$ is asymptotically stable. The key nuance between these two types of stability is that, in the case of an asymptotically stable critical point, all trajectories in its vicinity will eventually *converge* to it. In contrast, trajectories near a Lyapunov stable point may *oscillate* around it without approaching it directly.

What if there are no fixed points to analyse? Is such a system still worthy of our attention? Indeed, systems exist in which the vector field does not vanish at any point, indicating that the system is never at a state of rest locally. In such situations, trajectories cannot terminate or settle into equilibrium states; instead, the long-term behaviour is driven by other global structures such as periodic orbits (limit cycles) or more complex invariant sets.

2.1.2 Invariant sets

Important characters of the qualitative analysis of dynamical systems are invariant sets, as they represent subsets of the phase space that are *preserved* under the system's evolution. If a trajectory $\psi(t)$ originates within such a set, it remains within it for all future (and, when defined, past) times.

Definition 2.1.7 *A set $\mathbf{S} \subset \mathbf{X}$ is an **invariant set** of the flow ϕ^t on $\mathbf{X}$ if for every $\mathbf{x} \in \mathbf{S}$ and $\forall t \in T$, we have $\phi^t \mathbf{x} \in \mathbf{S}$.*

The simplest species that possess this property are the fixed points (Def. 2.1.4), for which $\phi^t \mathbf{x}_0 = \mathbf{x}_0$ for eternity. More interesting invariant sets may consist of entire trajectories or collections of trajectories. For instance, an invariant set may be a *curve* in phase space, such as a periodic orbit, heteroclinic orbit or a *line of fixed points*. In higher-dimensional systems, they can also take form of *surfaces* or even higher-dimensional *submanifolds* embedded in the phase space.

Invariant submanifolds typically occur when the vector fields $\mathbf{f}(\mathbf{x})$ are tangent to a lower-dimensional subset of the phase space. In practice, this situation arises when specific components of the dynamical system described by (2.1.1) become zero on

that subset. Other types of invariant submanifolds may emerge when the governing equations include extra constraints or symmetries – they effectively limit the dynamics to a lower-dimensional region within the phase space. Thus, physically, they can be viewed as representing a subset of physical systems that have a particular property or exhibit restricted evolution. These sets often characterize the asymptotic behaviour of a broad range of solutions as $t \to \infty$. Note that if a *global attractor* exists for the physical system, it must reside within the invariant state space, ensuring that it is accessible by trajectories confined to that space.

2.1.3 Linear stability theory

A major aspect of (certain) equilibrium points that we have omitted to mention so far is that they allow for a *local* linear analysis of nonlinear dynamics, enabling the examination of problems that initially appear intractable. This is a gist of the dynamical system technique. We are just one definition and one theorem away from concerning ourselves with characteristics of *linear dynamical systems* mainly from now on, as they provide a foundational framework for analysing the stability of nonlinear systems.

Definition 2.1.8 *A dynamical system $D_1 = \{T, \mathbf{X}, \phi^t\}$ is said to be **locally topologically equivalent** in the neighbourhood O_1 of a point $\mathbf{x}_1$ to a dynamical system $D_2 = \{T, \mathbf{X}, \psi^t\}$ in the neighbourhood O_2 of point $\mathbf{x}_2$ if there exists a homeomorphism $\mathbf{h} : O_1 \to O_2$ which maps the trajectories of D_1 in the neighbourhood O_1 to the trajectories of D_2 in the neighbourhood O_2, while preserving their orientation.*

In the language of physics, local topological equivalence means that the phase portrait in the vicinity of a point is unchanged under continuous deformation. A tiny observer placed nearby would be unable to distinguish the trajectories by watching the motion, as the direction of flow and connections between trajectories are preserved, despite potential differences in distances and angles.

Theorem 2.1.1 (Grobman–Hartman theorem) *The system $\dot{\mathbf{x}} = \mathbf{f}(\mathbf{x})$ is, in the vicinity of its hyperbolic equilibrium point $\mathbf{x}_0$, locally topologically equivalent to its linearization.*

This is highly valuable because if we manage to linearize a complicated system of ODEs, we immediately gain significant insight about the system as long as it possesses hyperbolic equilibrium points. We will address what that entails shortly. The proof of the Grobman–Hartman theorem can be found in the original 1960 publication [112].

Linear autonomous system

Let us suppose that (2.1) is of a form

$$\dot{\mathbf{x}} = \mathbf{A}\mathbf{x}\,, \tag{2.2}$$

where the matrix $\mathbf{A} \in \mathbb{R}^n \times \mathbb{R}^n$ and $\mathbf{x} \in \mathbb{R}^n$ is a vector of state variables, which are functions of time, i.e. $\mathbf{x} = \mathbf{x}(t) = (x_1(t), ..., x_n(t))$. This is a linear autonomous system of differential

equations studied extensively in math and physics literature. The general solution with initial value $\mathbf{x}_i$ can be expressed as

$$\mathbf{x}(t) = \mathbf{x}_i e^{\mathbf{A}t} , \tag{2.3}$$

which leads to the eigenvalue problem for the linear map $L : \mathbb{R}^n \to \mathbb{R}^n$ represented by the matrix $\mathbf{A}$. The resulting eigenvalues directly determine the growth or decay rates of solutions, while the corresponding eigenvectors specify the associated directions in phase space. This is achieved by solving the characteristic polynomial

$$\det(\mathbf{A} - \lambda \mathbf{I}) = 0 , \tag{2.4}$$

which yields n complex eigenvalues $\{\lambda_1, ..., \lambda_n\}$ along with their eigenvectors $\{\mathbf{v}_{\lambda_1}, ..., \mathbf{v}_{\lambda_n}\}$ forming the basis in $\mathbb{C}^n$.

An equilibrium point of (2.2) can be automatically identified with the origin $\mathbf{x}_0 = 0$ and the eigenvalues of $\mathbf{A}$ then directly decide its stability. In practice, linear systems may include a constant term $\mathbf{b}$, giving rise to

$$\dot{\mathbf{y}} = \mathbf{A}\mathbf{y} + \mathbf{b} . \tag{2.5}$$

Any isolated fixed point of such system can be translated to the origin via the transformation $\mathbf{x} = \mathbf{y} - \mathbf{y}_0$, where $\mathbf{y}_0$ satisfies $\mathbf{A}\mathbf{y}_0 + \mathbf{b} = 0$, provided that $\mathbf{A}$ is regular. Hence, without loss of generality, we can concentrate on fixed points at the origin.

Let us now categorize domains in phase space according to the signs of the real parts of the eigenvalues. Notice that if $\mathrm{Re}(\lambda) < 0$, then $e^{\lambda t} \to 0$ as $t \to \infty$, while if $\mathrm{Re}(\lambda) > 0$, then $e^{\lambda t} \to \infty$ as $t \to \infty$. If an eigenvalue is purely imaginary, $\mathrm{Re}(\lambda) = 0$, the corresponding trajectory neither grows nor decays but oscillates around the stationary point. In general case of complex eigenvalue $\lambda = \alpha + i\omega$, the real part α dictates whether the oscillation spirals toward ($\alpha < 0$) or away ($\alpha > 0$) from the equilibrium, giving rise to a spiral-type trajectory in the associated eigenspace. In turn, we define three subspaces of $\mathbb{R}^n$ formed by the eigenvectors $\mathbf{s}^i, \mathbf{u}^i, \mathbf{c}^i$:

the *stable* subspace:	$\mathbb{E}^{\mathrm{s}} = \mathrm{span}\{\mathbf{s}^1, ..., \mathbf{s}^{n_-}\},$	(2.6)
the *unstable* subspace:	$\mathbb{E}^{\mathrm{u}} = \mathrm{span}\{\mathbf{u}^1, ..., \mathbf{u}^{n_+}\},$	(2.7)
the *centre* subspace:	$\mathbb{E}^{\mathrm{c}} = \mathrm{span}\{\mathbf{c}^1, ..., \mathbf{c}^{n_0}\}.$	(2.8)

The first two subspaces govern the asymptotic (or hyperbolic) behaviour: all initial states in the stable subspace are attracted to the equilibrium point $\mathbf{x}_0 = 0$, while those in the unstable subspace are repelled by $\mathbf{x}_0 = 0$. The centre subspace is the most subtle one, as it captures persistent oscillatory motion and often determines the long-term *bounded* dynamics near marginally or *neutral* stable equilibria. In this way, the fixed points act as a "local organizing committee" of the flow.

This classification can be particularly conveniently visualized using the trace-determinant plane. In *two-dimensional* systems, the matrix $\mathbf{A}$ has two eigenvalues λ_1, λ_2, which are the roots of (2.4):

$$\lambda^2 - \sigma\lambda + \Delta = 0, \tag{2.9}$$

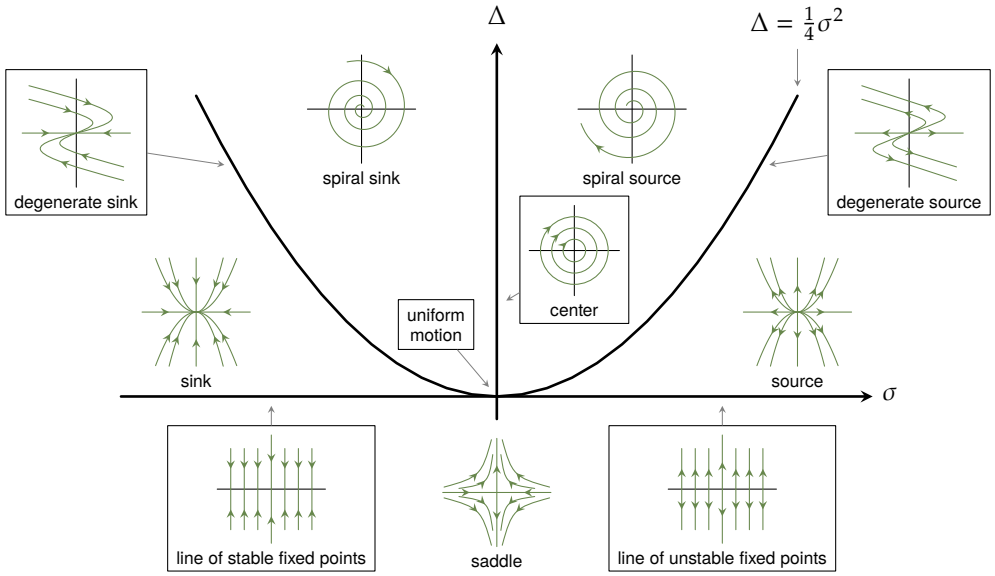

Figure 2.1: Trace-determinant diagram classifying the fixed points of two-dimensional linear dynamical systems. Adapted from a TikZ implementation by G. Salzer.

where $\sigma = \mathrm{tr}\mathbf{A} = \lambda_1 + \lambda_2$ is a trace of $\mathbf{A}$ and $\Delta = \det \mathbf{A} = \lambda_1\lambda_2$ its determinant. Thus, the necessary and sufficient conditions for the asymptotic stability of the point $\mathbf{x}_0 = 0$ in a two-dimensional plane are

$$\sigma = \mathrm{tr}\mathbf{A} < 0 \quad \text{and} \quad \Delta = \det \mathbf{A} > 0. \tag{2.10}$$

In summary, we can systematically classify types of equilibria in linear systems by probing their eigenvalues, and if those eigenvalues *do not* lie on the imaginary axis, we refer to them as *hyperbolic* fixed points.

Linearization of nonlinear system

The vector field $\mathbf{f}(\mathbf{x})$ on the right-hand side of equation (2.1) can be arbitrarily nonlinear. However, it is possible to scrutinize the dynamics of the entire nonlinear system in the vicinity of a fixed point $\mathbf{x}_0$ by performing a linearization around this point. This approach is justified when $\mathbf{f}$ in the general expression (2.1) is sufficiently smooth, allowing us to perform a Taylor expansion of $\mathbf{f}$ around $\mathbf{x}_0$. Since $\mathbf{f}(\mathbf{x}) = (f_1(\mathbf{x}), ..., f_n(\mathbf{x}))$, for each function $f_i(x_1, ..., x_n)$ we can write

$$f_i(\mathbf{x}) = f_i(\mathbf{x}_0) + \sum_{j=1}^{n} \frac{\partial f_i}{\partial x_j}(\mathbf{x}_0) y_j + \frac{1}{2!} \sum_{j,k=1}^{n} \frac{\partial^2 f_i}{\partial x_j \partial x_k}(\mathbf{x}_0) y_j y_k + \cdots, \tag{2.11}$$

where we have defined $\mathbf{y} = \mathbf{x} - \mathbf{x}_0$. As the term *linear stability* hints at, we focus only on the first-order partial derivatives, which correspond to *Jacobian matrix* in vector calculus,

expressed as

$$\mathbf{J} = D\mathbf{f}(\mathbf{x}_0) = \frac{\partial f_i}{\partial x_j}(\mathbf{x}_0) = \begin{pmatrix} \frac{\partial f_1}{\partial x_1}(\mathbf{x}_0) & \cdots & \frac{\partial f_1}{\partial x_n}(\mathbf{x}_0) \\ \vdots & \ddots & \vdots \\ \frac{\partial f_n}{\partial x_1}(\mathbf{x}_0) & \cdots & \frac{\partial f_n}{\partial x_n}(\mathbf{x}_0) \end{pmatrix}, \tag{2.12}$$

sometimes also called the *stability matrix*. Since $f_i(\mathbf{x}_0) = 0$, our system reduces, to first order, to

$$\dot{\mathbf{x}} = \mathbf{J}\mathbf{x} = D\mathbf{f}(\mathbf{x}_0)\mathbf{x}\,, \tag{2.13}$$

which is a linear autonomous system, similar to (2.2), governed by the matrix $\mathbf{J}$. Consequently the eigenvalues of the Jacobian matrix evaluated at the critical points $\mathbf{x}_0$ hold the information about the system's stability. Precisely, according to Grobman–Hartman theorem 2.1.1, the system described by (2.1) is locally topologically equivalent to its linearization (2.13) around $\mathbf{x}_0$, provided that none of the eigenvalues of $\mathbf{J}(\mathbf{x}_0)$ have zero real parts. In the opposite case, the point $\mathbf{x}_0$ is called *non-hyperbolic*, and the linear stability theory becomes inconclusive for such a point.

Definition 2.1.9 *An equilibrium point $\mathbf{x}_0$ of a dynamical system $\dot{\mathbf{x}} = \mathbf{f}(\mathbf{x})$ in $\mathbb{R}^n$ is referred to as a **local sink** or **attractor**, whenever the eigenvalues of the Jacobian matrix $D\mathbf{f}(\mathbf{x}_0)$ satisfy $\mathrm{Re}(\lambda_i) < 0$ for $i = 1, \cdots, n$. Conversely, it is called a **local source** or **repeller** if the eigenvalues satisfy $\mathrm{Re}(\lambda_i) > 0$ for $i = 1, \cdots, n$. A hyperbolic point with eigenvalues of differing signs is classified as a **saddle** point.*

In the nonlinear context, the invariant subspaces (2.6)–(2.8) of the linearized system generalize to local, generally curved invariant manifolds. These are tangent at the fixed point to the linear subspaces and remain invariant under the full nonlinear flow.

Theorem 2.1.2 *Let $\mathbf{x}_0$ be an equilibrium point of $\dot{\mathbf{x}} = \mathbf{f}(\mathbf{x})$ and let $\mathbb{E}^{\mathrm{s}}, \mathbb{E}^{\mathrm{u}}$ and $\mathbb{E}^{\mathrm{c}}$ denote the stable, unstable and centre subspaces of the linearization at $\mathbf{x}_0$. Then there exists locally*

the stable manifold $\mathcal{W}^{\mathrm{s}}$, tangent to $\mathbb{E}^{\mathrm{s}}$ at $\mathbf{x}_0$,
the unstable manifold $\mathcal{W}^{\mathrm{u}}$, tangent to $\mathbb{E}^{\mathrm{u}}$ at $\mathbf{x}_0$,
the centre manifold $\mathcal{W}^{\mathrm{c}}$, tangent to $\mathbb{E}^{\mathrm{c}}$ at $\mathbf{x}_0$.

Shortly, these invariant manifolds of the nonlinear system are nonlinear counterparts of the eigenspaces of the linearized system, sharing the same tangent directions at the fixed point. The stable and unstable manifolds consist solely of orbits that are asymptotic to $\mathbf{x}_0$ as t approaches positive or negative infinity, while a centre manifold includes all those whose long-term behaviour cannot be determined by linearization. Invariant manifolds $\mathcal{W}^{\mathrm{s}}, \mathcal{W}^{\mathrm{u}}, \mathcal{W}^{\mathrm{c}}$ inherit their dimensionality from the corresponding eigenspaces of the linearized system.

2.1.4 Beyond linear stability

For completeness, it is worth briefly mentioning the possible approaches that become relevant when linearization proves to be insufficient, namely, when an equilibrium point has at least one eigenvalue with a zero real part. In such scenarios, higher-order terms in the Taylor series become non-negligible, necessitating the use of advanced stability analysis methods. However, these will not be pursued further in this work.

One commonly applied method is *centre manifold theory*, which reduces the dimensionality of the dynamical system to a lower-dimensional invariant manifold $\mathcal{W}^{\mathrm{c}}$. This results in the analysis of the reduced system instead, whose stability properties decide the dynamics of the original system. For more information on this method, refer to [103].

Another valuable technique for assessing stability properties without explicitly solving the system or relying on linearization is the *Lyapunov method*, which can capture higher-order stabilizing effects. The concept lies in finding a so-called *Lyapunov function*, a scalar, differentiable $V(\mathbf{x}_0)$ analogous to an energy, which is zero in $\mathbf{x}_0$, positive in the vicinity of the investigated fixed point, and whose time derivative along trajectories is non-positive. The existence of such a function indicates that the system cannot deviate from the equilibrium, thereby confirming its stability. In the case of a strictly negative derivative, the equilibrium is asymptotically stable. Physically, this reflects systems in which an effective energy is dissipated over time, driving the system toward equilibrium.

2.1.5 Asymptotic evolution

Regarding full nonlinear systems, the focus is on determining their *future asymptotic behaviour* as time $t \to \infty$ or on examining the *asymptotic past* where $t \to -\infty$, which are global properties of each trajectory, nevertheless, they are dictated by local structures. This is captured through the concept of *limit sets*.

Definition 2.1.10 *Let ϕ^t be a flow on $\mathbb{R}^n$, and let $\mathbf{x}_{\mathrm{i}} \in \mathbb{R}^n$. A point $\mathbf{x}_*$ is an **ω-limit point** of $\mathbf{x}_{\mathrm{i}}$ means there exists a sequence $t_n \to \infty$ such that*

$$\lim_{n\to\infty} \phi^{t_n}(\mathbf{x}_{\mathrm{i}}) = \mathbf{x}_*.$$

*The set of all ω-limit points of $\mathbf{x}_{\mathrm{i}}$ is called the **ω-limit set** of $\mathbf{x}_{\mathrm{i}}$, denoted $\omega(\mathbf{x}_{\mathrm{i}})$. By using a sequence $t_n \to -\infty$, we similarly define **α-limit set** $\alpha(\mathbf{x}_{\mathrm{i}})$.*

The relationship between these global concepts and the previously discussed local linear stability analysis is described by the invariant manifolds associated with equilibrium points. Specifically, the stable manifold $\mathcal{W}^{\mathrm{s}}$ of a fixed point includes all initial conditions whose trajectories tend toward that point as their ω-limit set, while the unstable manifold $\mathcal{W}^{\mathrm{u}}$ comprises trajectories for which the point serves as their α-limit set. In this context, invariant manifolds serve to partition the phase space into regions characterized by different long-term behaviours.

As defined, the ω-limit set of an initial condition $\mathbf{x}_{\mathrm{i}}$ characterizes the long-term behaviour of the corresponding trajectory. However, this may not always be physically

significant as it can be sensitive to perturbations. Therefore, attention is directed toward the collective behaviour of multiple trajectories, which gives rise to the notion of an *attractor* – an invariant set that dictates a fate of a broad range of initial conditions.

Definition 2.1.11 *Given a flow ϕ^t on $\mathbb{R}^n$, the **future attractor** A^+ is the smallest closed invariant set such that $\omega(\mathbf{x}_i) \subset A^+$ for all $\mathbf{x}_i \in \mathbb{R}^n$ apart from a set of measure zero. The **past attractor** A^- is defined by replacing $\omega(\mathbf{x}_i)$ by the α-limit set $\alpha(\mathbf{x}_i)$.*

Thus, the attractors are the *physically observable outcomes*. If the system settles to a fixed point, then the limit set is precisely that point. If the system exhibits sustained oscillations, the limit set may encompass the entire periodic orbit. Although identifying all α- and ω-limit sets is generally a difficult task, two-dimensional systems are special due to the *Poincaré–Bendixson theorem* [108], which severely restrict possible asymptotic states.

2.2 Cosmological application

We are now ready to relate the discussed local analysis to cosmological research. One may already sense that addressing all possible states of our Universe simultaneously appears to be a nonlocal approach. Local analysis focuses on what occurs when near a specific fixed point, but does not quite determine whether this state is physically realized. In the case of cosmology, the relevant questions are: given a certain initial state of the Universe, what is its subsequent evolution, and what is its eventual configuration? Do different initial conditions converge to the same outcome? These inquiries are inherently *global* and relate to the concept of long-term evolution discussed in Section 2.1.5.

The challenge arises because in cosmology the attractors introduced in Definition 2.1.11 can (and do) correspond to extreme behaviours – for instance, near the Big Bang – with arbitrarily large values of variables such as ρ and H in the cosmological equations (1.58) and (1.60). For this reason, the phase space for these ODEs becomes unbounded, complicating the process of analysing the system globally. Fortunately, there is an effective approach: one can rescale all relevant dynamical quantities using the Hubble scalar H. This normalization enables us to interpret the evolution of these variables relative to the overall expansion rate of the Universe. The dimensionless variables arising through this procedure are known as *Expansion Normalized* (EN) variables and, in general, can be expressed as

$$\mathbf{y} = \frac{\mathbf{x}}{H^n}\,, \tag{2.14}$$

where n depends on the dimension of the original variable under consideration. In conjunction with this normalization, it is necessary to introduce a *dimensionless time variable*, typically denoted τ. This variable spans the entire real line, with $\tau \to -\infty$ belonging to the initial singularity and $\tau \to \infty$ at late times. It is defined by

$$\tau = \log \frac{a}{a_0}\,, \tag{2.15}$$

where $a(t)$ is the scale factor, a_0 its value at the present time, conventionally set to 1. From the definition of the Hubble parameter (1.59), it follows that:

$$\frac{\mathrm{d}\tau}{\mathrm{d}t} = H\,. \tag{2.16}$$

The benefits of this approach are threefold:

- *The normalized variables allow us to transform the Friedmann equation into a constraint. Such constraint can yield a compact phase space.*
- *The derivatives depend solely on the normalized variables themselves, not explicitly on t or $H(t)$, thereby making the application of machinery of dynamical systems straightforward.*
- *These quantities directly connect to cosmological observations.*

For the variables defined in this manner, it is intrinsically required that $H \neq 0$ and the sign of H must remain fixed.

In addition, if the goal is to determine the actual value of the Hubble parameter or the physical time afterwards, these must be reconstructed by integrating along the trajectory passing through an initial point $\mathbf{y}_0$ using the decoupled equations for $H(\tau)$ and $t(\tau)$. This emphasizes an important conceptual point: the normalized dynamical system does not specify the absolute scale of the Universe. In effect, each orbit within the dimensionless state space corresponds to a *one-parameter family of physical solutions*, differing only by an overall scaling of the Hubble parameter. This ambiguity is resolved once the observational input is taken into account. Specifically, the dimensionless combination

$$\alpha = tH\,, \tag{2.17}$$

known as the *age parameter*, evaluated at the present time as $\alpha_0 = t_0 H_0$, is constrained by observational data. As a consequence, this quantity becomes a well-defined function within the phase space and serves to *identify the point that marks the current state* $\mathbf{y}_0$ *of the Universe*. For a complete discussion of this remark, see [108].

Before finally delving into the analysis of concrete cosmological models, we briefly conclude and interpret key aspects of dynamical systems theory in our favoured context. Each trajectory in phase space represents a *possible cosmological history*, so the phase space as a whole encodes an ensemble of universes permitted by the theory, not a single realized one. In this setting, the central question is not merely the existence of particular solutions but which of them are dynamically realized for chosen initial conditions. Limit sets then characterize the asymptotic behaviour of trajectories and thereby translate the geometric structure of phase space into meaningful physical predictions about the past and future evolution of feasible universes.

Ultimately, this approach will effectively elucidate the overall properties of the gravitational model under examination, including its capacity to accurately replicate the observed evolution of the Universe, the occurrence of potential phase transitions, and whether these sequences are generally exhibited or require precise tuning.

2.2.1 Standard cosmology (ΛCDM)

As an introductory exercise, we shall begin by illustrating the dynamics of the standard cosmological paradigm, in which *dark energy* is represented by the cosmological constant, denoted Λ, and *dark matter* is characterized as non-relativistic Cold Dark Matter (CDM) with the EoS parameter $w_{\text{DM}} = 0$. It is anticipated that we recover a standard scenario, where our Universe experienced a radiation-dominated epoch in its early stages, followed by a matter-dominated period, and ultimately evolved into a dark energy-dominated era in its later stages, consistent with current observational evidence. Although each of these regimes can be analytically derived by neglecting the other components, such an approach does not capture the transitions between them. The dynamical systems framework provides a means to understand these transitions.

We start our analysis by neglecting the presence of spatial curvature, as $k \approx 0$ is in a well agreement with current observational evidence, indicating that our Universe is very close to being spatially flat [113]. From a theoretical standpoint, inflationary models provide additional support for this, as they dynamically lead the Universe toward spatial flatness.

However, the curvature parameter influences the cosmological evolution significantly, and becomes relevant particularly in the context of early Universe behaviour. Later, when examining modified theories of gravity, the role of spatial curvature term may become especially profound, as it may interact in complex ways with additional degrees of freedom or appear in the field equations nonlinearly, meaning that even a minor geometric contribution can exert a notable impact on the dynamics. It is thus necessary to address all instances of spatial geometry within the framework of the Standard cosmological model as well.

Flat spatial geometry

Assuming the curvature parameter $k = 0$, we drop the last terms of (1.57) and (1.58), remaining with

$$H^2 = \frac{\kappa}{3} \sum_i \rho_i + \frac{\Lambda}{3}\,, \tag{2.18}$$

$$2\dot{H} + 3H^2 = -\kappa \sum_i p_i + \Lambda\,. \tag{2.19}$$

To treat all contributions on an equal footing, it is often convenient to formally associate the cosmological constant with an effective energy density $\rho_\Lambda = \Lambda/\kappa$, which allows the Friedmann equation to be expressed as a sum of energy components, and with effective pressure $p_\Lambda = -\rho_\Lambda$, recalling that EoS parameter of dark energy is inferred to be $w_\Lambda = -1$. Then, accounting for matter (together with dark matter) in a form of pressureless fluid

($p_m = 0$) and for radiation ($p_r = \rho_r/3$), we can write

$$H^2 = \frac{\kappa}{3}\rho_m + \frac{\kappa}{3}\rho_r + \frac{\kappa}{3}\rho_\Lambda \,, \tag{2.20}$$

$$2\dot{H} + 3H^2 = -\frac{\kappa}{3}\rho_r + \kappa\rho_\Lambda \,, \tag{2.21}$$

and claim that the total energy density is

$$\rho_{tot} = \rho_m + \rho_r + \rho_\Lambda = \frac{3H^2}{\kappa} \,. \tag{2.22}$$

If those components do not interact, we further obtain the conservation laws

$$\dot{\rho}_m = -3H\rho_m \,, \tag{2.23}$$

$$\dot{\rho}_r = -4H\rho_r \,, \tag{2.24}$$

$$\dot{\rho}_\Lambda = 0 \,. \tag{2.25}$$

The common procedure involves identifying the following dimensionless variables

$$\Omega_m = \frac{\kappa\rho_m}{3H^2} \,, \quad \Omega_r = \frac{\kappa\rho_r}{3H^2} \,, \quad \Omega_\Lambda = \frac{\kappa\rho_\Lambda}{3H^2} \,, \tag{2.26}$$

which represent the relative energy densities of matter, radiation and the cosmological constant with respect to the total energy density (2.22). Since the energy densities ρ_m and ρ_r are strictly positive, the physical phase space in the (Ω_m, Ω_r)-plane is restricted through $\Omega_m > 0$ and $\Omega_r > 0$. The Friedmann equation in terms of these variables becomes a constraint

$$1 = \Omega_m + \Omega_r + \Omega_\Lambda \,. \tag{2.27}$$

This allows for the substitution of one variable in terms of the other two, reducing the dimensionality of the proposed system from three to two. It also implies that $\Omega_m + \Omega_r \leq 1$ must hold. Consequently, the physically meaningful dynamics happens inside the compact triangular region with vertices at the origin $(0, 0)$, the point $(1, 0)$ and the point $(0, 1)$. By implementing (2.26) into the equation (2.21) and rearranging, we obtain

$$\frac{\dot{H}}{H^2} = -\frac{1}{2}(3 + \Omega_r - 3\Omega_\Lambda) = -\frac{1}{2}(4\Omega_r + 3\Omega_m) \,. \tag{2.28}$$

Given that the deceleration parameter is defined as

$$q = -\frac{\ddot{a}a}{\dot{a}^2} = -\left(\frac{\dot{H}}{H^2} + 1\right) , \tag{2.29}$$

we can utilize equation (2.28) to infer which regions of the phase space correspond to decelerated or accelerated expansion. The accelerating region has $q < 0$, yielding, in this case, a linear boundary in phase space.

The 2D dynamical system itself is constructed by differentiating Ω_m and Ω_r (if we choose Ω_Λ as a constrained parameter) with respect to dimensionless time variable τ, as introduced in (2.15). Using the prime to represent the derivative with respect to τ, we arrive at

$$\Omega_m' = \frac{d\Omega_m}{d\tau} = \frac{1}{H}\frac{d\Omega_m}{dt} = \frac{\kappa\dot{\rho}_m}{3H^3} - \frac{2\kappa\rho_m\dot{H}}{3H^4} = \Omega_m(3\Omega_m + 4\Omega_r - 3)\,, \tag{2.30}$$

$$\Omega_r' = \frac{d\Omega_r}{d\tau} = \frac{1}{H}\frac{d\Omega_r}{dt} = \frac{\kappa\dot{\rho}_r}{3H^3} - \frac{2\kappa\rho_r\dot{H}}{3H^4} = \Omega_r(3\Omega_m + 4\Omega_r - 4)\,, \tag{2.31}$$

while noting again that all variables require $H \neq 0$. We immediately find two invariant submanifolds: $\Omega_m = 0$ and $\Omega_r = 0$. Next, the three critical points with their linear stability analysis, summarized in Table 2.1, divulge the following:

- *The origin,* $dS = (0, 0)$*, is a stable point, where the value of* Ω_Λ *reaches* 1*, indicating a universe dominated by the cosmological constant (dark energy). This is called the* ***de Sitter universe****.*
- *The unstable point* $F_r = (0, 1)$ *is entirely dominated by radiation, which is why we can refer to it as* ***radiation-dominated Friedmann universe****.*
- *The saddle point* $F_m = (1, 0)$ *is left for the solution characterized by non-relativistic matter dominance, thus corresponds to* ***matter-dominated Friedmann universe****.*

These are well-known limiting solutions depicted by dots in the accompanying phase portrait in Figure 2.2. The point F_r clearly functions as the past attractor, whereas the point dS represents the future attractor for all trajectories. Accordingly, every solution inside the triangle is a heteroclinic orbit connecting F_r (with $\tau \to -\infty$) to dS (as $\tau \to \infty$). The two different heteroclinic orbits are the axis $\Omega_r = 0$ and a line $\Omega_r = 1 - \Omega_m$, connecting F_r to F_m and F_m to dS, respectively. These trajectories correspond to a scenario with a vanishing cosmological constant or a universe devoid of radiation, which makes them physically less relevant. Nevertheless, it is important to note that, together, these two heteroclinics form a sequence $F_r \to F_m \to dS$, which holds fundamental significance. Because the measured value of the cosmological constant is positive but exceedingly tiny, we expect that our Universe's evolution closely follows a trajectory passing near the $\Omega_r = 1 - \Omega_m$ line. This implies an evolutionary path characterized by an initial radiation-dominated phase, followed by a matter-dominated period, and ultimately transitioning into a dark energy-dominated era.

Any initial condition with a slightly higher value of Ω_Λ would produce trajectories more distant from this line, resulting in a rapid transition from radiation dominance directly to dark energy domination, precluding the intermediate matter epoch to occur. This enhances the ongoing issue of *fine-tuning* the cosmological constant to its very small observed value.

Table 2.1: Fixed points and their stability for the 2D system (2.30)–(2.31).

Point	$\{\Omega_m, \Omega_r, \Omega_\Lambda\}$	Eigenvalues	Stability
dS	$\{0, 0, 1\}$	$\{-4, -3\}$	Attractor
F_r	$\{0, 1, 0\}$	$\{1, 4\}$	Repeller
F_m	$\{1, 0, 0\}$	$\{-1, 3\}$	Saddle

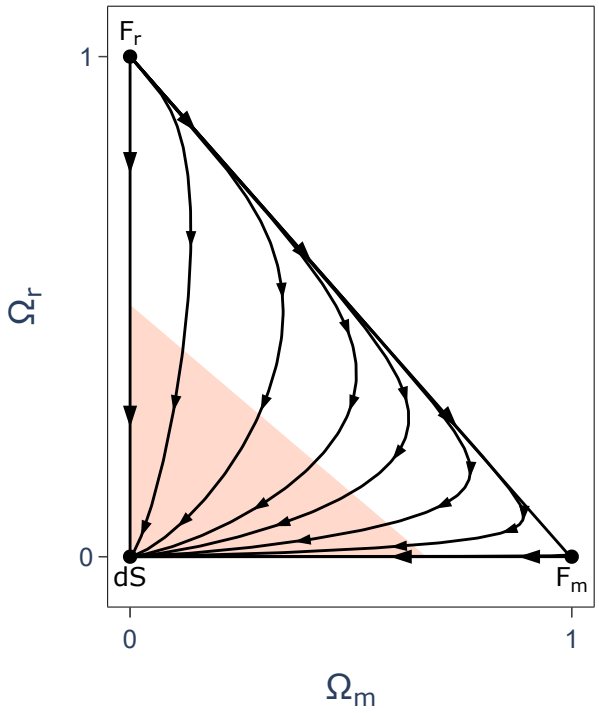

Figure 2.2: Phase portrait of the dynamical system (2.30)–(2.31) describing flat ΛCDM model containing two perfect fluids. The orange shaded area denotes the accelerating regime.

Open spatial geometry

The case of a hyperbolic universe, where $k = -1$, yields an analysis closely analogous to that of a flat universe, with a subtlety of bringing the curvature parameter Ω_k as a dynamical variable. To preserve the two-dimensional formulation, we can combine matter and radiation into a single effective fluid that obeys a barotropic equation of state, instead of introducing a separate variable for each.

Starting from the cosmological equations (1.57) and (1.58) with a single energy density, the definition of these EN variables is suggested

$$\Omega = \frac{\kappa\rho}{3H^2}\,, \quad \Omega_k = \frac{k}{a^2H^2}\,, \quad \Omega_\Lambda = \frac{\Lambda}{3H^2}\,, \tag{2.32}$$

which again results in a compact phase space, as long as we consider $k = -1$ only, hence $\Omega_k < 0$. The Friedmann constraint in this context reads

$$1 = \Omega - \Omega_{\rm k} + \Omega_\Lambda \tag{2.33}$$

with variables confined to the ranges $0 \leq \Omega \leq 1$, $-1 \leq \Omega_{\rm k} \leq 0$ and $0 \leq \Omega_\Lambda \leq 1$, resembling a triangle similar to its spatially flat counterpart. The deceleration parameter can be transformed into

$$\mathfrak{q} = \frac{3}{2}\Omega(w+1) - \Omega_{\rm k} - 1\,. \tag{2.34}$$

The derivatives of (2.32) with respect to the standard τ generate a dynamical system

$$\Omega' = \Omega[3(w+1)(\Omega-1) - 2\Omega_{\rm k}]\,, \tag{2.35}$$

$$\Omega_{\rm k}' = \Omega_{\rm k}[3(w+1)\Omega - 2(\Omega_{\rm k}+1)]\,. \tag{2.36}$$

Table 2.2: Fixed points and their stability for the 2D system (2.35)–(2.36).

Point	$\{\Omega, \Omega_{\rm k}, \Omega_\Lambda\}$	Eigenvalues	Stability	Solution
dS	$\{0, 0, 1\}$	$\{-2, -3(1+w)\}$	Attractor	de Sitter
F	$\{1, 0, 0\}$	$\{3(1+w), 1+3w\}$	Repeller	Friedmann
M	$\{0, -1, 0\}$	$\{2, -1-3w\}$	Saddle	Milne

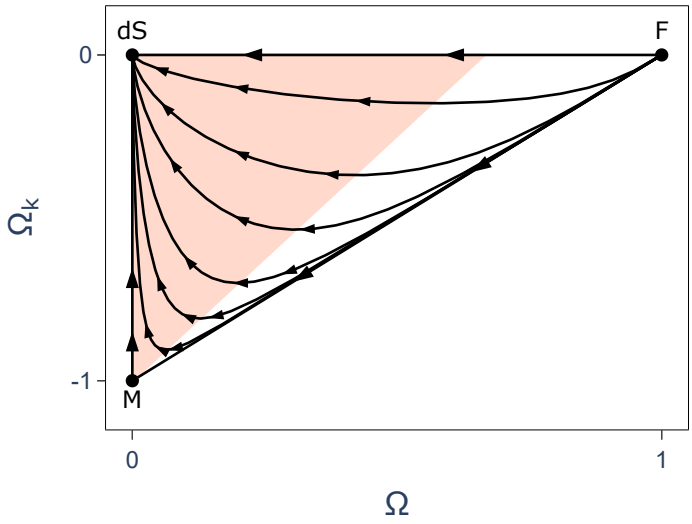

Figure 2.3: Phase portrait of the dynamical system (2.35)–(2.36) describing negatively spatially curved ΛCDM model with a single perfect fluid. The orange shaded area denotes the accelerating regime.

Once again, we observe equilibrium points, organized in Table 2.2, that correspond to the dominance of each dynamical variable over the others – specifically, the Friedmann solution, where the matter becomes predominant, and already notorious de Sitter attractor dS, where dark energy takes over. A new feature in this analysis is the identification of a critical point associated with curvature dominance, known as the Milne universe, thus marked as M. This solution is unstable: the introduction of a perturbation drives the system away from this limiting case.

Closed spatial geometry

When we address a universe described by $k = 1$, we can take advantage of the positive value of curvature parameter to suitably redefine the normalization factor. When utilizing

$$\eta = \sqrt{H^2 + \frac{k}{a^2}} \tag{2.37}$$

instead of the Hubble scale factor alone, it additionally becomes possible to analyse the system even near $H = 0$, which is a solution often associated with the *Einstein static universe*.

Considering Ω_m and Ω_r as parts of a single energy density parameter Ω again with an arbitrary barotropic EoS, $p = w\rho$, a new set of variables is given by

$$X = \frac{H}{\eta}\,, \quad \Omega = \frac{\kappa\rho}{3\eta^2}\,, \quad \Omega_\Lambda = \frac{\Lambda}{3\eta^2}\,, \tag{2.38}$$

where X is a new variable that encompasses the effect of curvature. In this case, one can constrain both relativistic and non-relativistic matter through

$$\Omega = 1 - \Omega_\Lambda\,. \tag{2.39}$$

This reduced formulation describes dynamics fully as the competition between the effective fluid component and the cosmological constant. Based on the definition of X, it follows that $-1 \leq X \leq 1$ and a constraint along with $\Omega \geq 0$ implies $0 \leq \Omega_\Lambda \leq 1$. As a result, the phase portrait will be confined within a compact rectangular region.

We recast cosmological equations as

$$X' = \frac{1}{\eta}\frac{\mathrm{d}X}{\mathrm{d}t} = (1 - X^2)\left[1 - \frac{3}{2}(w - 1)(1 - \Omega_\Lambda)\right], \tag{2.40}$$

$$\Omega_\Lambda' = \frac{1}{\eta}\frac{\mathrm{d}\Omega_\Lambda}{\mathrm{d}t} = 3\Omega_\Lambda X(w + 1)(1 - \Omega_\Lambda)\,, \tag{2.41}$$

where we have differentiated (2.38) with respect to the dimensionless time variable τ, defined via

$$\frac{\mathrm{d}\tau}{\mathrm{d}t} = \eta\,. \tag{2.42}$$

To identify the accelerated region of the phase space, we need to evaluate the expression that remains finite even when $H = 0$. This is not true when considering the form given by (2.28). Instead, we must examine when the following becomes positive:

$$\frac{\ddot{a}}{a\eta^2} = -\frac{1}{2}(1+3w) + \frac{3}{2}\Omega_\Lambda(1+w)\,. \tag{2.43}$$

Table 2.3: Fixed points and their stability for the 2D system (2.40)–(2.41).

Point	$\{X, \Omega_\Lambda, \Omega\}$	Eigenvalues	Stability
dS_+	$\{1, 1, 0\}$	$\{-2, -3(1+w)\}$	Attractor
dS_-	$\{-1, 1, 0\}$	$\{2, 3(1+w)\}$	Repeller
F_+	$\{1, 0, 1\}$	$\{3(1+w), 1+3w\}$	Repeller
F_-	$\{-1, 0, 1\}$	$\{-1-3w, -3(1+w)\}$	Attractor
E	$\left\{0, \frac{2}{3(w+1)}, \frac{3w+1}{3(w+1)}\right\}$	$\left\{\mp\frac{\sqrt{(1+w)^2(1+3w)}}{1+w}\right\}$	Saddle

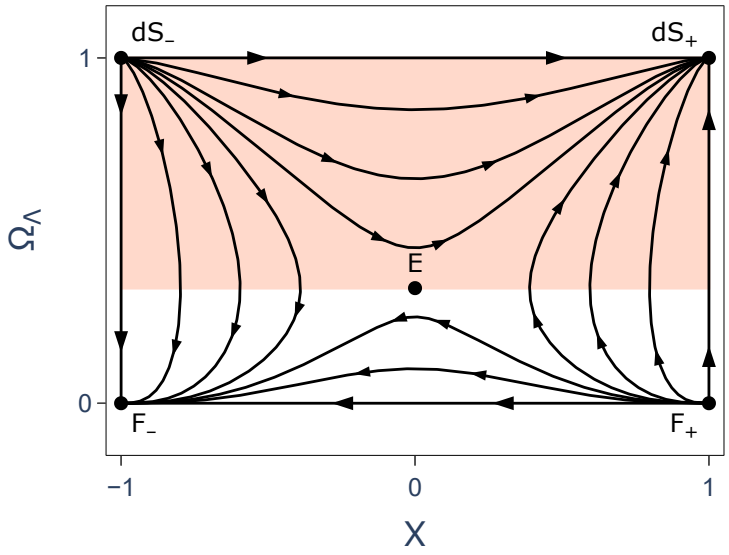

Figure 2.4: Phase portrait of the dynamical system (2.40)–(2.41) describing positively spatially curved ΛCDM model with a single perfect fluid. The orange shaded area denotes the accelerating regime.

We should stress that equation (2.43) does not reflect the numerical value of the deceleration parameter, that is, the flow along the trajectories may be distorted. However, the expression for the acceleration barrier remains valid regardless, as we are primarily concerned with its sign.

The system defined by (2.40)–(2.41) now admits four invariant submanifolds, $X = \pm 1, \Omega_\Lambda = 1, \Omega_\Lambda = 0$, and five fixed points, which are listed in Table 2.3. Friedmann and de Sitter solutions now appear in pairs, as the Hubble scalar H has been promoted to a dynamical variable, enabling both *contracting* and *expanding* versions. Contracting branches are not represented in the previous geometries. These four points form a rectangular configuration within which physically relevant solutions are found, as visualized in Figure 2.4.

In addition, a new equilibrium point E with saddle stability emerges, linked to Einstein static universe. This point gives rise to novel types of cosmic history. Trajectories that remain within the decelerated region throughout their evolution correspond to *re-collapsing universes*, which begin to contract after reaching their maximum size. Trajectories confined to the accelerated region on the opposite size exclusively represent *bouncing solutions*, starting with a contracting de Sitter universe and progressing toward de Sitter expansion. Furthermore, *loitering solutions* appear, associated with the transition between the regions, where the universe's expansion or contraction can approach a nearly static state.

For our purposes, bouncing solutions will be particularly important. They are defined as solutions for the scale factor $a(t)$ such that there is an instant t_b for which [114]

$$a_b \neq 0\,, \quad \dot{a}_b = 0 \quad \text{and} \quad \ddot{a}_b > 0\,. \tag{2.44}$$

2.2.2 Brans-Dicke cosmology

Here, we will begin to gradually move away from cosmologies based on GR with perfect fluid. Since we have already covered certain details and references concerning specific MG models, the focus will now be on presenting a brief technical overview of the cosmological phase spaces associated with some of these models, as outlined in several works.

Following the approach of [115], the cosmological equations (1.66)–(1.68) for the class of theories which introduce a scalar degree of freedom with an arbitrary potential non-minimally coupled to gravitational sector (or the generalized Brans-Dicke theory) can be transformed via the following dimensionless variables:

$$x = \frac{\dot{\phi}}{H\phi}\,, \qquad y = \frac{1}{H}\frac{\sqrt{V}}{\sqrt{3\phi}}\,, \qquad \lambda = -\frac{\phi}{V}\frac{\partial V}{\partial \phi}\,, \qquad \tilde{\Omega} = \frac{\kappa\rho}{3\phi H^2}\,. \tag{2.45}$$

As a reminder, a system (1.66)–(1.68) incorporates only a *flat spatial geometry*. Also, the variable y is only real when $V(\phi) > 0$, for negative V, it would require redefinition, which will not be addressed here. Additionally, $\tilde{\Omega}$ is only defined as positive when $\phi > 0$, which is, although, supported by gravity's attractive nature.

Nevertheless, these variables do not produce a closed autonomous system of equations until the form of scalar potential $V(\phi)$ is specified. Here, for a simple illustration, we will deal with a special case of a power-law potential function: a model of a quadratic potential given by

$$V(\phi) = V_0\phi^2\,, \tag{2.46}$$

which leads to

$$\lambda = -2 = \text{const.} \tag{2.47}$$

The modified Friedmann equation

$$3\phi H^2 + 3H\dot{\phi} - \frac{\omega_{\text{BD}}}{2}\frac{\dot{\phi}^2}{\phi} - V = \kappa\rho\,, \tag{2.48}$$

expressed in terms of the variables (2.45), simplifies to the Friedmann constraint

$$1 = \tilde{\Omega} + \frac{\omega_{\text{BD}}}{6}x^2 - x + y^2 = 1 + \Omega_\phi\,, \tag{2.49}$$

which restricts the physical dynamics to occur within a bounded region characterized by a compact ellipse, given that the effective energy density of the scalar field,

$$\Omega_\phi = \frac{\omega_{\text{BD}}}{6}x^2 - x + y^2, \tag{2.50}$$

stays positive, as ensured by assuming $\omega_{\text{BD}} > 0$. If that is not the case and ω_{BD} is negative, the phase space becomes non-compact and requires further asymptotic analysis, as extensively elaborated in [115]. We will stick to the first option.

The equation for the variable $\tilde{\Omega}$ can be eliminated using (2.49). Differentiating the remaining variables, x and y, with respect to standard τ (2.15) results in a 2D autonomous system:

$$\begin{aligned} x' = -3x\left[1 + x - \frac{\omega_{\text{BD}}}{6}x^2 - \frac{2+\omega_{\text{BD}}(1+w)}{3+2\omega_{\text{BD}}}\left(1 + x - \frac{\omega_{\text{BD}}}{6}x^2 - y^2\right)\right] \\ + 3\left(1 + x - \frac{\omega_{\text{BD}}}{6}x^2 - y^2\right)\frac{1-3w}{3+2\omega_{\text{BD}}}\,, \end{aligned} \tag{2.51}$$

$$y' = 3y\left[-\frac{x}{2} + \frac{\omega_{\text{BD}}}{6}x^2 + \frac{2+\omega_{\text{BD}}(1+w)}{3+2\omega_{\text{BD}}}\left(1 + x - \frac{\omega_{\text{BD}}}{6}x^2 - y^2\right)\right] \tag{2.52}$$

and

$$\frac{\dot{H}}{H^2} = 2x - \frac{\omega_{\text{BD}}}{2}x^2 - \frac{3}{3+2\omega_{\text{BD}}}y^2(2+\lambda) - 3\left(1 + x - \frac{\omega_{\text{BD}}}{6}x^2 - y^2\right)\frac{2+\omega_{\text{BD}}(1+w)}{3-2\omega_{\text{BD}}} \tag{2.53}$$

is delivering information on accelerated dynamics.

The choice of $V(\phi)$ (2.46) adopted in the present analysis is due to the fact that it provides the simplest physically consistent realization of Brans–Dicke cosmology with self-interaction. Notably, only quadratic or linear potential functions admit de Sitter solutions, while the quadratic potential uniquely yields a massive scalar field ϕ that exhibits well-defined behaviour in both Einstein and Jordan frames [116].

Table 2.4: Fixed points and their stability properties for the Brans–Dicke model with quadratic potential and a barotropic matter described by EoS parameter w, i.e. the 2D system (2.51)–(2.52). We denote ω_{BD} as ω for simplicity.

Point	$\{x, y, \tilde{\Omega}\}$
A_+	$\left\{\frac{3+\sqrt{6\omega+9}}{\omega}, 0, 0\right\}$
A_-	$\left\{\frac{3-\sqrt{6\omega+9}}{\omega}, 0, 0\right\}$
B	$\{0, 1, 0\}$
C	$\left\{\frac{1-3w}{\omega(1-w)+1}, 0, \frac{(2\omega+3)(3\omega+4+3w^2\omega-6w(1+\omega)}{6(\omega(w-1)-1)^2}\right\}$
D	$\left\{-\frac{3}{2}(1+w), \sqrt{\frac{1}{8}[5-3w+3\omega(1-w^2)]}, -\frac{3}{8}(1+w)(3+2\omega)\right\}$
Point	**Eigenvalues**
A_+	$\left\{3(1-w)+\frac{3+\sqrt{6\omega+9}}{\omega}, 3+\frac{3}{2}\frac{3+\sqrt{6\omega+9}}{\omega}\right\}$
A_-	$\left\{3(1-w)+\frac{3-\sqrt{6\omega+9}}{\omega}, 3+\frac{3}{2}\frac{3-\sqrt{6\omega+9}}{\omega}\right\}$
B	$\{-3, -3(1+w)\}$
C	$\left\{-\frac{3}{2}(1-w)-\frac{1}{2}\frac{1-3w}{\omega(1-w)+1}, \frac{3}{2}(1+w)+\frac{1-3w}{\omega(1-w)+1}\right\}$
D	$\left\{-\frac{3}{8}(1-w)+\frac{1}{2}\sqrt{\Delta}, -\frac{3}{8}(1-w)-\frac{1}{2}\sqrt{\Delta}\right\}$
	$\Delta = \frac{9}{16}(1-3w)^2+\frac{9}{2}[5-3w+3\omega(1-w^2)](1+w)$

The expressions (2.51)–(2.52) imply that the only invariant submanifold is $y = 0$, which corresponds to the original Brans–Dicke theory. It is evident that the critical points of this dynamical system and their stability properties are strongly influenced by the parameters w and ω_{BD}, which then opens the door to rich phenomenology (especially when $\omega_{\text{BD}} < 0$ is allowed). There can be up to five fixed points and we list them in Table 2.4. Points $A_\pm$ and C are associated with the kinetic dominance of the scalar field (where $y = 0$), representing stiff-fluid-like solutions that do not lead to accelerated expansion. Point B yields a scaling solution in which both the scalar field and matter contribute and evolve proportionally to each other; for appropriate parameter values, this solution may produce accelerated expansion. However, since it resides outside the invariant submanifold, it cannot function as a global attractor, as trajectories confined to this submanifold are unable to reach it. There is no potential dominated fixed point. Additionally, a critical point D may emerge within a physical region depending on w.

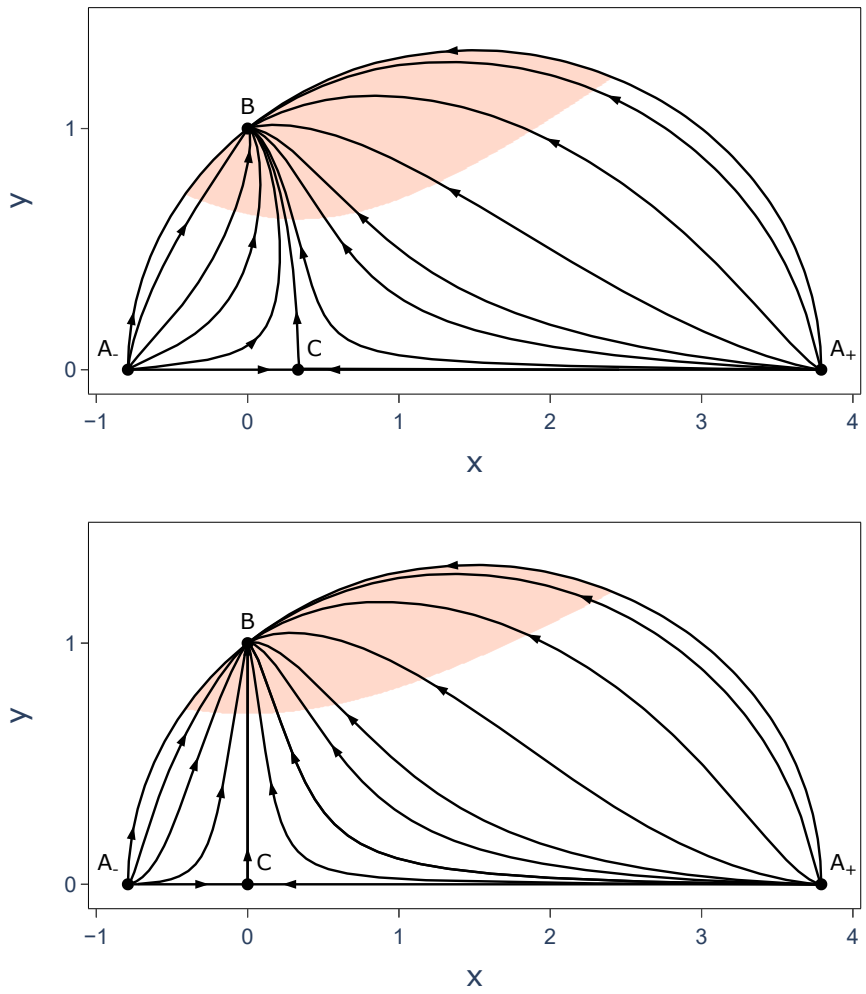

Figure 2.5: Phase portrait of the dynamical system (2.51)–(2.52) describing the Brans–Dicke model with quadratic potential. A universe is filled with pressureless dust ($w = 0$) at the top and with relativistic matter ($w = 1/3$) at the bottom. In the orange shaded area, the dynamics is accelerated.

For the attached illustrations in Figure 2.5, we selected values $\omega_{\text{BD}} = 2$ and $w = 0$ or $w = 1/3$, consequently, an equilibrium point D resides outside the allowed domain. Note that selecting ω_{BD} in such a way is well outside current observational constraints (see the discussion in Section 1.4.2). It is used here as a simplified toy model to demonstrate the qualitative structure of the phase space. For more realistic values of ω_{BD}, the phase space is compressed and the trajectories shift closer to the GR limit; however, the overall qualitative features remain consistent. We again stress that the situation becomes quite complex when considering other forms of potential $V(\phi)$ or when it remains entirely general.

2.2.3 R^n cosmology

As anticipated, navigating the multitude of potential modifications to GR leads to a rapid increase in the complexity and scope of cosmological models, and their analysis becomes vast and intricate. In the topic of $f(R)$ gravity as well, a fully general analysis is intractable, we will have to restrict our attention to a specific subclass of models in order to present a clear and interpretable example of the application of dynamical systems theory. The chosen category is the *power-law models*, commonly referred to as R^n *gravity*. After summarizing the methodology of the detailed study conducted in 2004 [117], we present phase portraits for a representative range of n.

The action for the gravitational interaction of R^n gravity reads

$$S_{R^n} = \int \mathrm{d}^4x\sqrt{-g}[\chi(n)R^n + 2\kappa\mathcal{L}_\mathrm{m}]\,, \tag{2.54}$$

compared to (1.69). Here, $\chi(n)$ is a function that equals 1 when $n = 1$, and is designed to maintain a positive sign even for negative n, ensuring that the attractive nature of the gravitational interaction is preserved. With this more concrete selection, the $f(R)$ cosmology equations from the first chapter, (1.70)–(1.73), become

$$H^2 + \frac{k}{a^2} = \frac{R}{6n}(1-n) - H\frac{\dot{R}}{R}(n-1) + \frac{2\kappa\rho}{3n\chi(n)R^{n-1}}\,, \tag{2.55}$$

$$2n\frac{\ddot{a}}{a} = -n(n-1)H\frac{\dot{R}}{R} - n(n-1)\frac{\ddot{R}}{R} - n(n-1)(n-2)\frac{\dot{R}^2}{R^2} + (1-n)\frac{R}{3} - \frac{\rho}{3n\chi(n)R^{n-1}}(1+3w)\,, \tag{2.56}$$

with

$$R = 6\left(\frac{\ddot{a}}{a} + \frac{\dot{a}^2}{a^2} + \frac{k}{a^2}\right)\,. \tag{2.57}$$

Vacuum case

We can simplify the analysis in the beginning by considering a universe where the matter is absent ($\rho = 0$). Proposing variables of the form

$$x = \frac{\dot{R}}{RH}(n-1)\,, \quad y = \frac{R}{6nH^2}(1-n)\,, \quad K = \frac{k}{a^2H^2}\,, \tag{2.58}$$

with one of them constrained by

$$1 + K + x - y = 0\,, \tag{2.59}$$

results in a non-compact two-dimensional phase space, parametrized by the value of n. In this way, x encodes the variation of the Ricci curvature and y captures its expansion normalized measure, while K is nothing but the standard variable connected to spatial curvature parameter of the FLRW model.

Table 2.5: Fixed points of the system describing R^n gravity in vacuum (2.60)–(2.61) and their eigenvalues.

Point	$\{x, y, K\}$	Eigenvalues
A	$\{0, 0, -1\}$	$\{-2, 2\}$
B	$\{-1, 0, 0\}$	$\left\{2, \frac{4n-5}{n-1}\right\}$
C	$\left\{\frac{2(n-2)}{2n-1}, \frac{4n-5}{2n-1}, 0\right\}$	$\left\{\frac{5-4n}{n-1}, \frac{4n+2-4n^2}{2n^2-3n+1}\right\}$
D	$\{2(1-n), 2(n-1)^2, 2n^2-2n-1\}$	$\left\{n-2+\sqrt{3n(3n-4)}, n-2-\sqrt{3n(3n-4)}\right\}$

Utilizing the standard time variable τ for differentiation, equation (2.56) is transformed into an autonomous system

$$x' = (2+x)y - 2x - 2x^2 - \frac{y(2+nx)}{n-1}\,, \tag{2.60}$$

$$y' = \frac{y}{n-1}[x(3-2n) - 2y + 2(n-1)]\,. \tag{2.61}$$

During the derivation process of these equations, we have implicitly arrived at a situation where $n = 1$ is forbidden. However, since this case corresponds to the standard GR, we are justified in disregarding it.

Each phase portrait can be partitioned into two regions using the deceleration parameter

$$\mathfrak{q} = -\frac{\dot{H}}{H^2} - 1 = -x - \frac{y}{n-1}\,, \tag{2.62}$$

where $\mathfrak{q} < 0$, we have accelerated expansion, as indicated by the orange regions in the corresponding Figure 2.6.

Setting x' and y' to zero, two categories of equilibrium points can be identified. The fixed points A and B are common to all variations of the R^n theory, while points C and D vary their positions with the parameter n. Notably, the coordinates of C even become divergent at $n = 1/2$. Another interesting observation is that the point C coincides with point B when $n = 5/4$, and with point D when $n = \frac{1}{2}(1+\sqrt{3})$. Points A and D would merge at $n = 1$, but since the system is not defined at this value, this case is excluded from consideration.

The eigenvalues derived from linear stability analysis are listed in Table 2.5. The point A possesses both positive and negative real eigenvalue, regardless of the value of n, indicating that it is always a saddle point. Additionally, it is situated at the origin with a K value of -1, this corresponds to the emergence of the Milne solution.

Given the complexity of analysing all possible stability configurations for each remaining point across the different ranges of n, we refer the reader to [117], where this has been conducted in detail. Also for the analysis at infinity, which is essential

for uncompactified phase spaces such as this one, see the same reference. The problem arises when fixed points exist as a result of x or y approaching infinity – that is, when the *kinetic* part of the curvature energy density dominates over the *potential* part, for example. The authors employed a Poincaré *compactification* method, which is beyond the scope of this work.

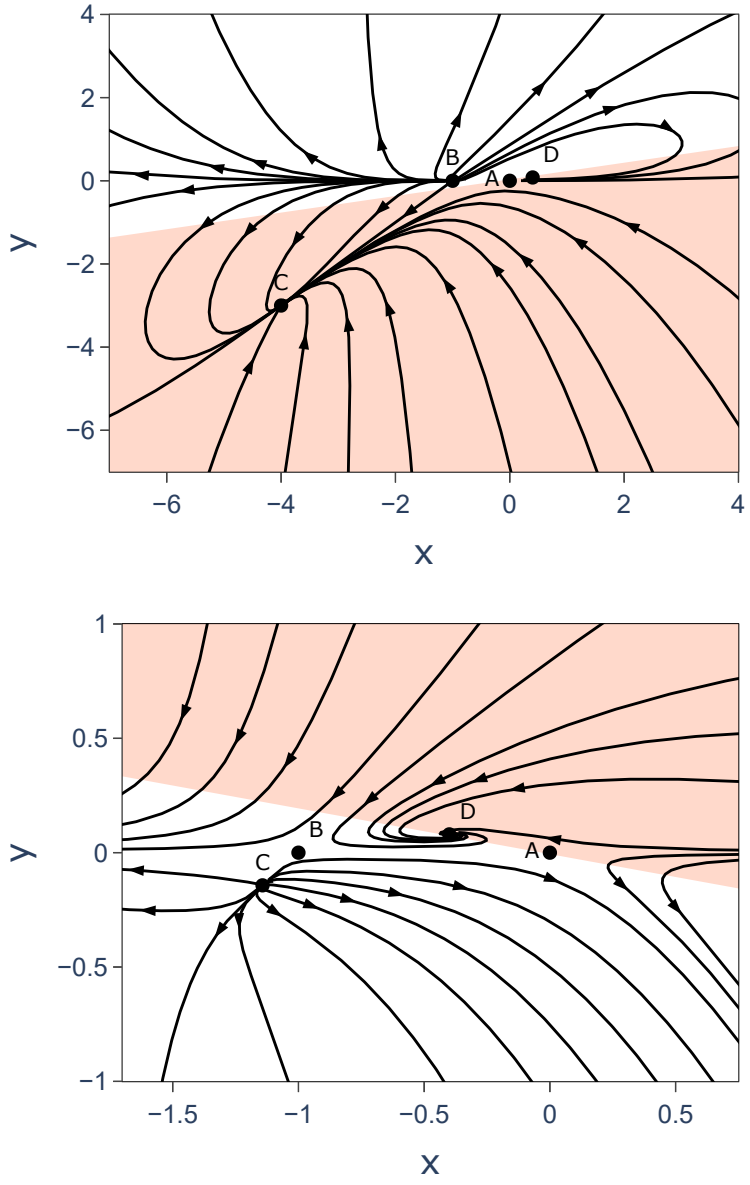

Figure 2.6: Phase portrait of the dynamical system (2.60)–(2.61) describing vacuum cosmological evolution in R^n gravity with $n = 4/5$ (top) and $n = 6/5$ (bottom). Orange shaded area denotes the accelerated expansion.

For our pictorial representation, we chose the power of n from the ranges $1/2 < n < 1$ and $1 < n < 5/4$ to demonstrate the stability alternation among the points B and C, as well as the differences in accelerated and decelerated evolutions. The point D exhibits complex eigenvalues with negative real parts within both of these intervals, meaning that we just encountered a stable spiral point for the first time in this work. This is the only other point where the curvature parameter K is nonzero, therefore exhibiting characteristics of the Milne model. In both selected intervals, the universe can transit (even multiple times) between accelerated and decelerated expansion before eventually stabilizing at $q = 0$.

For $n = 4/5$, the point B functions as a past attractor for all trajectories originating within the decelerated region. These may either approach the point D or, more interestingly, reach the C attractor, which gives rise to accelerated expansion – an alternative to dark energy.

For $n = 6/5$, this feature diminishes, the point C is transformed to a repeller in the decelerated region and the point B becomes a saddle. As a result, orbits starting in the decelerated region can only proceed toward continued decelerated evolution or spiral towards D. The latter represents the only pathway for the trajectories to cross from decelerated to accelerated expansion.

Matter case

Enriching our universe with some amount of baryonic matter in a form of perfect fluid substantially impacts its evolution, and an additional dimension is needed to conduct a comparable analysis. Notably, the matter terms in (2.55) are coupled with a generic power of the curvature R. This has a significant implication: since the sign of Ricci scalar is not fixed in general, these matter terms may not be well-defined for every n. Consequently, the field equations themselves can cease to be real-valued, indicating that not all R^n gravities remain consistent in the presence of standard matter. To ensure consistency, one must restrict n to integer values or rational numbers with odd denominators, for which real-valued roots of negative curvature are defined. Nonetheless, for $n = 6/5$ and $n = 4/5$ considered in vacuum example, these constraints on n are satisfied, allowing us to proceed with an extended set

$$x = \frac{\dot{R}}{RH}(n-1)\,, \quad y = \frac{R}{6nH^2}(1-n)\,, \quad z = \frac{2\kappa\rho}{3n\chi(n)H^2R^{n-1}}\,, \quad K = \frac{k}{a^2H^2}\,, \tag{2.63}$$

where the novel variable z traces the contribution of the energy density of standard matter weighted by a power of the Ricci scalar.

Deciding to constrain K via

$$1 + K + x - y - z = 0 \tag{2.64}$$

as previously, the three remaining variables evolve according to

$$x' = \frac{2y(n-2)}{n-1} - 2x - 2x^2 - \frac{xy}{n-1} + z(1+x) - 3wz\,, \tag{2.65}$$

$$y' = \frac{y}{n-1}[x(3-2n) - 2y + 2(n-1)(z+1)]\,, \tag{2.66}$$

$$z' = z\left(2z - 1 - 3x - \frac{2y}{n-1} - 3w\right)\,, \tag{2.67}$$

where the derivatives are taken with respect to logarithmic time, as previously.

Table 2.6: Fixed points of the system describing R^n gravity with matter modelled as a perfect fluid (2.65)–(2.67) and their eigenvalues.

Point	$\{x, y, z, K\}$
A	$\{0, 0, 0, -1\}$
B	$\{-1, 0, 0, 0\}$
C	$\left\{\frac{2(n-2)}{2n-1}, \frac{4n-5}{2n-1}, 0, 0\right\}$
D	$\{2(1-n), 2(n-1)^2, 0, 2n^2-2n-1\}$
E	$\{-1-3w, 0, -1-3w, -1\}$
F	$\{1-3w, 0, 2-3w, 0\}$
G	$\left\{\frac{-3(n-1)(1+w)}{n}, \frac{(n-1)[4n-3(w+3)]}{2n^2}, \frac{13+9w}{2n} - \frac{3(1+w)}{2n^2} - 4 - 3w, 0\right\}$
Point	**Eigenvalues**
A	$\{-2, 2, -1-3w\}$
B	$\left\{2, \frac{4n-5}{n-1}, 2-3w\right\}$
C	$\left\{\frac{4n-5}{n-1}, \frac{4n+2-4n^2}{2n^2-3n+1}, \frac{-2n^2(4+3w)+n(9w-13)-3(1+w)}{(n-1)(2n-1)}\right\}$
D	$\left\{n-2+\sqrt{3n(3n-4)}, n-2-\sqrt{3n(3n-4)}, 2n-3(1+w)\right\}$
E	$\left\{-2, \frac{2n-3(1+w)}{n-1}, 1+3w\right\}$
F	$\left\{2, \frac{4n-3(1+w)}{n-1}, 3w-2\right\}$
G	$\left\{\frac{3-2n+3w}{n}, \frac{P_1(n,w)-\sqrt{P_2(n,w)}}{4n(n-1)}, \frac{P_1(n,w)+\sqrt{P_2(n,w)}}{4n(n-1)}\right\}$
	$P_1(n,w) = 3(1+w) + 3n[w(2n-3)-1]$
	$P_2(n,w) = (n-1)[4n^2(8+3w)^2 - 4n^2\{152+3w(55+18w)\}$
	$+ 3n(1+w)(139+87w) - 81(1+w)^2]$

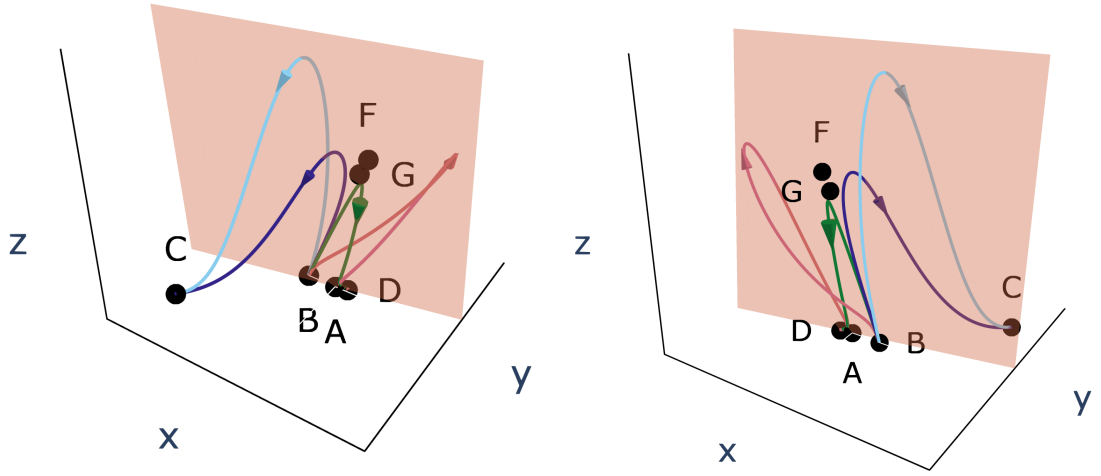

Figure 2.7: Some trajectories of the R^n gravity model with $n = 4/5$ containing baryonic matter, characterized by $w = 0$, presented from two perspectives. The two blue orbits represent potential evolutionary paths consistent with current observations. For clarity, the plane $\mathfrak{q} = 0$ is shaded, rather than the entire accelerated volume, noting that the point C resides within the $\mathfrak{q} < 0$ portion of the phase space.

In addition to the invariant submanifold defined by $y = 0$, the plane $z = 0$ also emerges as an invariant. Similarly to the vacuum case, a global attractor cannot exist in these models, as no single orbit is capable of traversing the entire phase space, and if it originates from $z_i, y_i \neq 0$, it can only approach these submanifolds asymptotically.

The equation

$$\mathfrak{q} = -\frac{\dot{H}}{H^2} - 1 = -x + z - \frac{y}{n-1} \tag{2.68}$$

equal to zero defines a plane that separates the accelerating ($\mathfrak{q} < 0$) and decelerating ($\mathfrak{q} > 0$) dynamics, which is depicted in Figure 2.7.

Instead of providing a detailed discussion of the stability of equilibrium points for each range of n, as presented in [117], we will supplement that work with a graphical representation for $n = 4/5$, as it falls within the range where meaningful agreement with the observed Universe evolution can be achieved. Notice that the four points encountered, A, B, C, D, remain fixed at the same coordinates and retain their stability properties. The points E and F are consistently saddle points. Regarding the point G, its eigenvalues cannot be computed explicitly for a general value of n; however, they can be evaluated numerically over specific intervals.

Within the selected range $0.71 \lesssim n \lesssim 1$, G functions as a pure saddle point when $w = 0$ and almost coincides with the saddle point F. These two can be interpreted as "almost-Friedmann" transient solutions with differing power-laws. They have the potential to influence trajectories such that they experience a matter-dominated era before subsequently reaching the C attractor, as illustrated by the two blue orbits in Figure 2.7. The presence of such orbits indicates that R^n gravity can effectively model the

accelerated expansion phenomenon as a higher order gravitational effect within a certain interval of n, while also reproducing cosmological history as we understand it today.

We also depicted certain trajectories, marked in green and red, which, although not immediately evident from the visualization, spiral towards D after experiencing a period of matter domination, rather than approaching the C attractor. The universes linked to these orbits exhibit several transitions between the decelerated and accelerated regimes before ultimately stopping to expand.

2.2.4 Einstein–Cartan cosmology

To complement the cosmological performance of dynamical systems, we give the floor to the effects of torsion. Unlike Brans–Dicke and R^n theories, the analysis of Einstein–Cartan evolution equations is relatively fast and minimalistic, which makes it well-suited for a graceful closing of this chapter. In addition, it offers a seamless transition to the upcoming core topic.

Spatially open universe

In order to transform equations (1.78) and (1.79) that describe the evolution of universe within a framework enriched by matter spin density, we may exploit a sign preceding the matter spin density and propose normalization

$$\eta = \sqrt{H^2 + \frac{\kappa\rho_{\mathrm{s}}}{3}}, \tag{2.69}$$

through which we establish the variables in the following fashion:

$$X = \frac{H}{\eta}\,, \quad \Omega_{\mathrm{m}} = \sqrt{\frac{\kappa\rho}{3\eta^2}}\,, \quad \Omega_{\mathrm{k}} = \sqrt{-\frac{k}{a^2\eta^2}}\,. \tag{2.70}$$

The Friedmann constraint associated with this selection of variables,

$$1 = \Omega_{\mathrm{m}}^2 + \Omega_{\mathrm{k}}^2\,, \tag{2.71}$$

reveals that we are even confined to a bounded phase space, a favourable contrast to working with an unbounded spatial domain defined by $k = -1$. Within this compact region, we will identify a finite area, characterized via

$$\frac{\ddot{a}}{a\eta^2} = -\frac{1}{2}\left[4(X^2 - 1) + \Omega_{\mathrm{m}}^2(1 + 3w)\right]\,. \tag{2.72}$$

Where the term in square brackets of (2.72) becomes negative, the evolution proceeds at an accelerated pace.

Table 2.7: Fixed points and their eigenvalues for the 2D system (2.73)–(2.74) describing the cosmological evolution within Einstein–Cartan theory in hyperbolic geometry ($k = -1$).

Point	$\{X, \Omega_m, \Omega_k\}$	Eigenvalues
F_+	$\{1, 1, 0\}$	$\{3w - 3, 3w + 1\}$
F_-	$\{-1, 1, 0\}$	$\{-1 - 3w, 3 - 3w\}$
M_+	$\{1, 0, 1\}$	$\left\{-4, \frac{1}{2}(-1 - 3w)\right\}$
M_-	$\{-1, 0, 1\}$	$\left\{4, \frac{1}{2}(1 + 3w)\right\}$

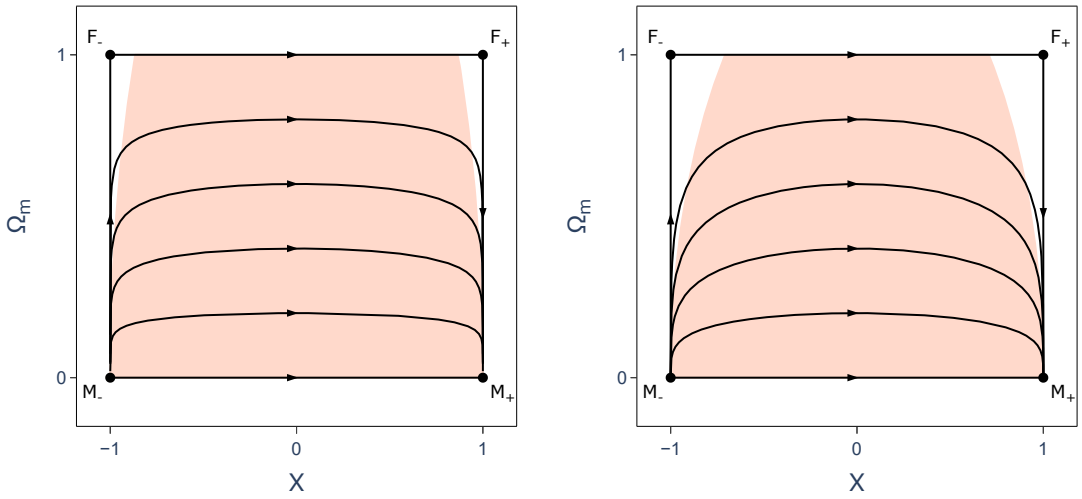

Figure 2.8: Phase portrait of the dynamical system (2.73)–(2.74) corresponding to the Einstein–Cartan cosmology in hyperbolic spatial geometry with $w = 0$ (left) and $w = 1/3$ (right). The orange portion of phase space denotes the accelerated regime.

The adjusted normalization (2.69) is propagated to the derivation of the autonomous dynamical system in a standard manner, i.e., $\mathrm{d}\tau = \eta\,\mathrm{d}t$, and we obtain

$$X' = \frac{1}{2}\left(X^2 - 1\right)\left[\Omega_m^2(1 + 3w) - 4\right], \tag{2.73}$$

$$\Omega_m' = \frac{1}{2}X\Omega_m(1 + 3w)\left(\Omega_m^2 - 1\right). \tag{2.74}$$

The walls of the phase portraits presented in Figures 2.8 are shaped by four invariant submanifolds: $X = \pm 1, \Omega_m = 0, \Omega_m = 1$. The last mentioned describes the flat universe composed solely of matter, as Ω_k vanishes along this line, while the opposite case, where Ω_m is zero, corresponds to evolution within universe with curvature only.

As observed, all orbits (except for GR limits present at $X = \pm 1$ boundaries) demonstrate the bounce scenario. In Einstein–Cartan theory, a spin–torsion coupling generates

an effective repulsive term at high densities, which causes trajectories starting with nonzero value of Ω_m to perceive *accelerated contraction* $\longrightarrow$ *bounce at* $\dot{a} = 0$ $\longrightarrow$ *accelerated expansion* before crossing to decelerated regime. Even within the Milne universe, a bounce is present; however, this universe remains confined to the accelerated region.

Spatially closed universe

Are bounces an unavoidable destiny of physically feasible trajectories in Einstein–Cartan theory, even within positively curved spatial geometries? To answer this completing inquiry, we want to normalize with a factor that also provides tickets to the $H = 0$ destination. In this case, we can make use of a familiar normalization

$$\eta = \sqrt{H^2 + \frac{k}{a^2}}, \tag{2.75}$$

used in Standard cosmology with $k = 1$. The variables can then be defined accordingly

$$X = \frac{H}{\eta}\,, \quad \Omega_m = \sqrt{\frac{\kappa\rho}{3\eta^2}}\,, \quad \Omega_s = \sqrt{\frac{\kappa\rho_s}{3\eta^2}}\,. \tag{2.76}$$

This appears similar to the formulation of (2.38), with the exception of the square roots, which are incorporated merely to facilitate a smoother and more algebraically manageable dynamical system. The key nuance is conveyed by a sign preceding ρ_s, which influences the alternative Friedmann constraint as

$$1 = \Omega_m^2 - \Omega_s^2\,. \tag{2.77}$$

As in the case of R^n gravity, we observe non-compact phase space. Although, in this context, it is less severe, since X is inherently bounded between 1 and -1, by definition. Also, since Ω_m^2 and Ω_s^2 are always positive, our phase space is restricted to a semi-infinite strip constrained by a hyperbolic equation (2.77). Notice that the Ω_s^2 component effectively behaves as a negative energy density.

It is particularly easy to evaluate the accelerated region in the resulting plots, as

$$\frac{\ddot{a}}{a\eta^2} = -\frac{1}{2}\left[4 + 3\Omega_m^2(w-1)\right] \tag{2.78}$$

crosses zero at a constant value of Ω_m, analogously to (2.43). Differentiating (2.76) with respect to τ, again defined via (2.42), we obtain the system

$$X' = \frac{1}{2}\left(X^2 - 1\right)\left[4 + 3\Omega_m^2(w-1)\right]\,, \tag{2.79}$$

$$\Omega_m' = \frac{3}{2}X\Omega_m(w-1)\left(\Omega_m^2 - 1\right)\,. \tag{2.80}$$

Table 2.8: Fixed points and their eigenvalues for the 2D system (2.79)–(2.80), describing the cosmological evolution within Einstein–Cartan theory in closed spatial geometry ($k = 1$).

Point	$\{X, \Omega_{\rm m}, \Omega_{\rm s}\}$	Eigenvalues
F_+	$\{1, 1, 0\}$	$\{3w - 3, 3w + 1\}$
F_-	$\{-1, 1, 0\}$	$\{-1 - 3w, 3 - 3w\}$
E	$\left\{0, \frac{2}{\sqrt{3(1-w)}}, \sqrt{-1 + \frac{4}{3(1-w)}}\right\}$	$\left\{-\sqrt{\frac{-2-4w+6w^2}{1-w}}, \sqrt{\frac{-2-4w+6w^2}{1-w}}\right\}$

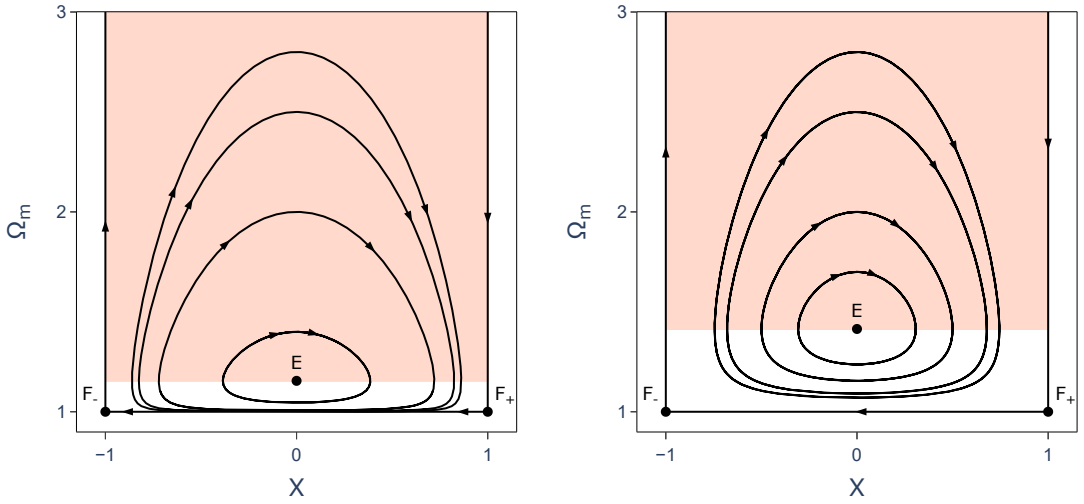

Figure 2.9: Phase portrait of the dynamical system (2.79)–(2.80) corresponding to the Einstein–Cartan cosmology in closed spatial geometry with $w = 0$ (left) and $w = 1/3$ (right). The orange portion of phase space denotes the accelerated regime.

As noted above, the variables are constructed so that infinite expansion or contraction rates are mapped to the finite boundaries, defined by invariant submanifolds $X = \pm 1$. On the other hand, the behaviour confined to the submanifold $\Omega_{\rm m} = 1$ corresponds to the standard GR in closed geometry, because $\Omega_{\rm s} = 0$ – the expanding Friedmann universe attains its maximum size at $X = 0$ and then collapses, as the curvature governs the turnaround point. The most prominent new feature, is that a combined contribution of both curvature and spin density parameters produces *cyclic universes*. The presence of a stable centre type fixed point E with purely imaginary eigenvalues (provided that w is physical) suggests the existence of *closed* trajectories, indicating oscillatory cosmological solutions. This represents a significant distinction from the GR single bounce solutions in a closed universe context, where all the orbits are heteroclinic and periodic cycles are not possible. This analysis affirms the natural capability of Einstein–Cartan theory to prevent the occurrence of cosmological singularity, as long as the universe seizes maximal spatial symmetry (FLRW geometry), thereby serving as an alternative to inflation.

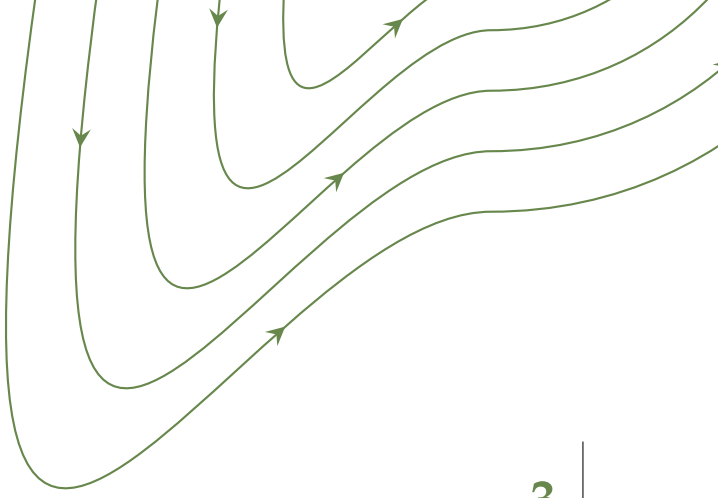

3

Minimal Exponential Measure model

The following pages offer an overview of the model we are focusing on. We outline the larger framework of Generalized Coupling Theories (GCT), as proposed by Feng and Carloni in 2020 [1], within which the Minimal Exponential Measure (MEMe) model emerges as the simplest case. We discuss certain model predictions and the observational constraints on its key parameter. Eventually, we demonstrate that, when combined with a single perfect fluid assumption, the MEMe model yields cosmological equations with unique characteristics and these equations can be solved *exactly* within the linearized version of the theory.

The primary distinguishing property of this model resides in its physical motivation and foundational principles. Specifically, the GCT family questions and re-evaluates the universality and nature of the minimal coupling between matter and geometry. This concept of re-examining the interaction between spacetime curvature and the energy-momentum tensor stems from the observation that the limitations of GR become evident when analysing systems involving numerous interacting particles (classical fluids) or matter fields, such as the behaviour of a perfect fluid in cosmology or the complex gravitational potentials present in galaxies and galaxy clusters. On the contrary, the most precise confirmations of GR – such as light deflection tests, perihelion shifts of planetary orbits, and gravitational wave detections – concern scenarios with only a limited number of test particles. Hence, it is primarily the vacuum Einstein's equations that have been thoroughly verified.

Regarding the perspective of modified gravity taxonomy encountered in Chapter 1, the MEMe model, along with its GCT parent branch, allows for several complementary classifications. Specifically, it can be viewed as a bimetric theory due to the existence of an auxiliary background metric in the presence of matter (see 1.2.1). It can also be classified as a minimally modified gravity model of type-I, as it does not introduce additional propagating gravitational degrees of freedom and admits an Einstein frame (see 1.3.1). Furthermore, it shares structural similarities with the Einstein–Cartan theory, since the additional tensor field exhibits behaviour analogous to the torsion tensor (see 1.4.2). This overlap provides benefits for fostering connections within the field of modified gravity.

3.1 Generalized coupling

In developing a consistent theory of gravity, Einstein required that his proposed equations (1.10) reproduce Poisson-like equations for the gravitational field in the weak-field limit, preserve the variational structure of the vacuum equations, and, mainly, naturally incorporate conservation of the matter energy-momentum continuum. This led to a straightforward proportionality relationship between the Einstein tensor $G_{\mu\nu}$ and the stress-energy tensor $T_{\mu\nu}$, as the Bianchi identity satisfied by spacetime curvature – $\nabla^\mu G_{\mu\nu} = 0$ – and the assumption of the usual conservation law – $\nabla^\mu T_{\mu\nu} = 0$ – then hold automatically. However, one can see this requirement also as the fact that the entire gravitational field equations are divergence free, while imposing that the Bianchi identities for $T_{\mu\nu}$ still hold, so that matter conservation laws are upheld.

By relaxing the assumption of minimal coupling, one may introduce an additional fundamental coupling tensor, $\chi_{\mu\nu}{}^{\alpha\beta}$, which acts as a mediator of the spacetime response to a particular matter distribution and extends Einstein's field equations in the following form:

$$G_{\mu\nu} = \chi_{\mu\nu}{}^{\alpha\beta} T_{\alpha\beta} \,. \tag{3.1}$$

An initial examination of this idea, its motivation, and general implications is presented in [118]. Certainly, the coupling tensor will be significantly constrained, namely $\nabla^\mu G_{\mu\nu} = 0$ restricts it to obey

$$\left(\nabla^\nu \chi_{\mu\nu}{}^{\alpha\beta}\right) T_{\alpha\beta} + \chi_{\mu\nu}{}^{\alpha\beta} \nabla^\nu T_{\alpha\beta} = 0 \,, \tag{3.2}$$

while, due to the symmetries of $G_{\mu\nu}$ and $T_{\mu\nu}$, it follows that

$$\chi_{(\mu\nu)(\alpha\beta)} = \chi_{\mu\nu\alpha\beta} \,. \tag{3.3}$$

To ensure the regularity of the field equations, this tensor is also supposed to be invertible.

An instructive analogy can be drawn with the elasticity theory, in which the deformation of a medium is governed by the stress-strain relationship encoded in the elasticity tensor, typically denoted as C^{ijkl}. In concrete,

$$T^{ij} = C^{ijkl} E_{kl} \,, \tag{3.4}$$

where T^{ij} represents the components of the Cauchy stress tensor and E_{kl} are components of the infinitesimal strain tensor. Both equations, (3.1) and (3.4), can be viewed as the most general linear relations between the two second-rank tensors. Classical electrodynamics also admits a similar formulation [119]. In fact, if we wish to treat the electromagnetic field within *macroscopic matter*, we should consider a generalized linear constitutive relation

$$\mathcal{H}^{ij} = \frac{1}{2} \tilde{\chi}^{ijkl} F_{kl} \,, \tag{3.5}$$

where $\mathcal{H}^{ij}$ is the *electromagnetic excitation* tensor (also known as the Maxwell tensor density), which describes the medium's response, F_{kl} is the standard electromagnetic field strength (Faraday) tensor, and $\tilde{\chi}^{ijkl}$ is the *constitutive* tensor characterizing the

properties of the medium. The factor $1/2$ in front accounts for the antisymmetry of F_{kl} and $\mathcal{H}^{ij}$, ensuring that the linear map $F \to \mathcal{H}$ is correctly normalized over independent components only. In this picture, the geometry of spacetime deforms under the influence of matter fields, and the specific character of this deformation depends on the properties or symmetries of the coupling tensor – just as in elasticity and electromagnetism, the behaviour of the medium simplifies in special cases such as isotropy.

Equation (3.1) can be formulated such that the vacuum phenomenology of General Relativity remains entirely unaffected. To preserve $G_{\alpha\beta} = 0$ in the absence of matter, an additional constraint has to be imposed. Such constraint can be obtained contracting both sides of (3.1) by the inverse of ${\chi_{\mu\nu}}^{\alpha\beta}$:

$$\chi^{\mu\nu}{}_{\alpha\beta} G_{\mu\nu} = T_{\alpha\beta} \,. \tag{3.6}$$

In this way it is clear that when $T_{\alpha\beta} = 0$ the 4-rank tensor has to reduce to a pair of Kronecker deltas (up to a factor $\kappa = 8\pi G/c^4$),

$${\chi_{\mu\nu}}^{\alpha\beta} = {\delta_\mu}^\alpha {\delta_\nu}^\beta \,. \tag{3.7}$$

Like that, GCTs overcome a common difficulty faced by many modified gravity theories, in which nontrivial vacuum solutions emerge and are often in tension with observational constraints.

The field equations (3.1) can be derived from an action principle. In theories with generalized coupling, the total action is constructed from multiple functionals that characterize the interaction among geometry, the matter sector, and the coupling field. This can be written as

$$S = \int \mathrm{d}^4x \left\{ \frac{1}{2\kappa} R\sqrt{-g} + L_\mathrm{m}[\varphi, \mathfrak{g}]\sqrt{-\mathfrak{g}} \right\} + S_\chi \,, \tag{3.8}$$

where $L_\mathrm{m}[\varphi, \mathfrak{g}]$ is the Lagrangian density associated with the matter fields φ and S_χ denotes the general action of the coupling field ${\chi_{\mu\nu}}^{\alpha\beta}$. In order to write this action, two separate metrics are used for convenience. It is clear from (3.8) that the familiar metric $g_{\mu\nu}$, which characterizes the geometric structure of spacetime, is no longer the one controlling the motion of matter. In fact, the Lagrangian L_m now contains the quantity $\mathfrak{g}_{\mu\nu}$ which acts as an additional effective metric minimally coupled to matter defined by

$$\mathfrak{g}_{\mu\nu} = {\chi_{\mu\nu}}^{\alpha\beta} g_{\alpha\beta} \,, \tag{3.9}$$

$$\mathfrak{g}^{\alpha\beta} = {\chi_{\mu\nu}}^{\alpha\beta} g^{\mu\nu} \,. \tag{3.10}$$

For simplicity, we can assume that the rank-4 coupling tensor ${\chi_{\mu\nu}}^{\alpha\beta}$ may be constructed from invertible rank-2 coupling tensors ${A_\mu}^\alpha$, along with a scalar function $\Psi(A_\cdot{}^\cdot)$, such that

$${\chi_{\mu\nu}}^{\alpha\beta} = \Psi(A_\cdot{}^\cdot) {A_\mu}^\alpha {A_\nu}^\beta \tag{3.11}$$

with a vacuum property $\Psi(\delta_{\cdot}^{\cdot}) = 1$ when

$$A_{\mu}{}^{\alpha} = \delta_{\mu}{}^{\alpha} \,, \tag{3.12}$$

where $\delta_{\mu}{}^{\alpha}$ is the Kronecker delta. The transformations (3.9)–(3.10) then become:

$$\mathfrak{g}_{\mu\nu} = \Psi(A_{\cdot}^{\cdot}) A_{\mu}{}^{\alpha} A_{\nu}{}^{\beta} g_{\alpha\beta} \,, \tag{3.13}$$

$$\mathfrak{g}^{\alpha\beta} = \Psi^{-1}(A_{\cdot}^{\cdot}) \bar{A}^{\alpha}{}_{\mu} \bar{A}^{\beta}{}_{\nu} g^{\mu\nu} \,. \tag{3.14}$$

The effective metric $\mathfrak{g}_{\mu\nu}$ may be referred to as the *Jordan frame* metric, while $g_{\mu\nu}$ as the *Einstein frame* metric. Furthermore, the coupling tensors $A_{\mu}{}^{\alpha}$ are assumed to be symmetric and nondynamical.

The decomposition (3.11) enables the action (3.8) to be expressed as follows [1]

$$\begin{aligned} S[\varphi, g^{\cdot\cdot}, A_{\cdot}^{\cdot}] = S_{\mathrm{EH}}[g^{\cdot\cdot}] + S_{\Lambda}[g^{\cdot\cdot}] + S_{\mathrm{A}}[A_{\cdot}^{\cdot}, g^{\cdot\cdot}] + S_{\mathrm{m}}[\varphi, \mathfrak{g}^{\cdot\cdot}] = \\ \frac{1}{2\kappa} \int \mathrm{d}^4x \sqrt{-g}(R - 2\Lambda) - \frac{\lambda}{\kappa} \int \mathrm{d}^4x \sqrt{-g}[1 - F(A_{\cdot}^{\cdot})] \\ + \int \mathrm{d}^4x \sqrt{-\mathfrak{g}} L_{\mathrm{m}}[\varphi, \mathfrak{g}^{\cdot\cdot}] \,, \end{aligned} \tag{3.15}$$

where as before S_{EH} is the Einstein–Hilbert action, a cosmological term has been introduced via S_{Λ} and the last term, S_{m}, is the matter action associated to L_{m}. The functional S_{χ} is now replaced by S_{A} whose role lays in encoding the physics of the generalized coupling, precisely through the function $F(A_{\cdot}^{\cdot})$. A specific form of $F(A_{\cdot}^{\cdot})$ must be specified to commence the investigation, similarly to how a function $f(R)$ must be selected to give meaning to any analysis of $f(R)$ theories, as indicated in Section 1.2.3. There is no unique formulation of $F(A_{\cdot}^{\cdot})$ that results in the constraint equation, $A_{\mu}{}^{\alpha} = \delta_{\mu}{}^{\alpha}$, as a solution in the absence of matter.

Two simple examples of classes of theories (distinguished by the structure of the $F(A_{\cdot}^{\cdot})$ function) are discussed in [1], and our focus will be on one of them in the following sections. It is important to note that both these choices involve *homogeneous* functions, i.e., they explicitly depend on the tensor $A_{\mu}{}^{\alpha}$, but not on its inverse $\bar{A}^{\mu}{}_{\alpha}$.

The inclusion of the term $1 - F(A_{\cdot}^{\cdot})$ in the functional S_{A}, instead of just $F(A_{\cdot}^{\cdot})$ alone, is intended to ensure the preservation of observational constraints. Later, we will find out that λ has to be very large and negative, which would provide the theory with both a wrong value and a wrong sign of the cosmological constant. To further clarify this point, we can reshuffle equation (3.15) as:

$$\begin{aligned} S[\varphi, g^{\cdot\cdot}, A_{\cdot}^{\cdot}] = \frac{1}{2\kappa} \int \mathrm{d}^4x \sqrt{-g}[R - 2(\Lambda - \lambda)] \\ - \frac{\lambda}{\kappa} \int \mathrm{d}^4x \sqrt{-g} F(A_{\cdot}^{\cdot}) + \int \mathrm{d}^4x \sqrt{-\mathfrak{g}} L_{\mathrm{m}}[\varphi, \mathfrak{g}^{\cdot\cdot}] \,. \end{aligned} \tag{3.16}$$

This formulation indicates that within a GCT, there is an inherent modification in the conceptual understanding of a cosmological constant term. In particular, the observed

tiny value of the cosmological constant emerges as an effective quantity resulting from the interplay between a (bare) cosmological constant from the geometrical sector, Λ, and a contribution from the coupling sector, λ, which tempts to relate to the vacuum energy density for quantum fields. Both must be of similar magnitude, which then causes the gravitational parameter, say $\tilde{\Lambda}$, related to the observed value of the cosmological constant, to be very small, given by $\tilde{\Lambda} = \lambda - \Lambda$. This, in turn, implies that GCT do not eliminate the fine-tuning issue associated with the cosmological constant; however, it can be mitigated to some extent (within the MEMe model specifically), potentially reducing its severity.

3.1.1 General field equations

Upon varying (3.15) with respect to the metric $g_{\mu\nu}$, we obtain

$$G_{\mu\nu} + [\Lambda - \lambda(1-F)]g_{\mu\nu} = \kappa\Psi|A|\bar{A}^{\alpha}{}_{\mu}\bar{A}^{\beta}{}_{\nu}\mathfrak{T}_{\alpha\beta}\,, \tag{3.17}$$

and, upon the variation with respect to $A_{\mu}{}^{\alpha}$, we get

$$(\delta_{\mu}{}^{\alpha} - A_{\mu}{}^{\alpha})f_{\alpha}{}^{\nu} = \Psi^2|A|\left[\mathfrak{T}_{\alpha\beta}\mathfrak{g}^{\mu(\alpha}\bar{A}^{\beta)}{}_{\nu} + \mathfrak{T}\frac{1}{2\Psi}\frac{\partial\Psi}{\partial A_{\mu}{}^{\nu}}\right], \tag{3.18}$$

where the Jordan frame energy-momentum tensor $\mathfrak{T}_{\alpha\beta}$ is defined as

$$\mathfrak{T}_{\alpha\beta} := -\frac{2}{\sqrt{-\mathfrak{g}}}\frac{\partial S_{\mathrm{m}}}{\partial \mathfrak{g}^{\alpha\beta}}\,, \tag{3.19}$$

the trace of $\mathfrak{T}_{\alpha\beta}$ is

$$\mathfrak{T} := \mathfrak{T}_{\alpha\beta}\mathfrak{g}^{\alpha\beta}\,, \tag{3.20}$$

$|A| = \det(A_{\cdot}{}^{\cdot})$ and $\bar{A}_{\mu}{}^{\nu}$ denotes the inverse of the coupling tensor $A_{\mu}{}^{\nu}$. The tensor $f_{\nu}{}^{\mu}$ is constructed from $A_{\mu}{}^{\alpha}$ such that

$$\frac{\delta F}{\delta A_{\mu}{}^{\nu}} = (A_{\nu}{}^{\alpha} - \delta_{\nu}{}^{\alpha})f_{\alpha}{}^{\mu}\,. \tag{3.21}$$

Some key conclusions can be drawn from these equations. Differently from other theories, such as the scalar-tensor ones, where the field ϕ is dynamical [see (1.17)], the equation (3.18) shows that the field $A_{\mu}{}^{\alpha}$ is nondynamical, i.e., it is *algebraically* connected to the stress energy tensor $\mathfrak{T}_{\alpha\beta}$. Thereby, $A_{\mu}{}^{\alpha}$ does not amount to additional degrees of freedom into the theory, coherently with the fact that GCTs are classified as type-I MMG. In addition, the relation (3.18) indicates that at points where the energy-momentum tensor $\mathfrak{T}_{\alpha\beta}$ vanishes, the coupling tensors satisfy $A_{\mu}{}^{\alpha} = \delta_{\mu}{}^{\alpha}$. Conversely, when $\mathfrak{T}_{\alpha\beta} \neq 0$, additional terms influence the coupling, causing deviation from this condition. Therefore, we can think of $A_{\mu}{}^{\alpha}$ as a bookkeeping device that drives a nontrivial geometry-matter relationship.

3.2 The exponential coupling prototype

To proceed and begin the detailed analysis of the GCT, we need to select a specific form of $F(A_{\cdot}^{\cdot})$. Following [1], we choose the so-called *exponential theories*. This class of theories can be represented by general functional for $F(A_{\cdot}^{\cdot})$

$$-\frac{\lambda}{\kappa}\int \mathrm{d}^4x\sqrt{-g}F(A_{\cdot}^{\cdot}) = -\frac{\lambda}{\kappa}\int \mathrm{d}^4x\sqrt{-g}|A|^n E(A_{\cdot}^{\cdot})\,, \tag{3.22}$$

where $E(A_{\cdot}^{\cdot})$ function has to satisfy the property $E(\delta_{\cdot}^{\cdot}) = 1$. From the constraint equation obtained by variation of (3.22) with respect to ${A_\beta}^\alpha$, it can be shown that $E(A_{\cdot}^{\cdot})$ takes the following form

$$E(A_{\cdot}^{\cdot}) = \exp[k - f_{\mathrm{p}}(A_{\cdot}^{\cdot})]\,. \tag{3.23}$$

In the above, $f_{\mathrm{p}}(A_{\cdot}^{\cdot})$ is a finite polynomial satisfying the constraint (to second order) and $k = f_{\mathrm{p}}(\delta_{\cdot}^{\cdot})$. The simplest choice [1] is to take $f_{\mathrm{p}} = nA$ and $k = 4n$. Thus, (3.22) becomes

$$-\frac{\lambda}{\kappa}\int \mathrm{d}^4x\sqrt{-g}|A|^n\exp[n(4-A)] = -\frac{\lambda}{\kappa}\int \mathrm{d}^4x\sqrt{-\mathfrak{g}}\,. \tag{3.24}$$

Considering also the transformation of the determinant (which can be derived using (3.13)–(3.14) relations),

$$\sqrt{-\mathfrak{g}} = \sqrt{-g}|A|\Psi^2\,, \tag{3.25}$$

we conclude that Ψ should take the form of an exponential of a polynomial in ${A_\mu}^\alpha$, and the simplest such form (where $n = 1$) is

$$\Psi = \exp\left(\frac{4-A}{2}\right). \tag{3.26}$$

This choice and its inherent simplicity are what lends the name to the resulting theory – the *Minimal Exponential Measure* model. The MEMe model is the simplest homogeneous theory that can be constructed.

3.2.1 MEMe model field equations

Employing the (3.26) in relation (3.13), we deduce that the effective metric and the spacetime metric are connected through

$$\mathfrak{g}_{\mu\nu} = e^{(4-A)/2}{A_\mu}^\alpha{A_\nu}^\beta g_{\alpha\beta}\,. \tag{3.27}$$

We can effectively characterize the MEMe model via the action

$$S_{\mathrm{MEMe}} = \int \mathrm{d}^4x\left\{\frac{1}{2\kappa}[R - 2(\Lambda - \lambda)]\sqrt{-g} + \left(L_{\mathrm{m}}[\phi, \mathfrak{g}^{\cdot\cdot}] - \frac{1}{q}\right)\sqrt{-\mathfrak{g}}\right\}, \tag{3.28}$$

which is just a reformulation of expression (3.15), where we wish to explicitly use the metric (3.27), and we have defined the coupling parameter of the model as

$$q := \frac{\kappa}{\lambda} \,. \tag{3.29}$$

Then, the constraint equation for the field ${A_\mu}^\alpha$ can be derived and expressed as

$${A_\beta}^\alpha - {\delta_\beta}^\alpha = q[(1/4)\mathfrak{T}{A_\beta}^\alpha - \mathfrak{T}_{\beta\nu}\mathfrak{g}^{\alpha\nu}] \tag{3.30}$$

and the gravitational field equations take the form

$$G_{\mu\nu} + [\Lambda - \lambda(1 - e^{4-A}|A|)]g_{\mu\nu} = \kappa e^{(4-A)/2}|A|\bar{A}^\alpha{}_\mu\bar{A}^\beta{}_\nu\mathfrak{T}_{\alpha\beta} \,. \tag{3.31}$$

The (3.31) are obtained by varying the action with respect to the spacetime metric $g_{\mu\nu}$ or, equivalently, by replacing F and Ψ in (3.17) with corresponding expressions for the MEMe model.

Furthermore, as equation (3.30) is algebraic in nature, taking its trace allows us to extract the scalar sector of the constraint. It follows that

$$A - 4 = q\mathfrak{T}(A/4 - 1) \,, \tag{3.32}$$

which implies that $A = 4$. Substituting this solution into the (3.31) yields

$$G_{\mu\nu} + [\Lambda - \lambda(1 - |A|)]g_{\mu\nu} = \kappa|A|\bar{A}^\alpha{}_\mu\bar{A}^\beta{}_\nu\mathfrak{T}_{\alpha\beta} \,, \tag{3.33}$$

the final, simplified form of the MEMe model gravitational field equations. From this expression, it is evident that the variation in the cosmological constant term – observed and discussed shallowly in the previous section within the context of the arbitrary GCT – can be represented as

$$\Lambda_{\text{eff}} = \Lambda - \lambda(1 - |A|) = \Lambda - \lambda\left(1 - \frac{\sqrt{\mathfrak{g}}}{\sqrt{g}}\right) , \tag{3.34}$$

which reduces to the standard Λ for $\mathfrak{g} \approx g$, but generally exhibits nonconstant behaviour.

3.2.2 Perfect fluid

The process of exploring the new theory begins with the simplest choices of matter models. In Chapter 1, it was stated that all possible spatial symmetries restrict the matter content to the form of a perfect fluid. Here, the choice of fluid affects the field equations themselves, not solely the metric $g_{\mu\nu}$.

There is a significant nuance concerning the form of the energy-momentum tensor for a perfect fluid, arising from the assumption that matter couples minimally to $\mathfrak{g}_{\mu\nu}$, not to $g_{\mu\nu}$. When expressed in terms of fluid four-velocity u^μ, it can be written as follows:

$$\mathfrak{T}_{\mu\nu} = (\rho + p)u_\mu u_\nu + p\mathfrak{g}_{\mu\nu} \,. \tag{3.35}$$

Here, we have to stress that observers who are comoving with the matter (and thus share the same four-velocity u^μ) will be in free fall with respect to the metric $\mathfrak{g}_{\mu\nu}$, as all physical kinematical quantities are defined with respect to it. So, timelike four-velocities satisfy

$$u_\mu u_\nu \mathfrak{g}^{\mu\nu} = -1\,, \tag{3.36}$$

whereas the standard normalization using $g^{\mu\nu}$ generally does not hold,

$$u_\mu u^\mu = u_\mu u_\nu g^{\mu\nu} \neq -1\,. \tag{3.37}$$

These statements indicate that observers free falling with respect to $g^{\mu\nu}$ can instead be described by a timelike unit vector U^μ, which is obtained by rescaling u^μ as

$$U^\mu := u^\mu/\sqrt{-\varepsilon}\,, \tag{3.38}$$

where

$$\varepsilon := u^\mu u_\mu\,. \tag{3.39}$$

This normalization is, of course, independent of the specific matter model and is preserved when the matter sector is specified as a perfect fluid.

With the established specifications in mind, the ansatz for the solution of (3.30) can be applied

$$A_\mu{}^\alpha = Y\delta_\mu{}^\alpha - \varepsilon Z U_\mu U^\alpha\,, \tag{3.40}$$

which is the most general $(1,1)$-tensor compatible with perfect fluid symmetry, and enables to compute the determinant as

$$|A| = Y^3(Y + \varepsilon Z)\,. \tag{3.41}$$

The coefficient Y can be considered related to effective pressure, as it governs the isotropic background component of the auxiliary tensor, while Z may be associated with the energy density of the fluid, since it captures the contribution aligned with the four-velocity of the fluid. With this approach, we simply reduce the $A_\mu{}^\alpha$ matrix to two scalar quantities. These can be explicitly expressed by combining our perfect fluid ansatz with the field equation (3.30). In particular, we get

$$Y = \frac{4(1-pq)}{4-q(3p-\rho)} \quad \text{and} \quad Z = -\frac{q(\rho+p)[4-q(3p-\rho)]}{4(q\rho+1)^2}\,. \tag{3.42}$$

Further details of this derivation are covered in [1]. The explicit form of the determinant in the MEMe model gravitational field equations (3.31) [or (3.33)] is given by [utilizing (3.41)]:

$$|A| = \frac{256(1-pq)^3(q\rho+1)}{[4-q(3p-\rho)]^4}\,. \tag{3.43}$$

Einstein-like equations

The physical consequences of the MEMe model can be better understood by rearranging the equation (3.31) to consolidate all matter-dependent modifications into a single object. This approach allows us to restore the structure of GR, as the geometric sector becomes isolated from the modified matter coupling. Consequently, deviations from GR can be interpreted purely as an effective stress-energy contribution. Once again, this should not be confused with the Ellis trick; while the algebraic operations are identical, there is no new geometric dynamics being reinterpreted, as the Einstein tensor remains unchanged. Precisely, we can recast (3.31) in the form

$$G_{\mu\nu} = \kappa T_{\mu\nu} \tag{3.44}$$

with

$$T_{\mu\nu} = T_1 U_\mu U_\nu + T_2 g_{\mu\nu}\,, \tag{3.45}$$

where

$$T_1 = |A|(p+\rho) \quad \text{and} \quad T_2 = \frac{|A|(pq-1)+1}{q} - \frac{\Lambda}{\kappa}\,. \tag{3.46}$$

When $q \to 0$ ($\lambda \to \infty$), the factor $|A|$ tends to unity, leading to the following limits,

$$T_1 \to p + \rho \quad \text{and} \quad T_2 \to p - \frac{\Lambda}{\kappa}\,, \tag{3.47}$$

indicating that no pathologies are present, even though q appears in the denominator of T_2. Notice that, in this limit, we have also obtained the same stress energy tensor as standard perfect fluid.

Characteristic scale of q

What is a physical significance of this key parameter? In [1], the motivation for GCT and the MEMe model is formulated within the framework of *semiclassical gravity*, where classical geometry couples to quantum matter expectation values. This approach results in identifying q with the vacuum energy; more concretely, $1/q = \lambda/\kappa$ could correspond to vacuum energy density associated with quantum fields. In addition, the parameter q essentially determines the scale at which $\mathfrak{g}_{\mu\nu}$ ceases to function as a valid spacetime metric. This occurs because when $pq \to 1$, or equivalently, when $p \to 1/q$, the determinant $|A|$ approaches zero [see (3.43)]. Consequently, $A_\mu{}^\alpha$ and $\mathfrak{g}_{\mu\nu}$ become degenerate (noninvertible) and $\mathfrak{g}_{\mu\nu}$ can no longer serve as a proper spacetime metric. Thus, the scale is set by the value of q at which the standard formulation of QFT on the effective background $\mathfrak{g}_{\mu\nu}$ becomes invalid. Although the bimetric theory description breaks down in this way, it does *not* imply that the MEMe model itself breaks down, as the gravitational metric $g_{\mu\nu}$ remains well defined (regular) in the limit $pq \to 1$. This scenario assumed a positive value of q, but a similar effect is present even when q is negative; in this case $|A|$ vanishes as $\rho q \to -1$. A negative q, which corresponds to λ being negative valued is actually preferred for three independent considerations:

- *it yields a high-density de Sitter phase relevant for early cosmology,*
- *it is well motivated by the dominance of fermionic vacuum contributions and string theory (AdS-type vacua),*
- *if MEMe model is regarded as a limit of a more fundamental dynamical theory, the term* $(\lambda/\kappa)\sqrt{-\mathfrak{g}}$ *can be interpreted as an effective potential, and physically meaningful solutions should lie in its minima.*

The final point concerning the assurance of dynamical stability offers the most compelling justification for selecting $\lambda < 0$.

3.3 MEMe model predictions

Having conferred the theoretical structure of the MEMe model, the next logical step involves assessing its phenomenological viability. Any extension of GR must not only possess internal mathematical consistency but must also be in accordance with stringent experimental and observational constraints. Since 2020, the MEMe model has been investigated within various physical contexts, ranging from studies of weak field relevant to solar system tests to high energy phenomena in the early Universe. Together, the analyses we will review here define the currently permissible parameter space of the model.

3.3.1 Speed of Gravitational waves

The foundational paper that settles the core theory provides an initial constraint at no additional cost [1]. Since bimetric theories generally feature light cones derived from each metric that may not perfectly coincide, the MEMe theory anticipates a nuanced difference in the propagation of gravitational waves (GW) compared to GR. Two different propagation speeds are involved, entailed by the fact that linearized gravitational waves propagate on background metric $g_{\mu\nu}$, while electromagnetic waves propagate according to the Jordan frame metric $\mathfrak{g}_{\mu\nu}$. These two speeds – the speed of light c and the speed of gravitational waves c_g – are linked through following formula

$$c_g = c\sqrt{1 + \Psi Z(Y + \varepsilon Z)}\,, \tag{3.48}$$

which can be derived from the dispersion relation. In other words, it is predicted that GW propagating through a matter distribution will travel at a different speed than GW in a vacuum. Specifically, for negative values of q within $\rho < 1/|q|$ range, the GW may exceed the speed of light in matter. As Earth presents a relatively dense medium through which detectable GW travel, constraints on q can be achieved from the uncertainty in the difference of arrival times between GW detectors. This approach has been applied to GW170817 event and resulted in the following upper bound:

$$|q| < 4 \times 10^{23}\,\mathrm{GeV}^{-4} \approx 2 \times 10^{-14}\,\mathrm{m}^3\,\mathrm{J}^{-1}\,. \tag{3.49}$$

This constraint is somewhat weak; if new physics is anticipated to become prominent at the TeV scale – currently the highest energy scale explored – then the value of $|q|$ should be of the order of $10^{-50}\mathrm{m}^3\,\mathrm{J}^{-1}$.

3.3.2 Circular orbits and G measurements

A crucial requirement for any MG is consistency with our solar system observations. Initially, it is essential to verify that the Newtonian limit of the model reproduces Poisson's equation at leading order. Following this, high-precision experiments – such as measurements of Mercury's perihelion precession – require considerations beyond this approximation to the *post-Newtonian order*, where relativistic corrections become detectable. The parametrized post-Newtonian (PPN) formalism is commonly employed to compare alternative metric theories with stringent experimental tests and to quantify deviations from GR predictions. In vacuum, the MEMe model is guaranteed to have the correct PPN behaviour by definition, because its vacuum phenomenology is the same as GR. This is not the case when one considers the PPN limit within a matter distributions, such as in the case of the pattern of the star in a galaxy modelled as continuous fluid vortex.

In these last cases, the PPN analysis of the MEMe theory requires an *extension* of the standard PPN, as new potentials arise due to nontrivial matter coupling. This extension, as presented in [120], demonstrates that all standard PPN parameters of the MEMe model are identical to those of GR, with the exception of one additional parameter that is proportional to the scale of q:

$$\nu = \frac{3q}{2G}\,. \tag{3.50}$$

Spherically symmetric matter distributions are then analyzed, revealing that the gravitational binding energy of particles within such distributions is reduced in the MEMe model compared to GR. This reduction is attributed to the monopole term of the potential associated with ν, which consequently results in a lower gravitational mass for an object outside the matter source than the sum of its individual components, due to a decreased gravitational binding energy. This can be interpreted as indicating a dependence of the effective gravitational constant on the compactness of the source. A proposed experiment utilizing thick spherical shells could be conducted to constrain the parameter ν by detecting possible variations in the effective gravitational constant. Such measurements may allow for a substantially more stringent upper limit on $|q|$ than provided by equation (3.49), that is

$$|q| \lessapprox 2\times 10^{13}\,\mathrm{GeV}^{-4} \approx 10^{-24}\mathrm{m}^3\,\mathrm{J}^{-1}\,, \tag{3.51}$$

which, however, remains 12 orders of magnitude weaker than the scales associated with the inverse of the highest energy densities studied in accelerator experiments, and 26 orders of magnitude lower than the energy density corresponding to a TeV-scale breakdown.

In addition, the same article examined circular geodesics within the context of spherically symmetric Gaussian and isothermal matter distributions to compare the

resulting tangential velocity rotation curves with those predicted by the Newtonian limit of GR. The findings indicate that the MEMe model shows significant differences primarily at very high matter densities and thus cannot account for galactic rotation curves without incorporating dark matter. Although, it is important to note that spiral galaxies are considerably more complex structures and do not conform to a spherically symmetric, static, perfect fluid model under exploration.

3.3.3 Sharp gradients

A subsequently published paper [121] addresses MEMe model's behaviour at sharp boundaries. In GR, smooth matching of spacetime is working well even with abrupt matter boundaries; it is then necessary to verify that any extensions of GR do not produce pathologies when sharp gradients of the energy-momentum tensor are present. These sharp gradients are often modelled as discontinuities in the metric components. To properly analyse such scenarios, a comprehensive formalism involving *singular hypersurfaces* and *junction conditions* – known as the Israel formalism – is required. While these situations are highly relevant from a physical perspective, we will not delve into the technical details here. The key point is that the auxiliary field $A_\mu{}^\alpha$, which induces the Jordan frame metric, is not guaranteed to remain continuous across the hypersurface, contrary to $g_{\mu\nu}$. This raises important concerns regarding the consistency of the theory.

The analysis in [121] indicates that, in the *static case* of a spherically symmetric density profile, no singularities are present, provided that the Einstein frame metric remains continuous and the matter and field dynamics are solved consistently. However, sharply defined boundaries of neutron stars in these conditions could introduce large discontinuities in the metric, potentially resulting in observable consequences such as additional heating of the neutron star crusts. This is in principle measurable and may allow for a tighter constraint on the value of the parameter q.

Dynamical collapse of spherical pressureless dust fluid (Oppenheimer-Snyder collapse) under MEMe model instead suggests peculiar differences in the underlying physics. For preferred values $q < 0$, a compressive force emerges that depends on the matter distribution and intensifies near sharp boundaries. As a result of this process, overdense regions are compressed, while underdense regions are expanded.

3.3.4 Baryogenesis constraint

The most stringent constraint to date has been derived from *matter-antimatter asymmetry* [122]. In fact, analysis of nuclear and subnuclear processes in the early Universe currently places the tightest known restrictions on gravitational theories overall. The matter-antimatter asymmetry, also known as baryon asymmetry, is a prominent unresolved issue in physical cosmology. Given that matter and antimatter form and behave in nearly identical ways, it is expected that they were created in approximately equal amounts during the Big Bang, whereas in reality matter comprises the vast majority of the Universe. This is favourable, as a symmetric universe would likely have resulted in

complete annihilation, but the reasons behind this imbalance – and why anything exists at all – remain an open puzzle.

There is a well-known parameter η that quantifies the baryon asymmetry in the Universe; it is derived through the combination of predictions of the Big Bang Nucleosynthesis (BBN), observations of the Cosmic Microwave Background (CMB), and the Large-Scale Structure (LSS) of the Universe. Denoting the number densities of baryons/antibaryons in the Universe as $n_{\rm B}/n_{\bar{\rm B}}$, we write the baryon-to-entropy ratio as [113]

$$\eta_{\rm s} \equiv \frac{n_{\rm B} - n_{\bar{\rm B}}}{s} \lesssim (9.2 \pm 0.5) \times 10^{-11} \,, \tag{3.52}$$

where s stands for the entropy density of the Universe, which remained relatively constant throughout its evolution.

The standard approach to baryogenesis relies on particle physics beyond the Standard Model and the production of a net baryon surplus (3.52) is possible if Sakharov's conditions are satisfied. These are:

1. *processes exist that violate the baryon number,*
2. *the discrete C (charge conjugation) and CP (charge conjugation + parity) symmetries are violated,*
3. *thermal equilibrium is broken.*

While conventional baryogenesis mechanisms depend on CP violation, they generally maintain CPT symmetry, which is inherently preserved in local Lorentz-invariant QFT. However, if an interaction introduces an effective CPT-violating term within a time-dependent background – such as through curvature couplings – it is possible to generate a nonzero baryon asymmetry (3.52) even when thermal equilibrium is preserved. In this context, the third Sakharov criterion can be effectively relaxed. This is a core idea of *gravitational baryogenesis*.

In this geometric framework, rather than incorporating exotic particle physics, the interaction responsible for inducing dynamical CPT violation is characterized by a coupling between the derivative of the Ricci scalar curvature $\partial_\mu R$ and the baryon/lepton current $\mathcal{J}^\mu$:

$$\frac{1}{M_*^2} \int {\rm d}^4x \sqrt{-g} \mathcal{J}^\mu \partial_\mu R \tag{3.53}$$

and M_* denotes the cutoff mass scale of the effective theory. In a universe with dynamical curvature, this interaction generates an effective chemical potential that distinguishes baryons from antibaryons within thermal equilibrium conditions. While in standard radiation-dominated GR the Ricci scalar is zero and this mechanism is thus ineffective, alternative gravity models can induce a nonzero time derivative of the curvature scalar, allowing for baryon asymmetry generation. Therefore, gravitational baryogenesis serves as a valuable tool for probing the high-energy early-universe regime of the MEMe model. More specifically, implementing this mechanism within the MEMe model scheme,

considering the decoupling temperature $\mathcal{T}_{\rm D} = 10^{15}\,\mathrm{GeV}$ and a mass scale for the effective theory of $M_* = 10^{15}\,\mathrm{GeV}$, leads to a constraint on the parameter

$$q \lesssim -4.1 \times 10^{-63}\,\mathrm{GeV}^{-4} \approx -2 \times 10^{-100}\,\mathrm{m}^3\,\mathrm{J}^{-1} \tag{3.54}$$

for a spatially flat universe, while the open universe is compatible with baryogenesis in the much lower limit,

$$q \lesssim -6 \times 10^{-78}\,\mathrm{GeV}^{-4} \approx -3 \times 10^{-115}\,\mathrm{m}^3\,\mathrm{J}^{-1}\,. \tag{3.55}$$

This result is particularly noteworthy, as the inverse of q provided by (3.54) corresponds to an energy density that is ten orders of magnitude lower than the quantum vacuum energy density,

$$\rho_\Lambda^{\rm theory} \sim 10^{72} \div 10^{76}\,\mathrm{GeV}^4\,, \tag{3.56}$$

whereas (3.55) suggests that the energy density related to q is one order above the estimated range of the zero point energy density (3.56). This outcome reinforces the interpretation of q as a parameter associated with the quantum vacuum of matter fields and appears to validate the view of the MEMe model as a classical coarse-grained approximation of QFT in curved spacetime. The loss of relevance of the Jordan frame beyond this energy scale would simply indicate that, at higher energies, the generalized coupling employed in the MEMe model is no longer sufficient to approximate quantum behaviour.

3.4 Cosmology of the MEMe model

We are now approaching the primary focus of this work. After surveying the broad landscape of modified gravity and zooming in on the generalized coupling region with its fundamental constituent, MEMe model, we are now fully prepared to confront its cosmological dynamics. The dynamical systems methodology established in Chapter 2 will allow us to systematically explore how the theory governs the evolution of a homogeneous and isotropic universe.

As stated previously in Section 1.4, the cosmological models built on the field equations pertaining to MG theories can divulge a lot about their feasibility. Specifically, the main aspiration is to assess their ability to replicate phenomena such as inflation or the properties of the dark universe. Here, the MEMe model becomes the protagonist of the cosmic drama, while we observe – and judge – its performance.

The derivation of the cosmological equations of the MEMe model proceeds along well-trodden lines: the assumption of the FLRW metric (1.54) together with the perfect fluid prescription (3.35)–(3.43) inserted into (3.33) yield the corresponding cosmological dynamics. Without going into a detailed elaboration, one obtains the following relations [1]:

$$3q\left(H^2 + \frac{k}{S^2}\right) = \kappa|A|(\rho q + 1) - \kappa + q\Lambda\,, \tag{3.57}$$

which is the modified Friedmann equation, and

$$6q\left(\dot{H}+H^2\right)=\kappa|A|\left[2-\rho q(3w+1)\right]+2(q\Lambda-\kappa)\,, \tag{3.58}$$

a MEMe model's version of the acceleration equation. These are formulated in the frame of reference observers characterized by the velocity field U^μ defined by (3.38), since the u^μ is not normalized with $g^{\mu\nu}$ nor is guaranteed to be time-like. We will briefly recall that we assumed a barotropic EoS for the fluid, $p=w\rho$, $H=\dot{a}/a$ is the Hubble parameter, and $|A|$ is given by (3.43). In addition, the Bianchi identity, $\nabla^\alpha T_{\alpha\beta}=0$, gives the conservation law:

$$\dot{\rho}=-\frac{3H\rho(w+1)[q^2\rho^2w(3w-1)+\rho(q-7qw)+4]}{q^2\rho^2w(3w-1)-q\rho(3w^2+13w+2)+4}\,. \tag{3.59}$$

Similarly as in the standard cosmological paradigm based on GR with a cosmological constant, the three equations above are redundant, as one of them can be derived from the other two.

3.4.1 Analysis of the late time behaviour

A concise and straightforward cosmological analysis has already been conducted [1], and we bring a brief review here. Following the standard procedure, one can make use of three dimensionless cosmological variables (2.32), together with one model-specific variable, χ, through which we rescale the Hubble parameter:

$$L=\frac{\Lambda}{3H^2}\,,\quad K=\frac{k}{H^2a^2}\,,\quad \Omega=\frac{\kappa\rho}{3H^2}\,,\quad \chi=\frac{qH^2}{\kappa}\,. \tag{3.60}$$

Substituting from these to the Friedmann equation of the MEMe model (3.57), we arrive at the constraint

$$L-K-\frac{256(3\chi\Omega+1)^2(3w\chi\Omega-1)^3}{3\chi[3\chi\Omega(1-3w)+4]^4}-\frac{1}{3\chi}=1\,, \tag{3.61}$$

which enables us to reduce the dimensionality of a system from four to three. Unfortunately, selecting this set of variables does not provide us with a compact phase space, on the other hand, due to the notorious definitions of L, K and Ω, the physical interpretation remains quite familiar. The equation for the decelerated factor takes the following form

$$\mathfrak{q}=-\frac{128(3\chi\Omega+1)(3w\chi\Omega-1)^3[3\chi\Omega(3w+1)-2]}{3\chi[3\chi\Omega(1-3w)+4]^4}-L+\frac{1}{3\chi}\,. \tag{3.62}$$

To recast the cosmological equations into a form of an autonomous system, the standard dimensionless time variable τ (2.15) can be employed. Differentiating with respect to τ and indicating this with a prime, we obtain a collection of three ordinary differential equations:

$$\chi' = \frac{1}{3}\chi\left\{6(L-1) + \frac{256(3\chi\Omega+1)(3w\chi\Omega-1)^3[3\chi\Omega(1+3w)-2]}{\chi[3\chi\Omega(1-3w)+4]^4} - \frac{2}{\chi}\right\}, \tag{3.63}$$

$$\Omega' = \frac{1}{3}\Omega\left\{6(1-L) - \frac{256(3\chi\Omega+1)(3w\chi\Omega-1)^3[3\chi\Omega(1+3w)-2]}{\chi[3\chi\Omega(1-3w)+4]^4} + \frac{2}{\chi} - \frac{9(w+1)(3w\chi\Omega-1)[3\chi\Omega(3w-1)-4]}{4-3\chi\Omega(3w^2+13w+2)+9w\chi^2\Omega^2(3w-1)}\right\}, \tag{3.64}$$

$$L' = \frac{1}{3}L\left\{6(1-L) - \frac{256(3\chi\Omega+1)(3w\chi\Omega-1)^3[3\chi\Omega(1+3w)-2]}{\chi[3\chi\Omega(1-3w)+4]^4} + \frac{2}{\chi}\right\}. \tag{3.65}$$

From the dynamical system above, three invariant submanifolds $\Omega = 0$, $L = 0$ and $\chi = 0$ can be determined instantly. Setting the derivatives on the left-hand side of (3.63)–(3.65) to zero, one recognizes two fixed points – M and F – that can be identified with Milne and Friedmann solutions, and two lines of fixed points – $d\mathcal{S}_1$ and $d\mathcal{S}_2$ – that correspond to two de Sitter solutions with different time constants. This means that MEMe model's cosmology naturally admits two distinct types of exponential expansion.

That said, the fixed line $d\mathcal{S}_2$ resides on the boundary of the system, defined by $3\Omega\chi = -1$, analogous to the limiting case $\rho q \to -1$. As we have adopted the U^μ frame, this condition does not manifest itself as an explicit feature of the phase space, but it still constitutes a hypersurface that separates physical orbits, for which $3\Omega\chi < -1$, from dynamically inaccessible configurations. Additionally, $d\mathcal{S}_2$ becomes asymptotic in the case of matter modelled as pressureless dust ($w = 0$). This also implies that a singular surface defined by $3\chi\Omega + 4 = 0$, which arises from the structure of (3.63)–(3.65) when $w = 0$, does not influence physically relevant solutions, as it exists outside the physically permissible region.

The discussed fixed points and their stability analyses are summarized in Table 3.1. The accompanying phase portraits demonstrate how a broad range of initial conditions can produce an inflationary phase. However, to achieve complete cosmic histories that align with observational data, and therefore transverse the yellow volume of decelerated expansion in Figures 3.1, some further fine-tuning is necessary to ensure that $\Lambda \ll \lambda$. This fine-tuning is significantly less severe than the cosmological constant problem, as λ can, in principle, be independent of the Planck scale.

Table 3.1: Fixed points and their stability for the 3D system (3.63)–(3.65).

Point(s)	$\{\chi, \Omega, L, K\}$	Eigenvalues	Stability
M	$\{0, 0, 0, -1\}$	$\{-2, 2, -1 - 3w\}$	Saddle
F	$\{0, 1, 0, 0\}$	$\{-3(1+w), 3(1+w), 1+3w\}$	Saddle
$d\mathcal{S}_1$	$\{\chi, 0, 1, 0\}$	$\{-2, 0, -3(1+w)\}$	Attractor
$d\mathcal{S}_2$	$\left\{\frac{1}{3w\Omega}, \Omega, 1+w\Omega, 0\right\}$	$\{0, -2, -1\}$	Attractor

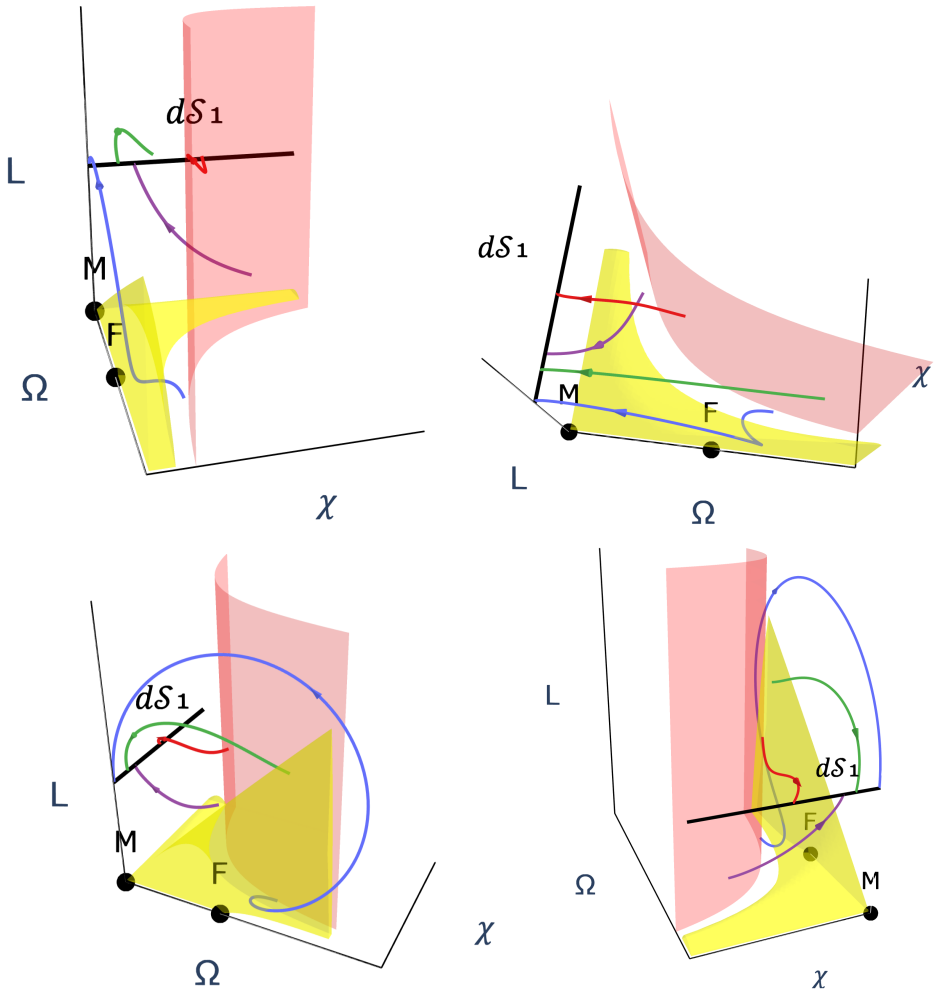

Figure 3.1: Three-dimensional phase portrait for the system (3.63)–(3.65) with $w = 0$ (top row) or $w = 1/3$ (bottom row) and $q < 0$ from two different eye-angles. The red surface indicates the boundary where $3\Omega\chi = -1$ within the phase space, only trajectories with initial conditions satisfying $3\Omega\chi < -1$ are taken into account. In the yellow region, the expansion is decelerating.

3.4.2 Linearized MEMe model cosmology

It is evident from the various analyses outlined in the previous Section 3.3 that the parameter q is indeed of a very small magnitude. Whenever such a hierarchy of scales arises in physics, it prompts us to perform a Taylor expansion with the expectation that the dominant behaviour can be captured by the leading-order terms of the established theory. A recent publication [123] is devoted to this precise question. There it is shown that linearization with respect to q permits an *exact solution* for the evolution of the scale factor. The linearized regime will guide much of the analysis developed in the remainder of this work.

Undoubtedly, the structure of the cosmological equations (3.57)–(3.58) indicates that, within the MEMe model, the gravitation of matter modelled as a perfect fluid differs substantially from that in GR, as described by (1.57)–(1.58). To approximate this influence to first order in q, one can perform a Taylor expansion of the conservation equation (3.59) around q, resulting in:

$$\dot{\rho} = -3\frac{\dot{a}}{a}(w+1)\rho\left[1+\frac{3}{4}q\rho(w+1)^2\right]. \tag{3.66}$$

The differential equation above can be solved exactly to give a function of density

$$\rho = \frac{4\rho_0}{a^{3w+3}[3q\rho_0(w+1)^2+4]-3q\rho_0(w+1)^2}, \tag{3.67}$$

where, although ρ_0 appears as an integration constant, the application of physical normalization conditions induces an *implicit dependence* on q, which should be considered when linearizing around $q=0$. This function, $\rho_0(q)$, is maintained in a fully general form, with its contribution treated consistently at linear order in q. Taking this into account via defining

$$\bar{\rho}_0 = \rho_0(0) \quad \text{and} \quad \bar{\rho}_0^{\dagger} = \left.\frac{\mathrm{d}\rho_0(q)}{\mathrm{d}q}\right|_{q=0}, \tag{3.68}$$

we may insert solution (3.67) into (3.57) to obtain the *linearized form of Friedmann equation*,

$$\frac{\dot{a}^2}{a^2} = -\frac{k}{a^2}+\kappa\left[\frac{4}{3}\frac{\bar{\rho}_0+q\bar{\rho}_0^{\dagger}}{a^{3(w+1)}}+2q(w+1)^2\frac{\bar{\rho}_0^2}{a^{6(w+1)}}\right]+\frac{\Lambda}{3}. \tag{3.69}$$

From this equation we can see that the modification term that emerged within the MEMe model with respect to GR is expected to have a huge impact at early times, as the second term in square parenthesis is proportional to $a^{-6(1+w)}$ and, when the scale factor a approaches zero, it becomes predominant. An effective equation of state can be attributed to this modification:

$$p_{\text{eff}} = (2w+1)\rho_{\text{eff}}. \tag{3.70}$$

Accordingly, this effective fluid adheres to a conservation law expressed as

$$\dot{\rho}_{\text{eff}} + 6H\rho_{\text{eff}} = 0, \tag{3.71}$$

which curiously resembles the evolution of the spin-induced correction in Einstein-Cartan cosmology (1.83). In fact, any quadratic density correction in cosmology will typically behave like a *stiff fluid* relative to the original matter content and dominate the very early dense universe.

The solution to (3.69) can be obtained for $k = 0$ only and takes the following form

$$a(t) = \left[A + Be^{-\sqrt{3\Lambda}(w+1)(t-t_0)} + Ce^{\sqrt{3\Lambda}(w+1)(t-t_0)}\right]^{\frac{1}{3w+3}} \tag{3.72}$$

with

$$A = -\frac{2\kappa(\bar{\rho}_0 + q\bar{\rho}_0^{\dagger})}{\Lambda}\,, \tag{3.73}$$

$$B = \frac{1}{2\Lambda(w+1)}\,, \tag{3.74}$$

$$C = \frac{\kappa(w+1)}{\Lambda}\left[2\kappa(\bar{\rho}_0 + q\bar{\rho}_0^{\dagger})^2 - 3\Lambda q\bar{\rho}_0^2(w+1)^2\right]\,. \tag{3.75}$$

This result describes a cosmic history with an initial phase of contraction followed by a nonsingular bounce and an expanding phase, which is at first decelerated and then accelerated. Due to the discrepancy between the B and C coefficients, the profiles of the contracting and expanding branches may behave differently. This *bounce asymmetry* is quite a peculiar characteristic that merits further investigation.

As initially suspected by the authors, due to the unique properties of a finite energy density value in a theory where matter and spacetime effectively decouple, complex dynamics are expected during early stages of the Universe. The decoupling occurs in the singular limit (the $|A|$ approaches zero only asymptotically), but the bounce mechanism enforces a nonvanishing scale factor and eliminates the singularity, thereby removing the decoupling point from the physical space.

A solution for $k \neq 0$ is not attainable in this way. Nevertheless, in the same study, the authors outlined the algorithm for deriving conditions that ensure the *existence of solutions* in nontrivial spatial geometries. When both the Friedmann equation and the acceleration equation are expanded to the first order in q and written in terms of parameters A, B and C given by (3.73)–(3.75), the conditions for the bounce, $\dot{a}_{\mathrm{b}} = 0$ and $\ddot{a}_{\mathrm{b}} > 0$, become

$$a^{6(1+w)} - 2Aa^{3(1+w)} - ka^{2(3w+2)} + A^2 - 4BC = 0 \tag{3.76}$$

and

$$\frac{a}{6B(w+1)}\left[2 + A(3w+1)a^{-3(w+1)} - (3w+2)(A^2 - 4BC)a^{-6(w+1)}\right] > 0\,, \tag{3.77}$$

respectively. Although it is generally feasible to perform this analysis, equation (3.76) constitutes a high-degree polynomial in a, which is not straightforward to solve when $k \neq 0$. Consequently, the resulting conditions are cumbersome, dependent on specific parameter intervals, and are not presented. This strongly highlights the motivation behind adopting the dynamical systems approach, which allows for a more transparent analysis of the underlying behaviour across a wide range of initial conditions.

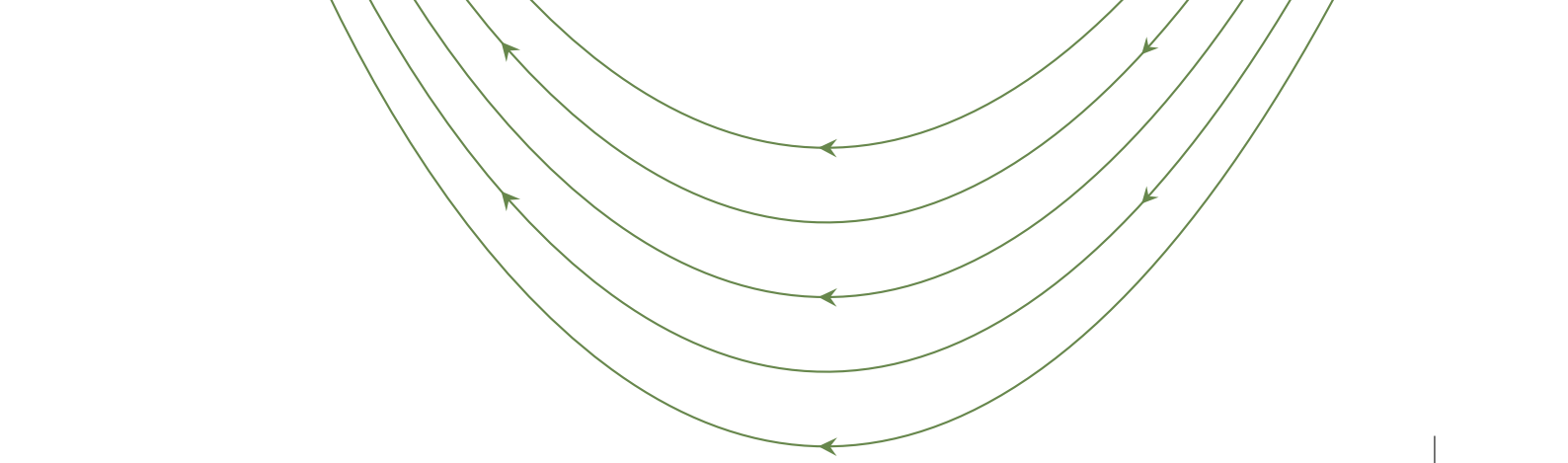

4

Analysis of the linearized MEMe model

Having walked patiently through the essential concepts from both the perspective of gravitational physics and of the mathematical methods used to visualize nonlinear differential equations, we proceed to explore further the dynamics of the MEMe model bringing it to previously unexplored depths.

Principally, the dynamical systems approach to MEMe model's cosmology reviewed at the end of the previous chapter (Section 3.4.1), while being simple, has certain limitations. Since variables (3.60) are defined within a standard EN framework, they prohibit us from circumventing the region of $H = 0$, where potential bouncing solutions occur. At the same time, the phase space presented is not compact and the line of fixed points associated with the early de Sitter phase resides outside the accessible range. For this reason, this analysis is well-suited to understand primary the late time cosmological evolution. Our purpose is to *extend* the analysis so that the admissible early cosmologies within the MEMe framework become directly observable.

While the analysis of Feng et al. conducted in [1] considers the full MEMe model driven by equations (3.57) and (3.58), where all nonlinearities are preserved, we begin here with a treatment of the linearized model: (3.66) and (3.69). This further simplification may overlook inherently nonlinear phenomena that could arise in regions distant from equilibrium configurations – that is the price we pay in the very beginning. What are the benefits of this approach? It provides a controlled approximation: isolating the leading order contribution to the dynamics enables the identification of the dominant physical mechanisms – such as the bounce – in a tractable form. These mechanisms inherently persist even within nonlinear equations.

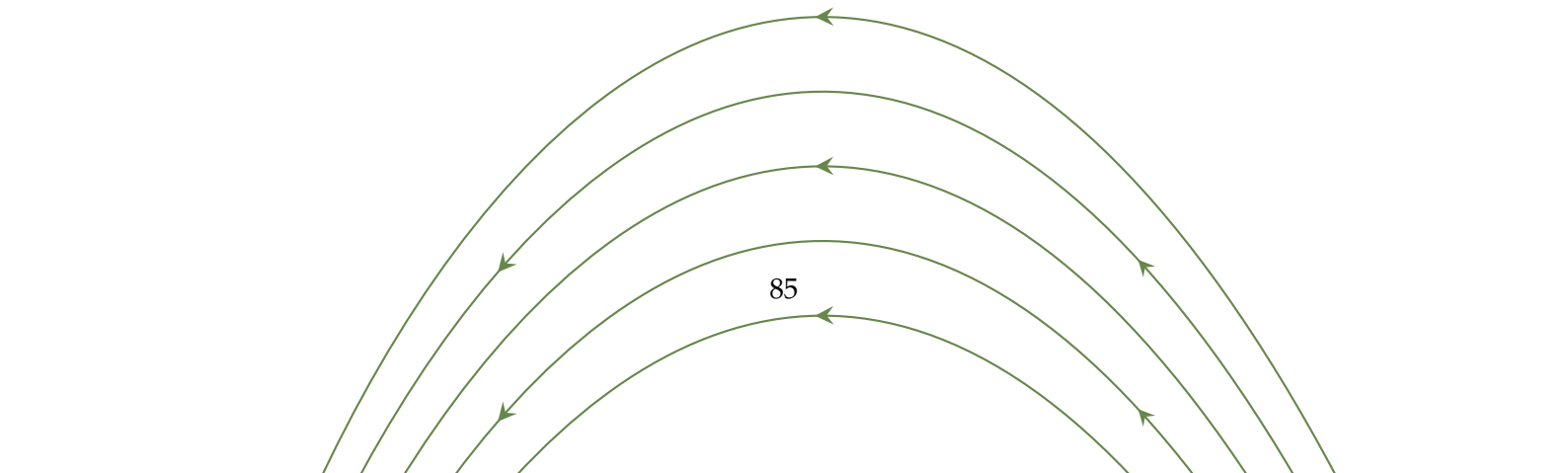

4.1 Spatially flat geometry

Let us start with the simplest possible setting, that is, assuming that the spatial curvature of our Universe is zero. As pointed out in the very end of the previous chapter, the analytical construction of a bouncing solution within the MEMe model when $k = 0$ provides a clear demonstration that nonsingular cosmological evolution can emerge directly from the theory without resorting to ad hoc modifications [123]. Although this establishes the existence of a bounce, it does not answer by itself to the question whether this solution is generic, structurally stable, or sensitive to initial conditions and/or parameter changes. Such a solution corresponds to a *specific choice* of initial conditions and parameters and thereby represents only a single trajectory in the phase space. For this reason, we will complement the analytical approach with a dynamical systems analysis.

Since a spatially flat universe corresponds to $k = 0$, we are left with the following formulation of the linearized Friedmann equation

$$H^2 = \kappa \left[\frac{4}{3} \frac{\bar{\rho}_0 + q\bar{\rho}_0^{\dagger}}{a^{3(w+1)}} + 2q(w+1)^2 \frac{\bar{\rho}_0^2}{a^{6(w+1)}} \right] + \frac{\Lambda}{3} \,. \tag{4.1}$$

Introducing the shorthand for the two types of energy densities present,

$$\rho_1 = \frac{4\kappa(\bar{\rho}_0 + q\bar{\rho}_0^{\dagger})}{a^{3(w+1)}} \quad \text{and} \quad \rho_2 = \frac{2\kappa q(w+1)^2\bar{\rho}_0^2}{a^{6(w+1)}} \,, \tag{4.2}$$

we propose the set of variables:

$$X = \frac{H}{\eta} \,, \qquad \Omega = \sqrt{\frac{\rho_1}{3\eta^2}} \,, \qquad L = \sqrt{\frac{\Lambda}{3\eta^2}} \,, \tag{4.3}$$

where

$$\eta = \sqrt{H^2 - \rho_2} \tag{4.4}$$

is the new normalization factor. Note that since $q < 0$, ρ_2 is always negative, which ensures that η is always real. Defining the dimensionless time variable τ as

$$\frac{\mathrm{d}\tau}{\mathrm{d}t} = \eta \,, \tag{4.5}$$

similarly to (2.42), we compute the autonomous system of differential equations as

$$X' = \frac{1}{\eta}\frac{\mathrm{d}X}{\mathrm{d}t} \,, \quad \Omega' = \frac{1}{\eta}\frac{\mathrm{d}\Omega}{\mathrm{d}t} \,, \quad L' = \frac{1}{\eta}\frac{\mathrm{d}L}{\mathrm{d}t} \,. \tag{4.6}$$

Equation (4.1) becomes a Friedmann constraint

$$1 = \Omega^2 + L^2 \,, \tag{4.7}$$

which defines a unit circle in the (Ω, L)-plane; seen in the full three-dimensional state space (X, Ω, L) it is the cylindrical surface that all physical orbits never leave. In particular, only the portion of this surface located within the first quadrant is physically relevant, since $\Omega \geq 0$ and $L \geq 0$ imply that $0 \leq \Omega \leq 1$ and $0 \leq L \leq 1$. The remaining variable X that represents the normalized Hubble rate is confined within the range $-1 \leq X \leq 1$, ensuring that the resulting phase space is compact.

Subsequently, the three differential equations (4.6) for the introduced variables can be reduced using the Friedmann constraint (4.7), allowing the analysis to be performed entirely within a convenient two-dimensional phase space. We have two attainable formulations. First,

$$X' = \frac{3}{2}(X^2 - 1)(1 + w)(\Omega^2 - 2)\,, \tag{4.8}$$

$$\Omega' = -\frac{3}{2}\Omega X(1 + w)(1 - \Omega^2)\,, \tag{4.9}$$

with L constrained by

$$L^2 = 1 - \Omega^2\,.$$

Alternatively,

$$X' = -\frac{3}{2}(X^2 - 1)(1 + w)(1 + L^2)\,, \tag{4.10}$$

$$L' = \frac{3}{2}LX(1 + w)(1 - L^2)\,, \tag{4.11}$$

with the corresponding constraint

$$\Omega^2 = 1 - L^2\,. \tag{4.12}$$

These options are equally valid. Since the vanishing k analysis is not highly complex, we can afford now, for the sake of clarity, to present both. Both phase spaces present invariant submanifolds, associated with $X = \pm 1$, and $\Omega = 0$ ($L = 1$) and $\Omega = 1$ ($L = 0$), respectively.

One can see that most of the trajectories in the accompanying Figures 4.1 and 4.2 exhibit a bouncing behaviour from the sequence of four prominent fixed points. All orbits inside the constrained region diverge from the contracting de Sitter solution (dS_-), bounce between matter-dominated saddles of contracting Friedmann (F_-) and expanding Friedmann (F_+), only to approach the de Sitter attractor (dS_+) of exponential expansion as $\tau \to \infty$. The exception is on the lines $X = \pm 1$. These represent the GR limit. In fact, one can write

$$X = \frac{H}{|H|}\frac{1}{\sqrt{1 - \frac{\rho_2}{H^2}}} \tag{4.13}$$

so that when $X = \pm 1$, $\rho_2 = 0$. Along these lines, we can recognize the transition between Friedmann and de Sitter solutions (expanding and contracting) typical of the GR systems (see Section 2.2.1).

Table 4.1: Fixed points and their stability for the system (4.8)–(4.9).

Point	$\{X, \Omega, L\}$	Eigenvalues	Stability
dS_-	$\{-1, 0, 1\}$	$\left\{6(1+w), \frac{3}{2}(1+w)\right\}$	Repeller
dS_+	$\{1, 0, 1\}$	$\left\{-6(1+w), -\frac{3}{2}(1+w)\right\}$	Attractor
F_-	$\{-1, 1, 0\}$	$\{-3(1+w), 3(1+w)\}$	Saddle
F_+	$\{1, 1, 0\}$	$\{-3(1+w), 3(1+w)\}$	Saddle

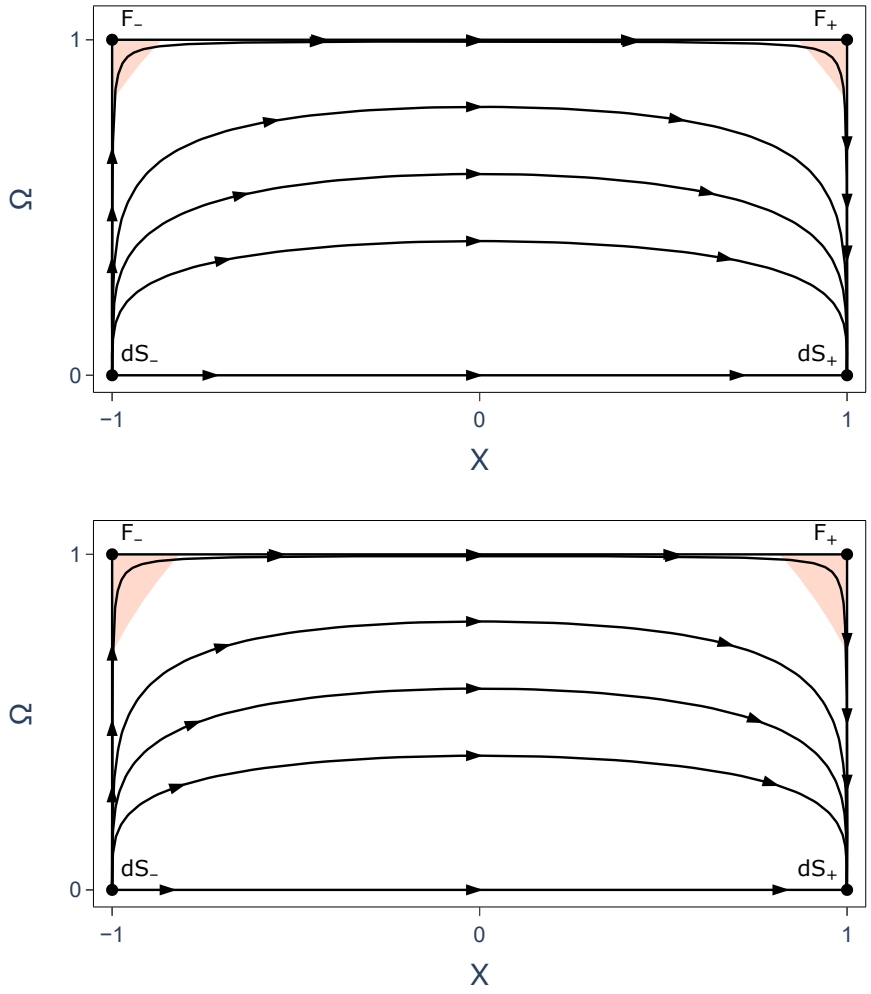

Figure 4.1: Two-dimensional phase portraits for the system (4.8)–(4.9) with $w = 0$ (top) and $w = 1/3$ (bottom) with L constrained. The orange region corresponds to decelerating universe.

Table 4.2: Fixed points and their stability for the system (4.10)–(4.11).

Point	$\{X, \Omega, L\}$	Eigenvalues	Stability
dS_-	$\{-1, 0, 1\}$	$\{6(1+w), 3(1+w)\}$	Repeller
dS_+	$\{1, 0, 1\}$	$\{6(1+w), 3(1+w)\}$	Attractor
F_-	$\{-1, 1, 0\}$	$\left\{3(1+w), -\frac{3}{2}(1+w)\right\}$	Saddle
F_+	$\{1, 1, 0\}$	$\left\{-3(1+w), \frac{3}{2}(1+w)\right\}$	Saddle

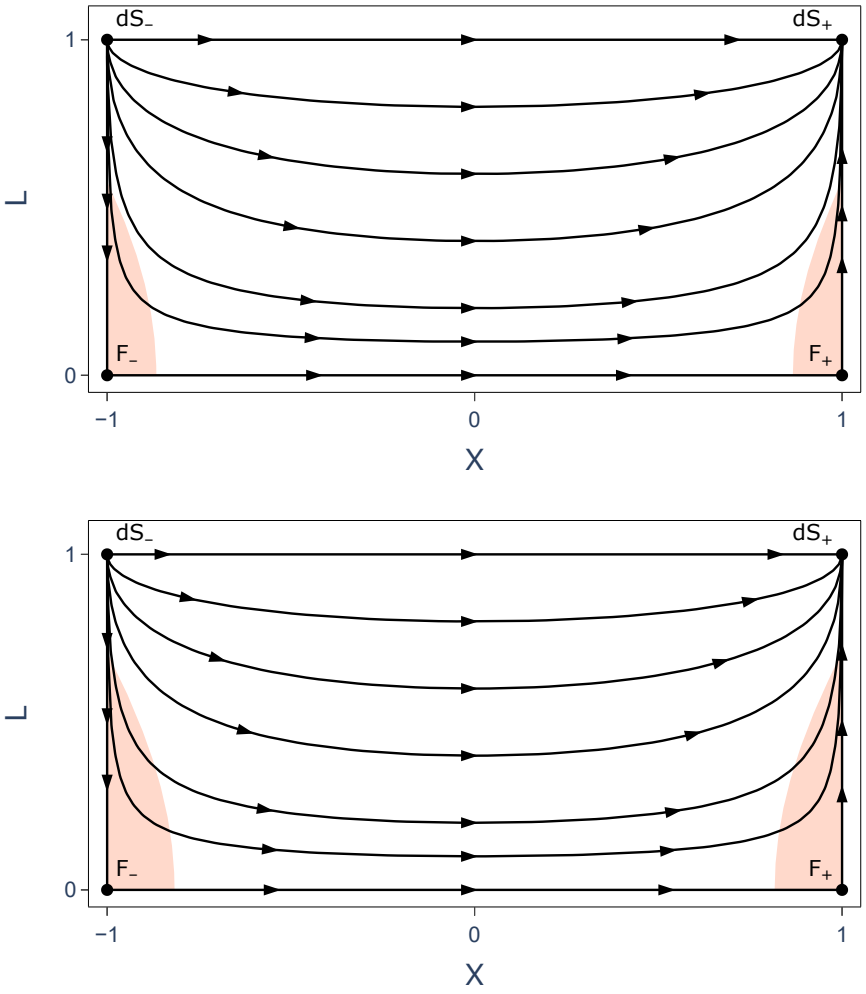

Figure 4.2: Two-dimensional phase portraits for the system (4.10)–(4.11) with $w = 0$ (top) and $w = 1/3$ (bottom) with Ω constrained. The orange region corresponds to decelerating universe.

Since dS_+ does not lie in every invariant submanifold, it cannot be classified as a global attractor in a strict sense, despite being approached by the majority of trajectories.

Choosing the first representation given by (4.8)–(4.9), we reformulate the acceleration equation accordingly

$$\frac{\ddot{a}}{a\eta^2} = -\frac{1}{2}\left[-6 + 4X^2 + 3\Omega^2 + 3w(-2 + 2X^2 + \Omega^2)\right] \,, \tag{4.14}$$

which turns positive when the entire bracket expression is negative. For both values of the EoS parameter w, the accelerating dynamics is contained within an elliptical interior, while the regions corresponding to the deceleration are indicated in orange in Figure 4.1.

Following analogous reasoning, considering the system described by (4.10)–(4.11), we obtain the following condition for the accelerated expansion/contraction:

$$3 + 3L^2(1 + w) - 4X^2 + w(3 - 6X^2) > 0 \,, \tag{4.15}$$

which, in this instance, corresponds to the region between the branches of a hyperbola. The decelerating complement is again indicated in orange in Figure 4.2. Aside from the confirmed occurrence of a bounce at $X = 0$ with a positive second derivative $\ddot{a} > 0$ in its vicinity, it is noteworthy that the accelerated regime encompasses nearly the entire phase space. All depicted trajectories originating with physically feasible initial conditions undergo acceleration in the contracting phase, near the bounce, as well as throughout the expansion period. However, passing also through the small orange region representing decelerated, matter-dominated expansion – consistent with our current understanding of cosmic evolution – requires precise fine-tuning.

There is a concealed subtlety regarding the reason of the bending of trajectories. Where does their shape originate? By focusing solely on the physical state space, we inherently excluded fixed points situated outside of it. Specifically, there exists a fixed point at $X = 0$ with a saddle nature, which is not dynamically reachable, and consequently has not been discussed at all. However, from a geometric standpoint, this fixed point still influences the structure of the vector field in its vicinity, thereby possibly impacting the shape of the orbits within the physical domain. This is especially intriguing in light of the conclusion drawn at the end of Chapter 3, where it was noted that the degeneracy of the theory – namely, the decoupling of spacetime and matter – is never achieved. Instead, this degeneracy resides *deeper* within the phase space, and the bounce mechanism acts as a protective feature that prevents the MEMe theory from reaching a singularity.

4.2 Spatially open geometry

We leverage the same property of the sign of ρ_2 to establish our normalization factor η for the hyperbolic universe. This extends further beyond the scope of the original paper on bounce analysis [123], which did not present a solution for the case of $k \neq 0$. In this section and the following one, we will demonstrate not only that solutions indeed exist for nonzero k, but also that they remain robust across all physically relevant initial conditions, similar to the case of a flat spatial geometry.

Employing the notation adopted in the beginning of our first analysis, (4.2), the Friedmann equation for $k \neq 0$ can be expressed as

$$H^2 = -\frac{k}{a^2} + \frac{\rho_1}{3} + \rho_2 + \frac{\Lambda}{3}\,. \tag{4.16}$$

Since we consider $k = -1$ in this first context, we may just define the extra variable that accounts for the spatial curvature, which will always be positive, while maintaining those proposed in the previous formulation (4.3). Accordingly, we proceed with

$$C = \sqrt{-\frac{k}{a^2}}\,, \qquad X = \frac{H}{\eta}\,, \qquad \Omega = \sqrt{\frac{\rho_1}{3\eta^2}}\,, \qquad L = \sqrt{\frac{\Lambda}{3\eta^2}}\,, \tag{4.17}$$

where η is as specified in (4.4). Again, we end up with a compact phase space, yet in three dimensions, since the Friedmann constraint reads:

$$1 = C^2 + L^2 + \Omega^2\,. \tag{4.18}$$

This equation delineates a spherical surface that the physical solutions never leave, while $0 \leq C \leq 1$, $0 \leq L \leq 1$ and $0 \leq \Omega \leq 1$ ensure that the relevant orbits are confined to the first quadrant once more.

In the same way as we treated previous variables (4.6), we construct the system from (4.17) as

$$X' = (X^2 - 1)\left[(1 + 3w)\left(\frac{\Omega^2}{2} - 1\right) - 1 - L^2\right]\,, \tag{4.19}$$

$$\Omega' = -\Omega X\left[\frac{(1 - \Omega^2)(1 + 3w)}{2} + L^2\right]\,, \tag{4.20}$$

$$L' = LX\left[\frac{\Omega^2}{2}(1 + 3w) + 1 - L^2\right]\,, \tag{4.21}$$

where prime denotes differentiation with respect to dimensionless time τ (4.5) and C is constrained by (4.18).

When analysing the behaviour of the system above, we can first point out that invariant submanifolds are now formed by planes – namely $\Omega = 0$, $L = 0$ and $X = \pm 1$ – which trajectories cannot ever cross. In Table 4.3, in addition to the four previously identified fixed points, which are assigned to the same solutions as before, we recognize

two new fixed points labelled M_- and M_+. They describe the contracting and expanding Milne's models, respectively.

It is especially noteworthy to compare the $L = 0$ submanifold, as displayed in the lower part of Figure 4.3, with Figure 2.8, which illustrates the Einstein–Cartan cosmology in a spatially open geometry. Since both the Einstein–Cartan and the linearized MEMe models involve two different types of energy densities with opposite signs, their evolution equations are very similar. In fact, setting $L = 0$ in (4.20) yields the same expression as in (2.74), with the variables related to matter density being scaled by numerically different η factors. From this observation, we can state that the Einstein–Cartan phase space in a hyperbolic universe has the same topology as the zero cosmological constant boundary of the MEMe model phase space in the hyperbolic case. As a consequence, these theories have a degenerate cosmological phenomenology. Any other initial condition with nonvanishing Λ converges to the de Sitter attractor, as expected.

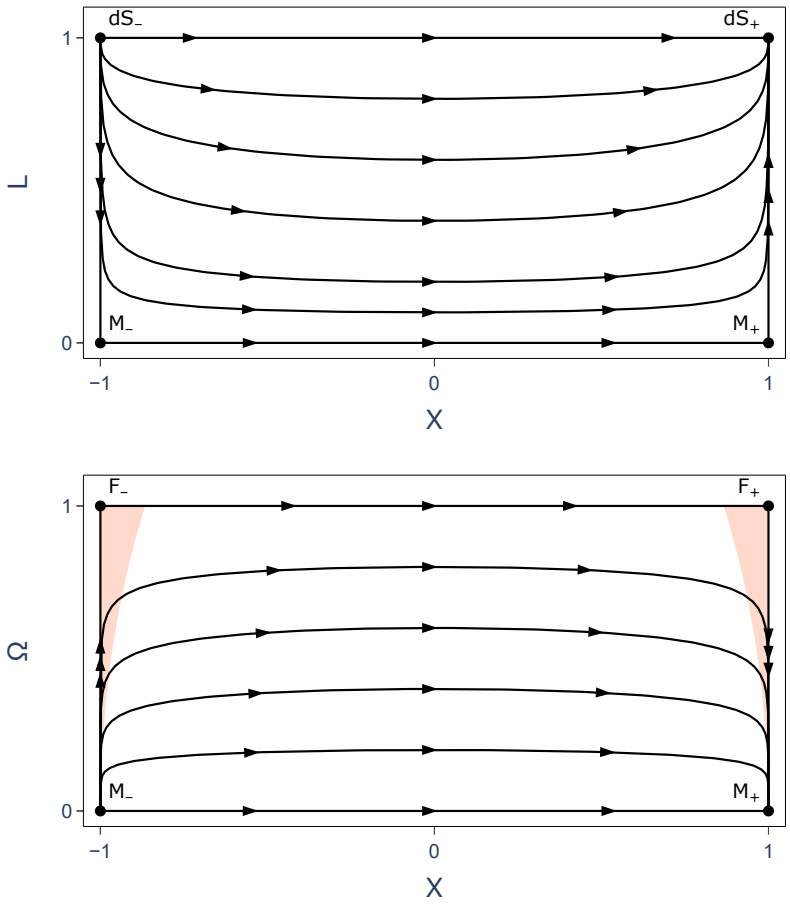

Figure 4.3: Two-dimensional invariant submanifolds of $\Omega = 0$ (top) and $L = 0$ (bottom) for the dynamical system (4.19)–(4.21) of an open universe with $w = 0$. The orange-shaded areas represent regions of decelerated dynamics.

To identify the region of acceleration within the three-dimensional phase space shown in Figures 4.4, we convert the acceleration equation into variables (4.17) as

$$\frac{\ddot{a}}{a\eta^2} = \frac{1}{2}\left[4 + 2L^2 - 4X^2 - \Omega^2 - 3w(-2 + 2X^2 + \Omega^2)\right] \ . \tag{4.22}$$

Requiring $\ddot{a} > 0$ now yields the area of a hyperboloid that encloses nearly the entire phase space. For this reason, marking the volume of decelerated dynamics remains a more effective means of visualization as before.

It can be concluded that, in the case of open geometry, the bounce inevitably takes place. Its occurrence is not sensitive to initial conditions nor to physical values of the EoS parameter w. As in the spatially flat scenario, an external structure exists outside the physical region – a line of fixed points at $X = 0$ – which influences the internal bouncing structure of the orbits. However, to transition into the intermediate decelerated epoch at some point, a similar level of fine-tuning is required as in the standard cosmological model.

Notice that, upon revisiting the case $k = 0$, it becomes evident that it can be incorporated into this analysis – if initial conditions for (X, Ω, L) are chosen such that they satisfy $\Omega^2 + L^2 = 1$, in other words, when we impose that $C = 0$, the resulting orbits will never leave the cylindrical blue surface depicted in Figure 4.5. Under these conditions, the system's structure is equivalent to the earlier case characterized by flat spatial geometry. This suggests that a single analysis that includes both values of k, 0 and -1, could have been formulated. However, the two-dimensional phase portraits presented earlier in Figures 4.1 and 4.2 capture the dynamics in a much simpler fashion, despite being two distinct projections of the same surface.

Table 4.3: Fixed points and their stability for the 3D system (4.19)–(4.21) describing the evolution of a spatially hyperbolic universe within the MEMe model.

Point	$\{X, \Omega, L, C\}$	Eigenvalues	Stability
dS_-	$\{-1, 0, 1, 0\}$	$\left\{2, 6(1+w), \frac{3}{2}(1+w)\right\}$	Repeller
dS_+	$\{1, 0, 1, 0\}$	$\left\{-2, -\frac{3}{2}(1+w), -6(1+w)\right\}$	Attractor
M_-	$\{-1, 0, 0, 1\}$	$\left\{-1, 2(2+3w), \frac{1}{2}(1+3w)\right\}$	Saddle
M_+	$\{1, 0, 0, 1\}$	$\left\{1, -2(2+3w), \frac{1}{2}(-1-3w)\right\}$	Saddle
F_-	$\{-1, 1, 0, 0\}$	$\left\{-\frac{3}{2}(1+w), -1-3w, 3(1+w)\right\}$	Saddle
F_+	$\{1, 1, 0, 0\}$	$\left\{-3(1+w), 1+3w, \frac{3}{2}(1+w)\right\}$	Saddle

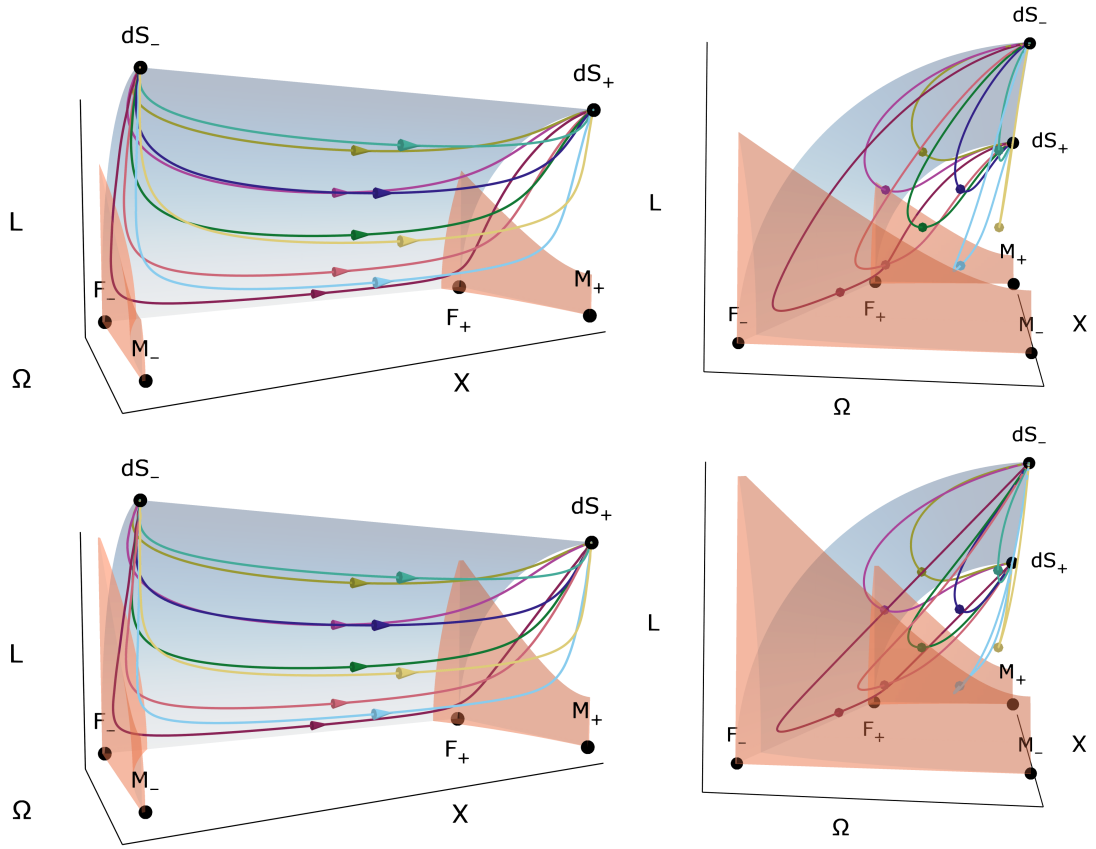

Figure 4.4: Three-dimensional phase space for the dynamical system (4.19)–(4.21) of an open universe with $w = 0$ (top row) and $w = 1/3$ (bottom row) from two different eye-angles. The blue surface corresponds to $C = 0$ and restricts all possible trajectories to stay underneath. The coordinates of the points present can be found in Table 4.3.

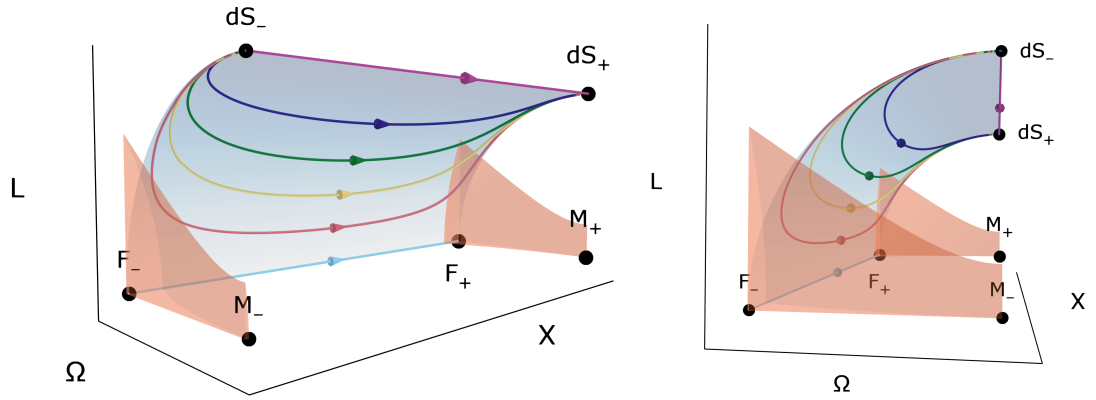

Figure 4.5: Three-dimensional phase portrait for the system (4.19)–(4.21) reduced to that of a flat universe ($C = 0$) with $w = 0$ from two different eye-angles. The cylindrical surface alone captures the dynamics equivalent to the one of systems (4.8)–(4.9) and (4.10)–(4.11).

4.3 Spatially closed geometry

Finally, we are left with the task of addressing a spatially closed universe. The premise of positive k favours adopting a standard approach, that is moving the curvature term to the left-hand side of (4.16) and set up variables using

$$\eta = \sqrt{H^2 + \frac{k}{a^2}}, \tag{4.23}$$

which is always real for $k = 1$. Next, we introduce

$$X = \frac{H}{\eta}, \qquad \Omega_1 = \sqrt{\frac{\rho_1}{3\eta^2}}, \qquad \Omega_2 = \sqrt{-\frac{\rho_2}{\eta^2}}, \qquad L = \sqrt{\frac{\Lambda}{3\eta^2}}, \tag{4.24}$$

where the minus sign preceding ρ_2 ensures that Ω_2 is real, since q of the MEMe model is preferred negative. Unfortunately, this choice of system variables fails to compactify the phase space, because (4.16) in terms of (4.24) yields

$$1 = L^2 + \Omega_1^2 - \Omega_2^2, \tag{4.25}$$

which defines a hyperbolic surface that extends along the Ω_2 direction. By differentiating (4.24) with respect to τ ($\mathrm{d}\tau = \eta\,\mathrm{d}t$), we find that the cosmological equations are now equivalent to

$$X' = -\frac{1}{2}\left(X^2 - 1\right)\left[-1 - 3w + 3(1+w)(L^2 + \Omega_2^2)\right], \tag{4.26}$$

$$L' = -\frac{3}{2}XL(1+w)\left(-1 + L^2 + \Omega_2^2\right), \tag{4.27}$$

$$\Omega_2' = -\frac{3}{2}X\Omega_2(1+w)\left(1 + L^2 + \Omega_2^2\right), \tag{4.28}$$

while we decide to constrain Ω_1 through (4.25). The expression that indicates whether the universe is experiencing acceleration or deceleration is given by

$$\frac{\ddot{a}}{a\eta^2} = \frac{1}{2}\left[-1 - 3w + 3(1+w)(L^2 + \Omega_2^2)\right]. \tag{4.29}$$

The considerably more intricate dynamics of the system (4.26)–(4.28) is demonstrated in the forthcoming Figures 4.6–4.11 for both values of the EoS parameter w. Again, we recognize the classical fixed points of the matter-dominated ($\mathrm{F}_-, \mathrm{F}_+$) and Λ-dominated ($\mathrm{dS}_-, \mathrm{dS}_+$) solutions, listed in Table 4.4, as well as the invariant submanifolds $\Omega_2 = 0$, $L = 0$ and $X = \pm 1$. The novel nontrivial features stem from the fixed curve C, situated within the $X = 0$ plane. When we investigate a three-dimensional phase space with initial conditions $L, \Omega_2 \neq 0$, we find two qualitatively distinct classes of trajectories: some orbits bounce toward the curve C and then recede, while others oscillate around it. This dual nature can be attributed to a change in linear stability that occurs at a specific point

with coordinates derivable from the nonzero eigenvalues associated with this curve. We can conclude that for $L > L_c$, where

$$L_c = \frac{\sqrt{2 + 9w(1+w)}}{3(1+w)}\,, \tag{4.30}$$

the fixed points of the line C are identified as saddles. When $L < L_c$, the two nonzero eigenvalues are purely imaginary, so orbits around the line C are closed curves indicating a periodic behaviour of cosmology.

In the special case of the invariant submanifold $\Omega_2 = 0$ depicted in Figure 4.12 on top, the point B marks the intersection of the fixed line C with the (X, L)-plane. On this plane, the cosmological equations and therefore the orbits are the same as the standard cosmological model with positive spatial curvature. One can then associate the point B with the point E of Figure 2.4, which represents Einstein's static universe, and conclude that the dynamics will include inevitable matter-dominated re-collapses, loitering solutions, and bounces that can never evolve toward decelerated regime.

Table 4.4: Fixed points and their stability for the 3D system (4.26)–(4.28) describing the evolution of a spatially closed universe within the MEMe model.

Point(s)	$\{X, L, \Omega_2, \Omega_1\}$
C	$\left\{0, L, \sqrt{\frac{1-3L^2+3w(1-L^2)}{3(1+w)}}, \sqrt{1-L^2+\frac{1-3L^2+3w(1-L^2)}{3(1+w)}}\right\}$
dS_-	$\{-1, 1, 0, 0\}$
dS_+	$\{1, 1, 0, 0\}$
F_-	$\{-1, 0, 0, 1\}$
F_+	$\{1, 0, 0, 1\}$
Point(s)	**Eigenvalues**
C	$\left\{0, \mp\sqrt{-2-9w-9w^2+9L^2(1+w)^2}\right\}$
dS_-	$\{2, 3(1+w), 3(1+w)\}$
dS_+	$\{-2, -3(1+w), -3(1+w)\}$
F_-	$\left\{-\frac{3}{2}(1+w), \frac{3}{2}(1+w), -1-3w\right\}$
F_+	$\left\{-\frac{3}{2}(1+w), \frac{3}{2}(1+w), 1+3w\right\}$

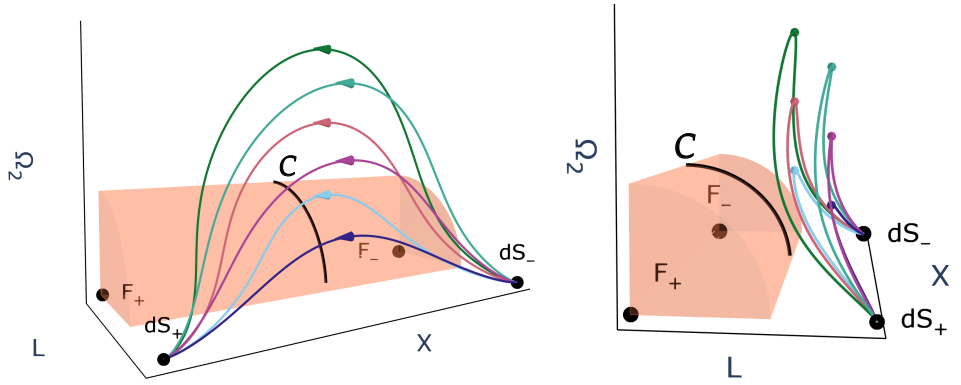

Figure 4.6: Six trajectories of the dynamical system (4.26)–(4.28) bouncing in region with $L > L_c$ in closed universe with $w = 0$ from two different eye-angles. The decelerated dynamics occurs in the orange volume.

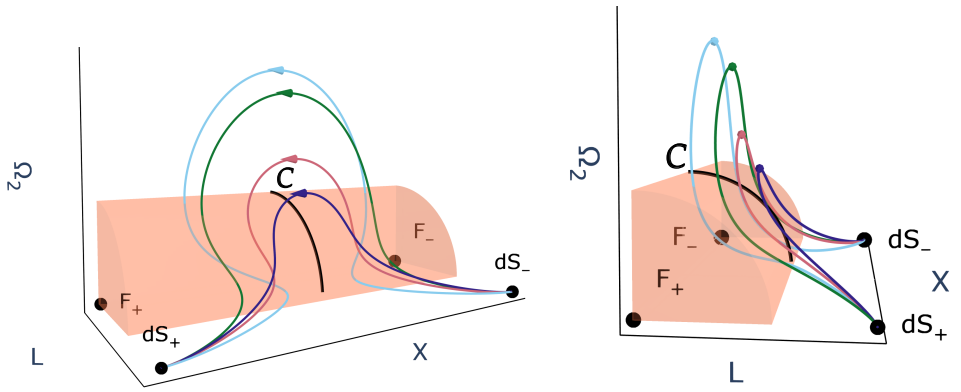

Figure 4.7: Four trajectories of the dynamical system (4.26)–(4.28) bouncing with $L < L_c$ in closed universe with $w = 0$ from two different eye-angles. The decelerated dynamics occurs in the orange volume.

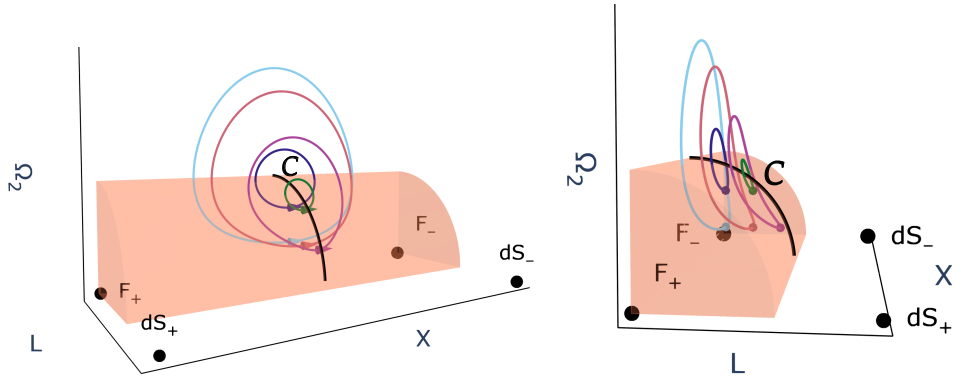

Figure 4.8: Five cyclically bouncing trajectories of the dynamical system (4.26)–(4.28) in closed universe with $w = 0$ from two different eye-angles. The decelerated dynamics occurs in the orange volume.

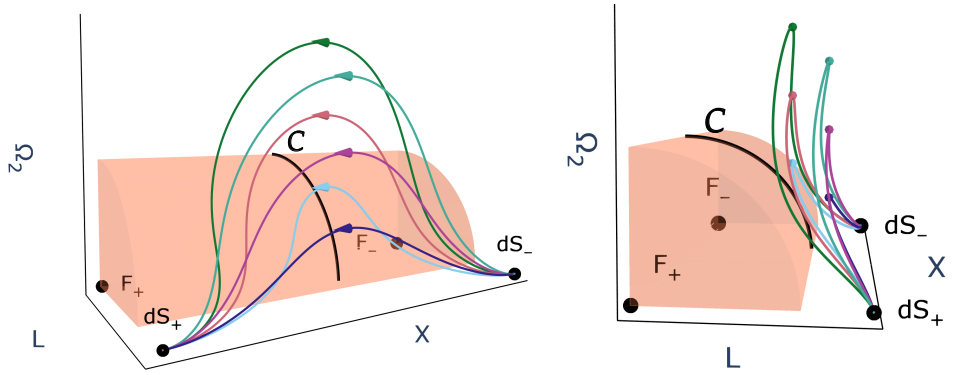

Figure 4.9: Six trajectories of the dynamical system (4.26)–(4.28) bouncing with value $L > L_c$ in closed universe with $w = 1/3$ from two different eye-angles. The decelerated dynamics occurs in the orange volume.

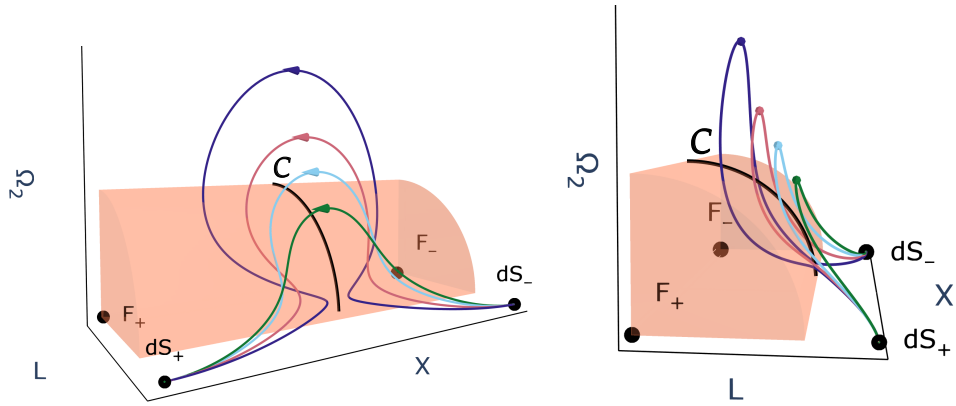

Figure 4.10: Four trajectories of the dynamical system (4.26)–(4.28) bouncing around $L < L_c$ in closed universe with $w = 1/3$ from two different eye-angles. The decelerated dynamics occurs in the orange volume.

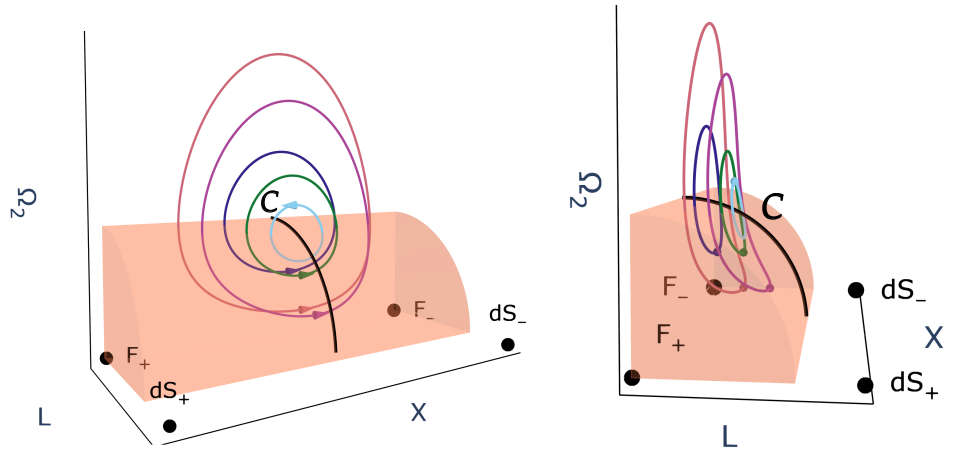

Figure 4.11: Five cyclically bouncing trajectories of the dynamical system (4.26)–(4.28) in closed universe with $w = 1/3$ from two different eye-angles. The decelerated dynamics occurs in the orange volume.

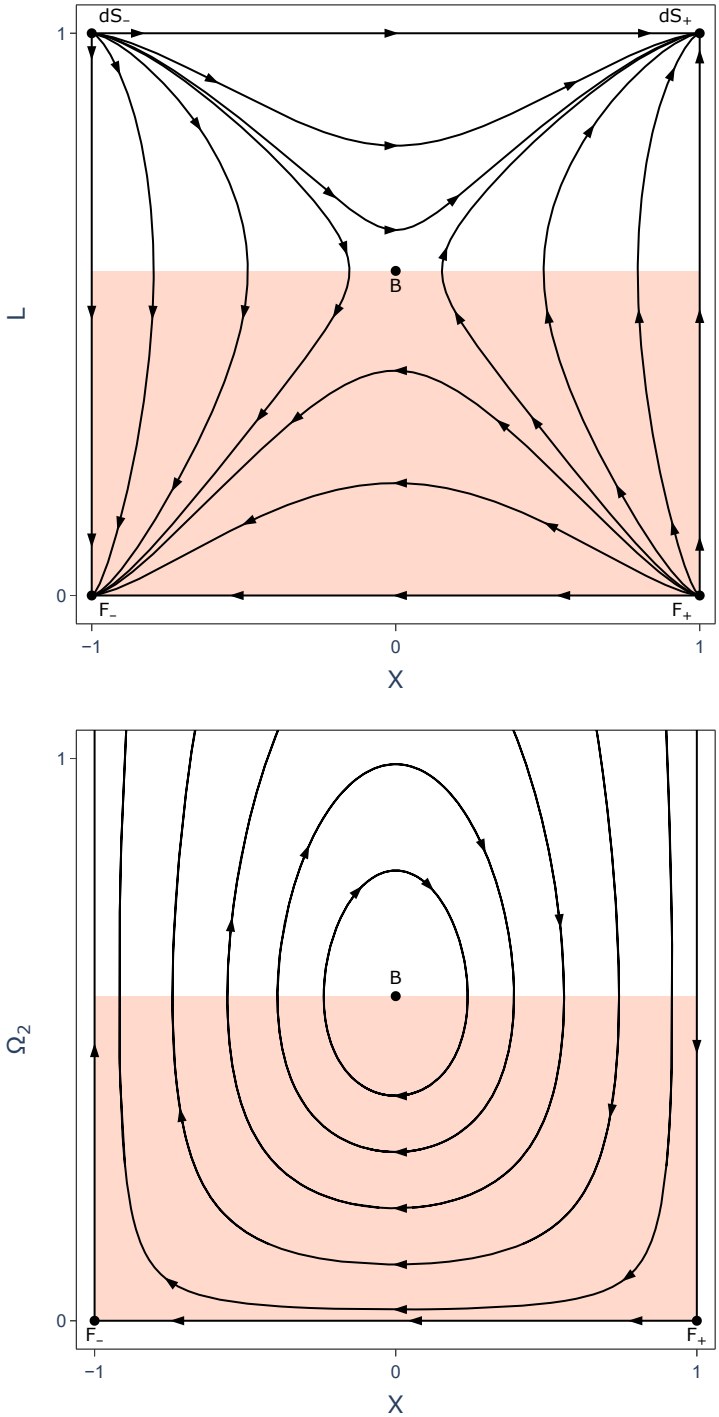

Figure 4.12: Two-dimensional invariant submanifolds of $\Omega_2 = 0$ (top) and $L = 0$ (bottom) for the dynamical system (4.26)–(4.28) of a closed universe with $w = 0$. The dynamics is decelerated in the orange region.

Within the invariant submanifold $L = 0$ on the bottom of Figure 4.12, all trajectories (with the exception where Ω_2 vanishes) are strictly cyclic around the intersection point with the fixed curve C, which we also marked as B. These trajectories correspond to periodic sequences of bounces and re-collapses resulting from the combined influence of positive spatial curvature within the model. This phenomenon closely resembles the behaviour encountered in Einstein–Cartan cosmology within a closed spatial geometry (see Figure 2.9). Again, we can view the analysis of the Einstein–Cartan theory as being contained within the MEMe model analysis for a closed universe in the limiting case where $\Lambda = 0$. Note, however, that the variable on the vertical axis differs between the two cases. In the Einstein-Cartan analysis, we plotted the unbounded matter density variable Ω_m, connected to the specific model parameter Ω_s as $\Omega_m = 1 + \Omega_s$. In the current presentation, we instead display the model variable Ω_2 directly.

At this stage, it would be valuable to scrutinize whether also the oscillations within the whole three-dimensional domain remain perpetual or eventually begin to diverge from or converge toward the fixed line. Is there a way to advance our analysis here? In other words, can we establish a proof that the oscillating trajectories are closed, or alternatively, demonstrate conditions under which the orbits might transition between the two regimes?

Let us take a closer look at the structure of the constructed 3D dynamical system, especially at the expressions (4.27) and (4.28). They share a common multiplicative factor, which includes a variable X. This means that our system exhibits a remarkable decoupling property: when considering the ratio of the evolution equations for L and Ω_2, the dependence on X can be completely removed. This induces a closed differential relation in the (L, Ω_2)-plane alone:

$$\frac{\Omega_2'}{L'} = \frac{\mathrm{d}\Omega_2}{\mathrm{d}L} = \frac{\Omega_2(L^2 + \Omega_2^2 + 1)}{L(L^2 + \Omega_2^2 - 1)} \,. \tag{4.31}$$

As a result, the dynamics is foliated by infinitely many invariant submanifolds, labelled by (L, Ω_2), each defined by a set of solutions to this reduced equation. In simpler terms, the relative evolution of L and Ω_2 is fixed, X only controls the rate at which we progress along these trajectories, functioning similarly to a reparametrization of time.

Although the explicit solution $\Omega_2(L)$ can be calculated in principle, it is much more insightful to derive the implicit relationship in this case, as it directly reveals a conserved quantity. Specifically, we seek a function $F(L, \Omega_2)$ such that $\mathrm{d}F = 0$. This can be achieved by identifying an appropriate integrating factor and eventually uncovering the key relation:

$$K = \frac{1 - L^2 + \Omega_2^2}{L\Omega_2} = \frac{\Omega_1^2}{L\Omega_2} \,, \tag{4.32}$$

where K is a constant characterizing a hyperbolic subspace. This is an additional constraint that our system always satisfies – choosing the value of K becomes equivalent to selecting the particular two-dimensional submanifold, which, much in the same way as the invariant submanifolds discussed above, cannot be crossed by any orbits. Using

(4.32) to eliminate L, we can reduce the system (4.26)–(4.28) to only two equations, which are parametrized by K:

$$X' = -\frac{1}{4}\left(X^2-1\right)\left[4+3\Omega_2^2\left(4+K^2\right)(1+w)-3K\Omega_2(1+w)\sqrt{4+\Omega_2^2\left(4+K^2\right)}\right], \quad (4.33)$$

$$\Omega_2' = -\frac{3}{4}X\Omega_2(1+w)\left[4+\Omega_2^2\left(4+K^2\right)-K\Omega_2\sqrt{4+\Omega_2^2\left(4+K^2\right)}\right]. \quad (4.34)$$

This reduced system corresponds to a set of representative two-dimensional phase portraits, illustrated in Figures 4.13–4.15. The number of equilibrium points in the system varies from two to four, depending on the specific value of K. In particular, the points labelled dS_- and dS_+ from the full three-dimensional system, as detailed in Table 4.4, remain present across all values of K. At the critical value K_c, which can be determined by substituting (4.30) and the corresponding $\Omega_{2,c}$ into (4.32) as

$$K_c = \frac{4(2+3w)}{\sqrt{1+3w}\sqrt{2+9w(1+w)}}, \quad (4.35)$$

a new degenerate fixed point with $X = 0$ appears, marked as B in Figure 4.14. Specifically, for $w = 0$ and $w = 1/3$, these critical values are

$$K_c = 4\sqrt{2} \quad \text{and} \quad K_c = 2\sqrt{3} \quad (4.36)$$

respectively. Each corresponds to the *separatrix* – a boundary that delineates regions of the phase space with differing properties. Not surprisingly, these values of K describe surfaces that are tangent to the curve C.

For any $K < K_c$ the dynamics shows a direct transition from a de Sitter-like contraction to a de Sitter-like expansion without any intervening matter-dominated phase (see Figure 4.13). Decelerated patches are present only when the submanifolds with $K > K_c$ immerse themselves in the cylindrical volume defined by the equation (4.29) (see Figure 4.15). They intersect the fixed curve C *twice*, designated by points B_1 and B_2 .

This analysis highlights a significant conclusion: all cyclic trajectories correspond to invariant closed curves, which enhance our overall understanding. Within a positively spatially curved universe, as well as in previous geometries, all orbits in the physical phase space demonstrate bounce solutions and, furthermore, if the initial conditions for L and Ω_2 satisfy

$$\frac{1-L_0^2+\Omega_{2,0}^2}{L_0\Omega_{2,0}} > K_c \quad (4.37)$$

some universes directed by MEMe model are destined to undergo perpetual cycles. Except for these cyclic cosmologies, that dominate in the $K > K_c$ section as we approach the $L = 0$ submanifold, we also find various loitering solutions, where the contraction or expansion slows down substantially. Those are parts of some orbits "squeezed" towards the saddle part of the equilibrium curve, associated with the transition between the accelerating and decelerating epochs.

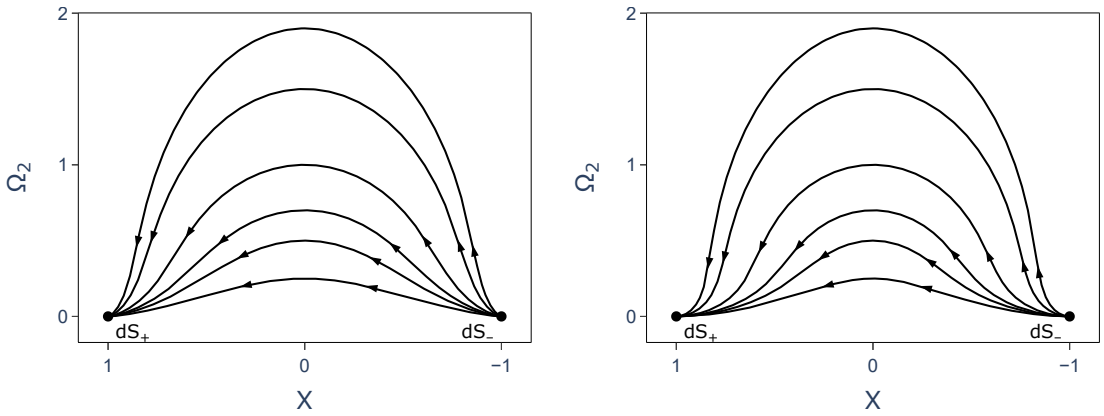

Figure 4.13: An example of a phase portrait for the reduced system (4.33)–(4.34) with $K = 2 < K_c$ for $w = 0$ (left) and $w = 1/3$ (right).

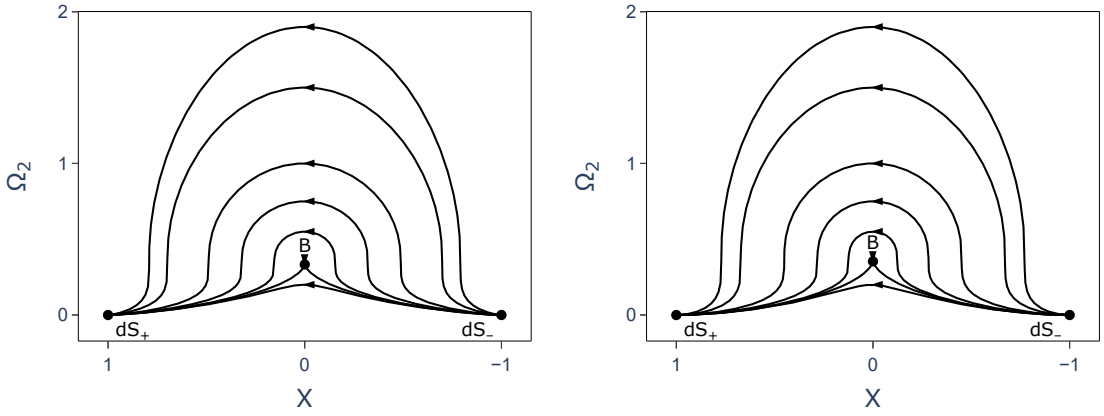

Figure 4.14: A separatrix of the system (4.33)–(4.34) corresponding to $K = K_c$ for $w = 0$ (left) and $w = 1/3$ (right). The downward-pointing arrow indicates the very slow flow in the vicinity of a contact point B.

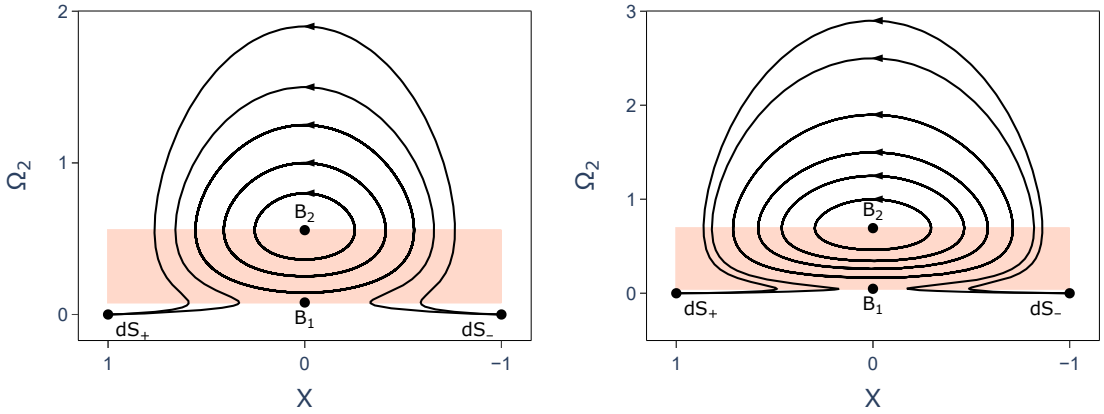

Figure 4.15: An example of a phase portrait for the reduced system (4.33)–(4.34) with $K = 15 > K_c$ for $w = 0$ (left) and $w = 1/3$ (right). The points B_1 and B_2 mark two intersections of the invariant hyperbolic submanifold with a fixed curve C. The decelerated regime is indicated in orange.

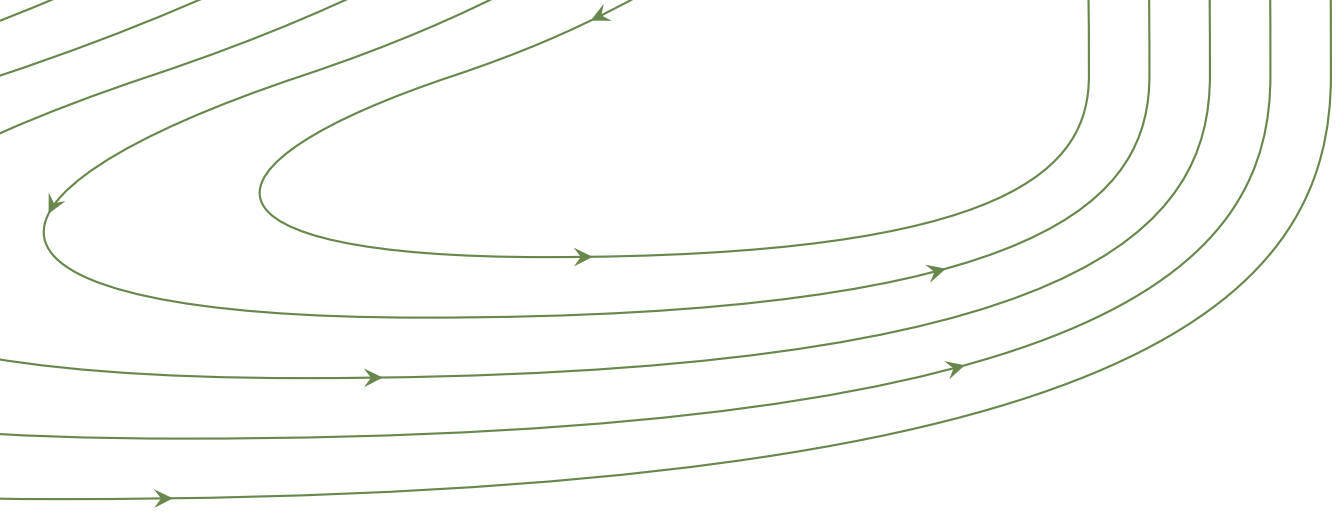

Conclusion

To enhance our understanding of hidden cosmic dynamics, researchers are extensively investigating possible extensions to Einstein's theory of gravitation. Many of these alternative theories introduce additional propagating degrees of freedom, which have not been observed. On the other hand, more restrictive modifications to gravity preserve the same number of degrees of freedom as General Relativity. The Minimal Exponential Measure model within the Generalized Coupling Theory framework can be categorized as such a minimal modification, since the non-trivial coupling, represented by a rank-4 tensor, can be decomposed into two rank-2 tensors which do not propagate.

The objective of this thesis was to elaborate on the bounce cosmologies within the MEMe theory framework, which are connected to the phenomenon of *spacetime-matter decoupling* at a critical value of energy density. Via applying the dynamical systems approach, we specifically focused on confirming the occurrence of the bounce across all values of the spatial curvature parameter k and on examining the range of initial conditions that lead to this behaviour.

Regarding the linearized version of the MEMe model, we have demonstrated that, for all three spatial geometries, the phase space trajectories *consistently present a bounce solution*, provided that their initial conditions are physical. This was accomplished by properly selecting three sets of dynamical variables and representing the phase portraits of the corresponding dynamical systems, as described in Chapter 4. We have determined that both flat and hyperbolic universes can be effectively analysed within a single three-dimensional system of ordinary differential equations. Within a closed spatial geometry, alongside single-bounce solutions, cyclic cosmologies have emerged under specific initial conditions. This has been verified through *dimensional reduction*, which allowed a more efficient analysis, ultimately summarizing the study within three two-dimensional phase portraits for each EoS parameter w in Figures 4.13–4.15. The system (4.26)–(4.28) exhibited the distinctive property of comprising infinitely many invariant submanifolds, each defined by an equation of a hyperbolic surface.

In dynamical systems analysis, selecting appropriate variables can be likened to choosing a suitable "dress code": each selection highlights certain properties of the

dynamics while potentially obscuring others, much as an outfit advisable in one setting may be entirely out of place in another. Some formulations enable a more compact representation of the phase space, facilitating global analysis, but may conceal specific features. Other choices emphasize particular characteristics, possibly at the expense of simplicity or generality. Consequently, this process involves a series of *trade-offs*, with each decision driven by the specific aspects of the dynamics that are of interest. Thus, different variable choices serve as complementary perspectives rather than universally superior descriptions.

In our work, this principle was clearly manifested: clarifying specific aspects of the MEMe model's dynamics, particularly the investigation concerning $H = 0$, came at the cost of separating the analyses for three distinct types of curvature parameter. This proved beneficial, since for $k = -1$ and $k = 0$, a compact phase space could be obtained while maintaining a positive normalization factor, owing to the properties of the model parameter q. This outcome was not achievable with the standard EN variables used in the initial analysis performed in [1]. On the other hand, for $k = 1$, a similar analysis to that of standard cosmology was employed. Although this second approach did not result in an entirely compact phase space, it revealed a broader range of cosmological scenarios.

We have also observed that the dynamical properties of Einstein–Cartan cosmology discussed at the end of Chapter 2 are encapsulated within the MEMe model on the boundary when the cosmological constant Λ becomes negligible. This is attributable to the fact that both models incorporate corrections to General Relativity characterized by an effective contribution of *negative energy density*, which is dominant at early times, when the scale factor a is very small.

Addressing the time asymmetry associated with the bounce in the exact solution (3.72) for a scale factor in flat spatial geometry would be an interesting avenue for future investigation, as we have not examined potential differences in time flow along the phase space orbits in any case. Another future prospect involves identifying appropriate variables for a full MEMe model, described by equations (3.57) and (3.58), which would enable the attainment of behaviour around $H = 0$ while preserving all nonlinear model properties. Here we addressed only the linearized version of the theory.

In conclusion, the dynamical systems formulation developed in this work provides a consistent and physically transparent framework for analysing bounce cosmologies within the MEMe model and therefore helps to elucidate the role of minimal modifications to gravity in addressing early-universe singularities. Although the analysis has been restricted to the linearized regime, we found that it is able to capture the key qualitative features of the theory: the generic occurrence of nonsingular bounce solutions across all spatial geometries under physically admissible initial conditions.

Bibliography

[1] J. C. Feng and S. Carloni. New class of generalized coupling theories. *Physical Review D*, 101(6), March 2020. ISSN 2470-0029. doi: 10.1103/physrevd.101.064002. URL http://dx.doi.org/10.1103/PhysRevD.101.064002.

[2] E. N. Saridakis et al. *Modified Gravity and Cosmology: An Update by the CANTATA Network*. Springer International Publishing, 2021. ISBN 9783030837150. doi: 10.1007/978-3-030-83715-0. URL http://dx.doi.org/10.1007/978-3-030-83715-0.

[3] B. P. Abbott et al. Observation of gravitational waves from a binary black hole merger. *Physical Review Letters*, 116(6), February 2016. ISSN 1079-7114. doi: 10.1103/physrevlett.116.061102. URL http://dx.doi.org/10.1103/PhysRevLett.116.061102.

[4] K. Aoki, A. D. Felice, C. Lin, S. Mukohyama, and M. Oliosi. Phenomenology in type-i minimally modified gravity. *Journal of Cosmology and Astroparticle Physics*, 2019 (01):017–017, January 2019. ISSN 1475-7516. doi: 10.1088/1475-7516/2019/01/017. URL http://dx.doi.org/10.1088/1475-7516/2019/01/017.

[5] C. Brans and R. H. Dicke. Mach's Principle and a Relativistic Theory of Gravitation. *Physical Review*, 124(3):925–935, November 1961. doi: 10.1103/PhysRev.124.925.

[6] A. G. Riess et al. Observational evidence from supernovae for an accelerating universe and a cosmological constant. *The Astronomical Journal*, 116(3):1009–1038, September 1998. ISSN 0004-6256. doi: 10.1086/300499. URL http://dx.doi.org/10.1086/300499.

[7] S. Perlmutter et al. Cosmology from type ia supernovae, 1998. URL https://arxiv.org/abs/astro-ph/9812473.

[8] P. A. R. Ade et al. Planck 2015 results: Xiv. dark energy and modified gravity. *Astronomy amp; Astrophysics*, 594:A14, September 2016. ISSN 1432-0746. doi:

10.1051/0004-6361/201525814. URL http://dx.doi.org/10.1051/0004-6361/201525814.

[9] D. J. Eisenstein et al. Detection of the baryon acoustic peak in the large-scale correlation function of sdss luminous red galaxies. *The Astrophysical Journal*, 633(2):560–574, November 2005. ISSN 1538-4357. doi: 10.1086/466512. URL http://dx.doi.org/10.1086/466512.

[10] V. C. Rubin. A brief history of dark matter. In Mario Livio, editor, *The Dark Universe: Matter, Energy and Gravity*, volume 15, pages 1–13, January 2003.

[11] F. Zwicky. On the Masses of Nebulae and of Clusters of Nebulae. *The Astrophysical Journal*, 86:217, October 1937. doi: 10.1086/143864.

[12] C. W. Misner, K. S. Thorne, and J. A. Wheeler. *Gravitation*. W. H. Freeman, San Francisco, 1973. ISBN 978-0-7167-0344-0, 978-0-691-17779-3.

[13] R. M. Wald. *General Relativity*. Chicago Univ. Pr., Chicago, USA, 1984. doi: 10.7208/chicago/9780226870373.001.0001.

[14] M. P. Hobson, G. P. Efstathiou, and A. N. Lasenby. *General relativity: An introduction for physicists*. 2006.

[15] E. Poisson. *A Relativist's Toolkit: The Mathematics of Black-Hole Mechanics*. Cambridge University Press, 12 2009. doi: 10.1017/CBO9780511606601.

[16] J. M. Lee. *Introduction to Riemannian Manifolds*, volume 176 of *Graduate Texts in Mathematics*. Springer, Cham, 2nd edition, 2018.

[17] W. Rindler. *Relativity: Special, general, and cosmological*. 2006.

[18] W. M. Clifford. *Theory and Experiment in Gravitational Physics*. 2018. doi: 10.1017/9781316338612.

[19] D. Lovelock. The Four-Dimensionality of Space and the Einstein Tensor. *Journal of Mathematical Physics*, 13(6):874–876, June 1972. doi: 10.1063/1.1666069.

[20] T. Clifton, P. G. Ferreira, A. Padilla, and C. Skordis. Modified gravity and cosmology. *Physics Reports*, 513(1–3):1–189, March 2012. ISSN 0370-1573. doi: 10.1016/j.physrep.2012.01.001. URL http://dx.doi.org/10.1016/j.physrep.2012.01.001.

[21] H. Goldstein, C. Poole, and J. Safko. *Classical Mechanics (3rd Edition)*. 06 2001. ISBN 0201657023.

[22] G. D. Birkhoff and R. E. Langer. *Relativity and modern physics*. 1923.

[23] S. Capozziello, S. Nojiri, and S.D. Odintsov. Dark energy: the equation of state description versus scalar-tensor or modified gravity. *Physics Letters B*, 634(2–3):93–100, March 2006. ISSN 0370-2693. doi: 10.1016/j.physletb.2006.01.065. URL http://dx.doi.org/10.1016/j.physletb.2006.01.065.

[24] M. Milgrom. A modification of the Newtonian dynamics as a possible alternative to the hidden mass hypothesis. *The Astrophysical Journal*, 270:365–370, 1983. doi: 10.1086/161130.

[25] A. A. Starobinsky. Spectrum of relict gravitational radiation and the early state of the universe. *Soviet Journal of Experimental and Theoretical Physics Letters*, 30:682, December 1979.

[26] V. Faraoni, E. Gunzig, and P. Nardone. Conformal transformations in classical gravitational theories and in cosmology, 1998. URL https://arxiv.org/abs/gr-qc/9811047.

[27] G. W. Horndeski. Second-order scalar-tensor field equations in a four-dimensional space. *International Journal of Theoretical Physics*, 10(6):363–384, September 1974. doi: 10.1007/BF01807638.

[28] T. Kobayashi, M. Yamaguchi, and J. Yokoyama. Generalized g-inflation: –inflation with the most general second-order field equations–. *Progress of Theoretical Physics*, 126(3):511–529, September 2011. ISSN 1347-4081. doi: 10.1143/ptp.126.511. URL http://dx.doi.org/10.1143/PTP.126.511.

[29] J. Gleyzes, D. Langlois, F. Piazza, and F. Vernizzi. Exploring gravitational theories beyond horndeski. *Journal of Cosmology and Astroparticle Physics*, 2015(02):018–018, February 2015. ISSN 1475-7516. doi: 10.1088/1475-7516/2015/02/018. URL http://dx.doi.org/10.1088/1475-7516/2015/02/018.

[30] L. Heisenberg. Generalised Proca Theories, 2017. URL https://arxiv.org/abs/1705.05387.

[31] C. de Rham, G. Gabadadze, and A. J. Tolley. Resummation of Massive Gravity. *Physical Review Letters*, 106(23), June 2011. ISSN 1079-7114. doi: 10.1103/physrevlett.106.231101. URL http://dx.doi.org/10.1103/PhysRevLett.106.231101.

[32] S. F. Hassan and R. A. Rosen. Bimetric gravity from ghost-free massive gravity. *Journal of High Energy Physics*, 2012(2), February 2012. ISSN 1029-8479. doi: 10.1007/jhep02(2012)126. URL http://dx.doi.org/10.1007/JHEP02(2012)126.

[33] N. Rosen. General Relativity and Flat Space. I. *Phys. Rev.*, 57:147–150, Jan 1940. doi: 10.1103/PhysRev.57.147. URL https://link.aps.org/doi/10.1103/PhysRev.57.147.

[34] N. Rosen. A bi-metric theory of gravitation. *Gen. Rel. Grav.*, 4(6):435–447, 1973. doi: 10.1007/BF01215403.

[35] I. T. Drummond. Bimetric gravity and "dark matter". *Physical Review D*, 63 (4), January 2001. ISSN 1089-4918. doi: 10.1103/physrevd.63.043503. URL http://dx.doi.org/10.1103/PhysRevD.63.043503.

[36] Mordehai Milgrom. Bimetric MOND gravity. *Physical Review D*, 80(12), December 2009. ISSN 1550-2368. doi: 10.1103/physrevd.80.123536. URL http://dx.doi.org/10.1103/PhysRevD.80.123536.

[37] J. Khoury and A. Weltman. Chameleon cosmology. *Physical Review D*, 69(4), February 2004. ISSN 1550-2368. doi: 10.1103/physrevd.69.044026. URL http://dx.doi.org/10.1103/PhysRevD.69.044026.

[38] Y. Shtanov and V. Sahni. Bouncing braneworlds. *Physics Letters B*, 557(1–2): 1–6, March 2003. ISSN 0370-2693. doi: 10.1016/s0370-2693(03)00179-5. URL http://dx.doi.org/10.1016/S0370-2693(03)00179-5.

[39] T. Kaluza. On the unification problem in physics. *International Journal of Modern Physics D*, 27(14):1870001, October 2018. ISSN 1793-6594. doi: 10.1142/s0218271818700017. URL http://dx.doi.org/10.1142/S0218271818700017.

[40] O. Klein. The Atomicity of Electricity as a Quantum Theory Law. *Nature*, 118 (2971):516, October 1926. doi: 10.1038/118516a0.

[41] K. Akama. An Early Proposal of "Brane World", 2000. URL https://arxiv.org/abs/hep-th/0001113.

[42] V. A. Rubakov and M. E. Shaposhnikov. Do we live inside a domain wall? *Physics Letters B*, 125(2-3):136–138, May 1983. doi: 10.1016/0370-2693(83)91253-4.

[43] V. A. Rubakov. Large and infinite extra dimensions. *Physics-Uspekhi*, 44(9):871–893, September 2001. ISSN 1468-4780. doi: 10.1070/pu2001v044n09abeh001000. URL http://dx.doi.org/10.1070/PU2001v044n09ABEH001000.

[44] A. Lukas, B. A. Ovrut, K. S. Stelle, and D. Waldram. Universe as a domain wall. *Physical Review D*, 59(8), March 1999. ISSN 1089-4918. doi: 10.1103/physrevd.59.086001. URL http://dx.doi.org/10.1103/PhysRevD.59.086001.

[45] N. Arkani–Hamed, S. Dimopoulos, and G. Dvali. The hierarchy problem and new dimensions at a millimeter. *Physics Letters B*, 429(3–4):263–272, June 1998. ISSN 0370-2693. doi: 10.1016/s0370-2693(98)00466-3. URL http://dx.doi.org/10.1016/S0370-2693(98)00466-3.

[46] L. Randall and R. Sundrum. Large Mass Hierarchy from a Small Extra Dimension. *Physical Review Letters*, 83(17):3370–3373, October 1999. ISSN 1079-7114. doi: 10.1103/physrevlett.83.3370. URL http://dx.doi.org/10.1103/PhysRevLett.83.3370.

[47] L. Randall and R. Sundrum. An alternative to compactification. *Physical Review Letters*, 83(23):4690–4693, December 1999. ISSN 1079-7114. doi: 10.1103/physrevlett.83.4690. URL http://dx.doi.org/10.1103/PhysRevLett.83.4690.

[48] C. Charmousis, R. Gregory, and V. A. Rubakov. Wave function of the radion in a brane world. *Physical Review D*, 62(6), August 2000. ISSN 1089-4918. doi: 10.1103/physrevd.62.067505. URL http://dx.doi.org/10.1103/PhysRevD.62.067505.

[49] M. Ishak and J. Moldenhauer. A minimal set of invariants as a systematic approach to higher order gravity models. *Journal of Cosmology and Astroparticle Physics*, 2009 (01):024–024, January 2009. ISSN 1475-7516. doi: 10.1088/1475-7516/2009/01/024. URL http://dx.doi.org/10.1088/1475-7516/2009/01/024.

[50] Thomas P. Sotiriou and Valerio Faraoni. $f(R)$ theories of gravity. *Reviews of Modern Physics*, 82(1):451–497, March 2010. ISSN 1539-0756. doi: 10.1103/revmodphys.82.451. URL http://dx.doi.org/10.1103/RevModPhys.82.451.

[51] T. P. Sotiriou and S. Liberati. The metric-affine formalism of $f(R)$ gravity. *Journal of Physics: Conference Series*, 68:012022, May 2007. ISSN 1742-6596. doi: 10.1088/1742-6596/68/1/012022. URL http://dx.doi.org/10.1088/1742-6596/68/1/012022.

[52] C. M. Will. *Theory and Experiment in Gravitational Physics*. Cambridge University Press, 9 2018. ISBN 978-1-108-67982-4, 978-1-107-11744-0.

[53] A. D. Dolgov and M. Kawasaki. Can modified gravity explain accelerated cosmic expansion? *Physics Letters B*, 573:1–4, October 2003. ISSN 0370-2693. doi: 10.1016/j.physletb.2003.08.039. URL http://dx.doi.org/10.1016/j.physletb.2003.08.039.

[54] N. Lanahan-Tremblay and V. Faraoni. The Cauchy problem of $f(R)$ gravity. *Classical and Quantum Gravity*, 24(22):5667–5679, November 2007. ISSN 1361-6382. doi: 10.1088/0264-9381/24/22/024. URL http://dx.doi.org/10.1088/0264-9381/24/22/024.

[55] A. Iglesias, N. Kaloper, A. Padilla, and M. Park. How (not) to use the Palatini formulation of scalar-tensor gravity. *Physical Review D*, 76(10), November 2007. ISSN 1550-2368. doi: 10.1103/physrevd.76.104001. URL http://dx.doi.org/10.1103/PhysRevD.76.104001.

[56] E. Barausse, T. P. Sotiriou, and J. C. Miller. A no-go theorem for polytropic spheres in Palatini $f(R)$ gravity. *Classical and Quantum Gravity*, 25(6):062001, March 2008. ISSN 1361-6382. doi: 10.1088/0264-9381/25/6/062001. URL http://dx.doi.org/10.1088/0264-9381/25/6/062001.

[57] E. Barausse, T. P. Sotiriou, and J. C. Miller. Curvature singularities, tidal forces and the viability of Palatini $f(R)$ gravity. *Classical and Quantum Gravity*, 25(10):105008, May 2008. ISSN 1361-6382. doi: 10.1088/0264-9381/25/10/105008. URL http://dx.doi.org/10.1088/0264-9381/25/10/105008.

[58] L. P. Eisenhart. *Riemannian Geometry*. Princeton University Press, Princeton, 1926. URL https://archive.org/details/in.ernet.dli.2015.524829. Also published by Oxford University Press (London).

[59] F. W. Hehl, J. D. McCrea, E. W. Mielke, and Y. Ne'eman. Metric-affine gauge theory of gravity: field equations, Noether identities, world spinors, and breaking of dilation invariance. *Physics Reports*, 258(1–2):1–171, July 1995. ISSN 0370-1573. doi: 10.1016/0370-1573(94)00111-f. URL http://dx.doi.org/10.1016/0370-1573(94)00111-F.

[60] J. B. Jiménez and T. S. Koivisto. Lost in translation: The Abelian affine connection (in the coincident gauge). *International Journal of Geometric Methods in Modern Physics*, 19(07), April 2022. ISSN 1793-6977. doi: 10.1142/s0219887822501080. URL http://dx.doi.org/10.1142/S0219887822501080.

[61] A. Delhom-Latorre, G. J. Olmo, and M. Ronco. Observable traces of non-metricity: New constraints on metric-affine gravity. *Physics Letters B*, 780:294–299, May 2018. ISSN 0370-2693. doi: 10.1016/j.physletb.2018.03.002. URL http://dx.doi.org/10.1016/j.physletb.2018.03.002.

[62] R. Aldrovandi and J. G. Pereira. *Teleparallel Gravity: An Introduction*. Springer, 2013. ISBN 978-94-007-5142-2, 978-94-007-5143-9. doi: 10.1007/978-94-007-5143-9.

[63] J. M. Nester and H-J Yo. Symmetric teleparallel general relativity, 1999. URL https://arxiv.org/abs/gr-qc/9809049.

[64] J. B. Jiménez, L. Heisenberg, and T. S. Koivisto. The Geometrical Trinity of Gravity, 2019. URL https://arxiv.org/abs/1903.06830.

[65] É Cartan. On manifolds with an affine connection and the theory of general relativity. 1986. URL https://api.semanticscholar.org/CorpusID:117835856.

[66] S. Capozziello and M. De Laurentis. Extended theories of gravity. *Physics Reports*, 509(4–5):167–321, December 2011. ISSN 0370-1573. doi: 10.1016/j.physrep.2011.09.003. URL http://dx.doi.org/10.1016/j.physrep.2011.09.003.

[67] F. W. Hehl. Four lectures on poincaré gauge field theory, 2023. URL https://arxiv.org/abs/2303.05366.

[68] R. T. Hammond. Torsion gravity. *Rept. Prog. Phys.*, 65:599–649, 2002. doi: 10.1088/0034-4885/65/5/201.

[69] H. Weyl. *Space, Time, Matter*. Dover Books on Advanced Mathematics. Dover Publications, 1952. ISBN 9780486602677. URL https://books.google.cz/books?id=ztI6ezRvPXYC.

[70] H. Weyl. Republication of: Purely infinitesimal geometry by Hermann Weyl. *General Relativity and Gravitation*, 54(6):51, June 2022. doi: 10.1007/s10714-022-02931-6.

[71] C. Pfeifer. Finsler spacetime geometry in physics. *International Journal of Geometric Methods in Modern Physics*, 16(supp02):1941004, November 2019. ISSN 1793-6977. doi: 10.1142/s0219887819410044. URL http://dx.doi.org/10.1142/S0219887819410044.

[72] M. Hohmann, C. Pfeifer, and N. Voicu. Finsler gravity action from variational completion. *Physical Review D*, 100(6), September 2019. ISSN 2470-0029. doi: 10.1103/physrevd.100.064035. URL http://dx.doi.org/10.1103/PhysRevD.100.064035.

[73] E. Harikumar and V. O. Rivelles. Noncommutative gravity. *Classical and Quantum Gravity*, 23(24):7551–7560, November 2006. ISSN 1361-6382. doi: 10.1088/0264-9381/23/24/024. URL http://dx.doi.org/10.1088/0264-9381/23/24/024.

[74] R. Ferraro and F. Fiorini. Modified teleparallel gravity: Inflation without an inflaton. *Physical Review D*, 75(8), April 2007. ISSN 1550-2368. doi: 10.1103/physrevd.75.084031. URL http://dx.doi.org/10.1103/PhysRevD.75.084031.

[75] G. R. Bengochea and R. Ferraro. Dark torsion as the cosmic speed-up. *Physical Review D*, 79(12), June 2009. ISSN 1550-2368. doi: 10.1103/physrevd.79.124019. URL http://dx.doi.org/10.1103/PhysRevD.79.124019.

[76] R. Ferraro and F. Fiorini. Non-trivial frames for $f(t)$ theories of gravity and beyond. *Physics Letters B*, 702(1):75–80, August 2011. ISSN 0370-2693. doi: 10.1016/j.physletb.2011.06.049. URL http://dx.doi.org/10.1016/j.physletb.2011.06.049.

[77] L. Heisenberg. Review on $f(q)$ gravity, 2023. URL https://arxiv.org/abs/2309.15958.

[78] J. Lu, X. Zhao, and G. Chee. Cosmology in symmetric teleparallel gravity and its dynamical system, 2019. URL https://arxiv.org/abs/1906.08920.

[79] V. Gakis, M. Krššák, J. L. Said, and E. N. Saridakis. Conformal gravity and transformations in the symmetric teleparallel framework. *Physical Review D*, 101(6), March 2020. ISSN 2470-0029. doi: 10.1103/physrevd.101.064024. URL http://dx.doi.org/10.1103/PhysRevD.101.064024.

[80] N. J. Poplawski. Cosmological consequences of gravity with spin and torsion. *The Astronomical Review*, 8(3):108–115, July 2013. doi: 10.1080/21672857.2013.11519725.

[81] I. P. Lobo and C. Romero. Experimental constraints on the second clock effect. *Physics Letters B*, 783:306–310, August 2018. ISSN 0370-2693. doi: 10.1016/j.physletb.2018.07.019. URL http://dx.doi.org/10.1016/j.physletb.2018.07.019.

[82] M. P. Hobson and A. N. Lasenby. Note on the absence of the second clock effect in weyl gauge theories of gravity. *Physical Review D*, 105(2), January 2022. ISSN 2470-0029. doi: 10.1103/physrevd.105.l021501. URL http://dx.doi.org/10.1103/PhysRevD.105.L021501.

[83] J. B. Jiménez and K. F. Dialektopoulos. Non-linear obstructions for consistent new general relativity. *Journal of Cosmology and Astroparticle Physics*, 2020(01): 018–018, January 2020. ISSN 1475-7516. doi: 10.1088/1475-7516/2020/01/018. URL http://dx.doi.org/10.1088/1475-7516/2020/01/018.

[84] R. Ferraro and M. J. Guzmán. Hamiltonian formalism for $f(T)$ gravity. *Physical Review D*, 97(10), May 2018. ISSN 2470-0029. doi: 10.1103/physrevd.97.104028. URL http://dx.doi.org/10.1103/PhysRevD.97.104028.

[85] T. Koivisto and G. Tsimperis. The spectrum of teleparallel gravity, 2018. URL https://arxiv.org/abs/1810.11847.

[86] R. Arnowitt, S. Deser, and C. W. Misner. Republication of: The dynamics of general relativity. *General Relativity and Gravitation*, 40(9):1997–2027, August 2008. ISSN 1572-9532. doi: 10.1007/s10714-008-0661-1. URL http://dx.doi.org/10.1007/s10714-008-0661-1.

[87] C. Lin and S. Mukohyama. A class of minimally modified gravity theories. *Journal of Cosmology and Astroparticle Physics*, 2017(10):033–033, October 2017. ISSN 1475-7516. doi: 10.1088/1475-7516/2017/10/033. URL http://dx.doi.org/10.1088/1475-7516/2017/10/033.

[88] K. Aoki, C. Lin, and S. Mukohyama. Novel matter coupling in general relativity via canonical transformation. *Physical Review D*, 98(4), August 2018. ISSN 2470-0029. doi: 10.1103/physrevd.98.044022. URL http://dx.doi.org/10.1103/PhysRevD.98.044022.

[89] A. D. Felice, A. Doll, and S. Mukohyama. A theory of type-ii minimally modified gravity. *Journal of Cosmology and Astroparticle Physics*, 2020(09):034–034, September 2020. ISSN 1475-7516. doi: 10.1088/1475-7516/2020/09/034. URL http://dx.doi.org/10.1088/1475-7516/2020/09/034.

[90] N. Afshordi, D. J. H. Chung, and G. Geshnizjani. Causal field theory with an infinite speed of sound. *Physical Review D*, 75(8), April 2007. ISSN 1550-2368. doi: 10.1103/physrevd.75.083513. URL http://dx.doi.org/10.1103/PhysRevD.75.083513.

[91] S. Weinberg. *Cosmology*. 2008. ISBN 978-0-19-852682-7.

[92] D. Tong. Cosmology, 2019. URL https://www.damtp.cam.ac.uk/user/tong/cosmo.html. Lecture notes, Department of Applied Mathematics and Theoretical Physics, University of Cambridge.

[93] S. Bahamonde, C. G. Böhmer, S. Carloni, E. J. Copeland, W. Fang, and N. Tamanini. Dynamical systems applied to cosmology: Dark energy and modified gravity. *Physics Reports*, 775–777:1–122, November 2018. ISSN 0370-1573. doi: 10.1016/j.physrep.2018.09.001. URL http://dx.doi.org/10.1016/j.physrep.2018.09.001.

[94] B. Bertotti, L. Iess, and P. Tortora. A test of general relativity using radio links with the Cassini spacecraft. *Nature*, 425:374–376, 2003. doi: 10.1038/nature01997.

[95] M. Gasperini. Spin-dominated inflation in the einstein-cartan theory. *Phys. Rev. Lett.*, 56:2873–2876, Jun 1986. doi: 10.1103/PhysRevLett.56.2873. URL https://link.aps.org/doi/10.1103/PhysRevLett.56.2873.

[96] F. W. Hehl, P. von der Heyde, G. D. Kerlick, and J. M. Nester. General relativity with spin and torsion: Foundations and prospects. *Rev. Mod. Phys.*, 48:393–416, Jul 1976. doi: 10.1103/RevModPhys.48.393. URL https://link.aps.org/doi/10.1103/RevModPhys.48.393.

[97] Q. Huang, H. Huang, B. Xu, and K. Zhang. Evolution of the Early Universe in Einstein–Cartan Theory. *Universe*, 11(5):147, 2025. doi: 10.3390/universe11050147.

[98] J. Ginoux and C. Letellier. Van der pol and the history of relaxation oscillations: Toward the emergence of a concept. *Chaos: An Interdisciplinary Journal of Nonlinear Science*, 22(2), April 2012. ISSN 1089-7682. doi: 10.1063/1.3670008. URL http://dx.doi.org/10.1063/1.3670008.

[99] I. Kovacic and M.J. Brennan. *The Duffing Equation: Nonlinear Oscillators and their Behaviour*. Wiley, 2011. ISBN 9780470977866. URL https://books.google.cz/books?id=1dwZiol4qm0C.

[100] T. Matsumoto. A chaotic attractor from chua's circuit. *IEEE Transactions on Circuits and Systems*, 31(12):1055–1058, 1984. doi: 10.1109/TCS.1984.1085459.

[101] E. N. Lorenz. Deterministic Nonperiodic Flow. *Journal of the Atmospheric Sciences*, 20(2):130–148, March 1963. doi: 10.1175/1520-0469(1963)020<0130:DNF>2.0.CO;2.

[102] S. H. Strogatz. *Nonlinear Dynamics and Chaos: With Applications to Physics, Biology, Chemistry and Engineering*. Westview Press, 2000.

[103] S. Wiggins. *Introduction to Applied Nonlinear Dynamical Systems and Chaos*. Texts in Applied Mathematics. Springer New York, 2013. ISBN 9781475740684. URL https://books.google.cz/books?id=p64LswEACAAJ.

[104] L. Perko. *Differential equations and dynamical systems*. Springer-Verlag, Berlin, Heidelberg, 1991. ISBN 0387974431.

[105] J. Maruskin. *Dynamical Systems and Geometric Mechanics: An Introduction*. 08 2018. ISBN 9783110597806. doi: 10.1515/9783110597806.

[106] L. Přibylová. *Nelineární dynamika [online]*. Elportál. Masarykova univerzita, 1. vyd. edition, 2021. ISBN 978-80-280-0111-7, 978-80-280-0111-7 (html). URL http://is.muni.cz/elportal/?id=1756857.

[107] L. Přibylová. *Teorie bifurkací, chaos a fraktály [online]*. Elportál. Masarykova univerzita, 1. vyd. edition, 2021. ISBN 978-80-280-0112-4, 978-80-280-0112-4 (html). URL http://is.muni.cz/elportal/?id=1799998.

[108] J. Wainwright and G. F. R. Ellis. Dynamical systems in cosmology: Subject index. 1997. URL https://api.semanticscholar.org/CorpusID:117790265.

[109] C. G. Böhmer and N. Chan. *Dynamical Systems in Cosmology*, page 121–156. WORLD SCIENTIFIC (EUROPE), December 2016. ISBN 9781786341044. doi: 10.1142/9781786341044_0004. URL http://dx.doi.org/10.1142/9781786341044_0004.

[110] A. A. Coley. Dynamical systems in cosmology, 1999. URL https://arxiv.org/abs/gr-qc/9910074.

[111] F. Verhulst. *Nonlinear differential equations and dynamical systems*. Springer-Verlag, Berlin, Heidelberg, 1990. ISBN 0387506284.

[112] P. Hartman. A lemma in the theory of structural stability of differential equations. 1960. URL https://api.semanticscholar.org/CorpusID:6411725.

[113] R. Adam et al. Planck 2015 results: I. overview of products and scientific results. *Astronomy amp; Astrophysics*, 594:A1, September 2016. ISSN 1432-0746. doi: 10.1051/0004-6361/201527101. URL http://dx.doi.org/10.1051/0004-6361/201527101.

[114] M. Novello and S. Bergliaffa. Bouncing cosmologies. *Physics Reports*, 463(4): 127–213, July 2008. ISSN 0370-1573. doi: 10.1016/j.physrep.2008.04.006. URL http://dx.doi.org/10.1016/j.physrep.2008.04.006.

[115] Orest Hrycyna and Marek Szydłowski. Dynamical complexity of the brans-dicke cosmology. *Journal of Cosmology and Astroparticle Physics*, 2013(12):016–016, December 2013. ISSN 1475-7516. doi: 10.1088/1475-7516/2013/12/016. URL http://dx.doi.org/10.1088/1475-7516/2013/12/016.

[116] V. Faraoni. Scalar field mass in generalized gravity. *Classical and Quantum Gravity*, 26(14):145014, June 2009. ISSN 1361-6382. doi: 10.1088/0264-9381/26/14/145014. URL http://dx.doi.org/10.1088/0264-9381/26/14/145014.

[117] S. Carloni, P. Dunsby, S. Capozziello, and A. Troisi. Cosmological dynamics of R^n gravity. *Classical and Quantum Gravity - CLASS QUANTUM GRAVITY*, 22: 4839–4868, 11 2005. doi: 10.1088/0264-9381/22/22/011.

[118] S. Carloni. Generalising the coupling between spacetime and matter. *Physics Letters B*, 766:55–58, March 2017. ISSN 0370-2693. doi: 10.1016/j.physletb.2016.12.053. URL http://dx.doi.org/10.1016/j.physletb.2016.12.053.

[119] F. W. Hehl, Y. N. Obukhov, and G. F. Rubilar. Classical electrodynamics: A tutorial on its foundations, 1999. URL https://arxiv.org/abs/physics/9907046.

[120] J. C. Feng, S. Mukohyama, and S. Carloni. Minimal exponential measure model in the post-newtonian limit. *Physical Review D*, 103(8), April 2021. ISSN 2470-0029. doi: 10.1103/physrevd.103.084055. URL http://dx.doi.org/10.1103/PhysRevD.103.084055.

[121] J. C. Feng, S. Mukohyama, and S. Carloni. Junction conditions and sharp gradients in generalized coupling theories. *Physical Review D*, 105(10), May 2022. ISSN 2470-0029. doi: 10.1103/physrevd.105.104036. URL http://dx.doi.org/10.1103/PhysRevD.105.104036.

[122] A. Troisi, G. Lambiase, and S. Carloni. Matter-antimatter asymmetry in generalized coupling theories. *Journal of Cosmology and Astroparticle Physics*, 2025(09):043, September 2025. ISSN 1475-7516. doi: 10.1088/1475-7516/2025/09/043. URL http://dx.doi.org/10.1088/1475-7516/2025/09/043.

[123] A. Troisi and S. Carloni. Bounce cosmologies in generalized coupling theories. *Physics Letters B*, 864:139426, May 2025. ISSN 0370-2693. doi: 10.1016/j.physletb.2025.139426. URL http://dx.doi.org/10.1016/j.physletb.2025.139426.